2023

MITOCHONDRIA AS CAUSES OF AND THERAPEUTIC TARGETS IN CHRONIC POST-SEPSIS SKELETAL MUSCLE WEAKNESS

Meagan Scott Kingren
University of Kentucky, kingrensmeagan@gmail.com
Author ORCID Identifier:
https://orcid.org/0000-0002-9262-2936
Digital Object Identifier: https://doi.org/10.13023/etd.2023.244

Right click to open a feedback form in a new tab to let us know how this document benefits you.

STUDENT AGREEMENT:

I represent that my thesis or dissertation and abstract are my original work. Proper attribution has been given to all outside sources. I understand that I am solely responsible for obtaining any needed copyright permissions. I have obtained needed written permission statement(s) from the owner(s) of each third-party copyrighted matter to be included in my work, allowing electronic distribution (if such use is not permitted by the fair use doctrine) which will be submitted to UKnowledge as Additional File.

I hereby grant to The University of Kentucky and its agents the irrevocable, non-exclusive, and royalty-free license to archive and make accessible my work in whole or in part in all forms of media, now or hereafter known. I agree that the document mentioned above may be made available immediately for worldwide access unless an embargo applies.

I retain all other ownership rights to the copyright of my work. I also retain the right to use in future works (such as articles or books) all or part of my work. I understand that I am free to register the copyright to my work.

REVIEW, APPROVAL AND ACCEPTANCE

The document mentioned above has been reviewed and accepted by the student's advisor, on behalf of the advisory committee, and by the Director of Graduate Studies (DGS), on behalf of the program; we verify that this is the final, approved version of the student's thesis including all changes required by the advisory committee. The undersigned agree to abide by the statements above.

Meagan Scott Kingren, Student

Dr. Hiroshi Saito, Major Professor

Dr. Howard Glauert, Director of Graduate Studies

2023

MITOCHONDRIA AS CAUSES OF AND THERAPEUTIC TARGETS IN CHRONIC POST-SEPSIS SKELETAL MUSCLE WEAKNESS

Meagan Scott Kingren

STUDENT AGREEMENT:

I represent that my thesis or dissertation and abstract are my original work. Proper attribution has been given to all outside sources. I understand that I am solely responsible for obtaining any needed copyright permissions. I have obtained needed written permission statement(s) from the owner(s) of each third-party copyrighted matter to be included in my work, allowing electronic distribution (if such use is not permitted by the fair use doctrine) which will be submitted to UKnowledge as Additional File.

I hereby grant to The University of Kentucky and its agents the irrevocable, non-exclusive, and royalty-free license to archive and make accessible my work in whole or in part in all forms of media, now or hereafter known. I agree that the document mentioned above may be made available immediately for worldwide access unless an embargo applies.

I retain all other ownership rights to the copyright of my work. I also retain the right to use in future works (such as articles or books) all or part of my work. I understand that I am free to register the copyright to my work.

REVIEW, APPROVAL AND ACCEPTANCE

The document mentioned above has been reviewed and accepted by the student's advisor, on behalf of the advisory committee, and by the Director of Graduate Studies (DGS), on behalf of the program; we verify that this is the final, approved version of the student's thesis including all changes required by the advisory committee. The undersigned agree to abide by the statements above.

Meagan Scott Kingren, Student

Dr. Hiroshi Saito, Major Professor

Dr. Howard Glauert, Director of Graduate Studies

MITOCHONDRIA AS CAUSES OF AND THERAPEUTIC TARGETS IN
CHRONIC POST-SEPSIS SKELETAL MUSCLE WEAKNESS

_____

DISSERTATION
_____

A dissertation submitted in partial fulfillment of the
requirements for the degree of Doctor of Philosophy in the
College of Medicine
at the University of Kentucky

By
Meagan Scott Kingren
Lexington, Kentucky
Director: Dr. Hiroshi Saito, Professor of Surgery
Lexington, Kentucky
2023

ABSTRACT OF DISSERTATION

MITOCHONDRIA AS CAUSES OF AND THERAPEUTIC TARGETS IN POST
SEPSIS-SKELETAL MUSCLE WEAKNESS

Sepsis, or the organ damage that ensues after the body fails to properly contain a local infection, is the leading cause of in-patient hospitalization in the United States. Advances in critical care medicine over the last 20 years have enabled most sepsis patients to survive the life-threatening dysregulated immune response. However, a majority of survivors report chronic weakness and fatigue years after sepsis, and the cause of this weakness remains largely unknown. This dissertation work focused first on elucidating the major causes of post-sepsis muscle weakness (Aim 1). This aim involved a time-course study to determine when muscle weakness was the greatest, combining functional and molecular analyses to further reveal the underlying causes. These data indicated mitochondrial abnormalities cause progressive muscle weakness after sepsis, as noted by persisting transcriptional, functional, and proteomic changes. Then I evaluated the effectiveness of the mitochondrial protecting enzyme MnSOD in preventing post-sepsis skeletal muscle weakness (Aim 2). This study examined if overexpression led to differences in skeletal muscle function following severe sepsis when compared to wildtype mice and how these functional deficits related to non-sepsis control mice. Finally, therapeutic strategies were evaluated in Aim 3. Neither providing higher oxygen concentrations during acute sepsis nor allowing for voluntary exercise after sepsis survival reduced debilitating muscle weakness. However, pharmacological treatments showed significant promise. The mitochondria-localizing tetrapeptide SS-31 provided protection against skeletal muscle weakness when administered after the development of severe sepsis. A combination of functional, histological, and biochemical techniques was utilized to provide a comprehensive overview on how mitochondrial protection prevented

long-term weakness. Collectively, these studies demonstrate that mitochondrial abnormalities cause muscle weakness after sepsis. Mitochondria therefore serve as viable therapeutic targets in post-sepsis skeletal muscle weakness. Accordingly, this work suggests that mitochondria-targeting therapeutic approaches could allow sepsis survivors to recover from post-sepsis muscle weakness.

KEYWORDS: Muscle weakness, Post-sepsis syndrome, Sepsis, Mitochondria, Myopathy

Meagan Scott Kingren

(Name of Student)

03/31/2023

Date

MITOCHONDRIA AS CAUSES OF AND THERAPEUTIC TARGETS IN CHRONIC POST-SEPSIS SKELETAL MUSCLE WEAKNESS

By

Meagan Scott Kingren

Hiroshi Saito, PhD
_____
Director of Dissertation

Howard Glauert, PhD
_____
Director of Graduate Studies

03/31/2023
_____
Date

ACKNOWLEDGMENTS

Don't for one second think I am forgetting my best support system in my friends and family. Thank you all so much for supporting me, giving me reality checks, and overall just straight up ensuring my ability to complete this craziness. To my family, I truly wouldn't have done it without you all. Mom, thank you for the trips up to see me and make food and the long phone calls discussing experiments, frustrations, and life plans. Mitch, thanks for our monthly calls this last year to talk about plans… it was on the phone with you I realized where I really wanted to go for my next step in my career. Dad, never did I think I'd go from having you edit my constitutional debate speeches to my NIH grants… wow. Thank you for all your help and for your trips up to watch Stevie. Mossy, Calvin, Steph, Sheryl, and the rest of the gang—the trips to Auburn, Pensacola, and up to see me were always at perfect times and with the perfect company because of you all. Thanks for making sure I took breaks and had fun during them.

To Stevie, my sweet, silly girl, thank you for always being there to brighten my day after 12-hour timepoints, a rough round of function testing, or a bad Western and never failing to celebrate my successes. Not that you can even read, but thank you for keeping me sane, active, and laughing. I love you and can't wait to get you a yard in the coming years.

To all my friends: gosh I love you all. Erica, Chan, Amy—from high school to now, thanks for being my constants. Carol, Jessie, Hannah, Natalie, Ryan, and Georgeann, I am so glad we all met in college and y'all have stuck. My grad school friends… I can't even fathom having done the last four years without you. Rea, Liv, Tanner, and Lesley, my cohort buds, our Keeneland trips, Shrek party, trivia nights, and random hangs are so special me. Sydney, Gabi, Sara, Kellea, Zack, Micah, Genesee, Courtney, Lyndsay, Nermin, Julia—thank you all for commiserating with me and making this process fun. Sami and Rea, y'all have been my rocks, especially the last year and a half—thanks for always picking up the phone, grabbing lunch, and being down to just grab groceries or make sure we all eat. Thank you all for making me a better person.

And with that, I have one last thing to say: Stevie dog, we freaking did it!! We got through this process, and I still love research.

TABLE OF CONTENTS

LIST OF TABLES

LIST OF FIGURES

CHAPTER 1.BACKGROUND AND INTRODUCTION

1.1 Sepsis

1.1.1 Sepsis pathophysiology

Sepsis is the life-threatening organ damage that results from the body's failure to contain a standard infection (**Figure 1.1**) (1). This dysregulated host response to a bacterial, viral, fungal, or parasitic insult drives endothelial dysfunction, organ damage, and, in some cases, subsequent death. Altered body temperature, heart rate, respiration, urine output, white blood cell count, and platelet, creatinine, lactate, and bilirubin levels are all indications of sepsis (1). Increased age complicates these potential biomarkers and makes sepsis diagnosis harder. As such, there are several age-associated comorbidities that contribute to worsened sepsis, increased susceptibility, and/or increased mortality (**Figure 1.2**).

While most patients have fevers (temperature >38°C), fevers are absent in older sepsis patients up to 50% of the time (2). In addition, hypothermia (temperature <36°C) is more common in older adults and is also associated with higher mortality rates (2). This trend of hypothermia is seen in murine models, with older animals exhibiting more profound along with increased systemic inflammatory cytokine production and mortality (2). As a result, we perform our sepsis experiments in middle-aged animals, aiming to replicate the sequelae of most human sepsis patients.

Disseminated intravascular coagulation (DIC), resulting from inflammation-driven microvascular endothelial cell damage and vascular leakage, is a particularly deadly complication in sepsis. Not only does inflammation drive coagulation, but also increased coagulation further perpetuates inflammation, resulting in a positive feedback loop (2, 3). Hypotension, compromised blood circulation, tissue ischemia, and organ failure are all downstream consequences of increased coagulation (2). DIC also commonly results in coagulopathy (bleeding) once platelets and coagulation factors are exhausted (2, 4, 5). Kelm *et*

al. reported that DIC development in sepsis led to higher mortality rates when compared with sepsis controls without DIC (68% instead of 38%) (2, 6, 7). Lyons *et al.* found that as the severity of sepsis-associated coagulopathy increased, the duration of hospitalization and the requirement for ICU care did as well (2, 8, 9). This study also found an association between increased mortality and coagulopathy (2, 9). ''Sepsis-induced coagulopathy'' that can progress to DIC was recently introduced to better describe and diagnose the fibrinolytic phenotype of coagulopathy in sepsis (2, 4, 10). However, its relation to aging has yet to be characterized (2). Notably, individuals that suffer from sepsis commonly suffer from post-sepsis syndrome, a complication of sepsis survival that causes symptoms such as cognitive impairment, a weakened immune system, and significant skeletal muscle weakness.
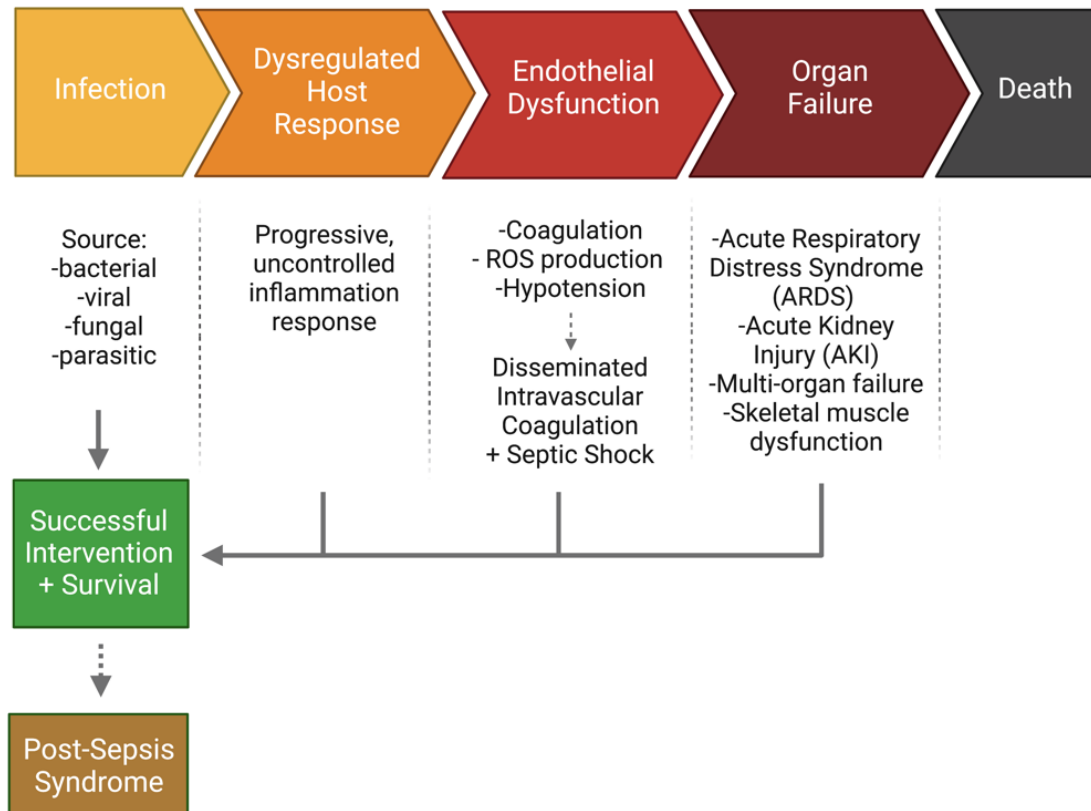
Figure 1-1 Sepsis Progression.

Sepsis is the organ damage that results from the immune system's failure to contain a local infection. Progressive, uncontrolled inflammation results, thus triggering endothelial dysfunction. Coagulation occurring with endothelial dysfunction can result in hypotension and even disseminated intravascular coagulation (DIC) and septic shock if intervention does not occur. This can cause damage to multiple organs, ultimately leading to death.
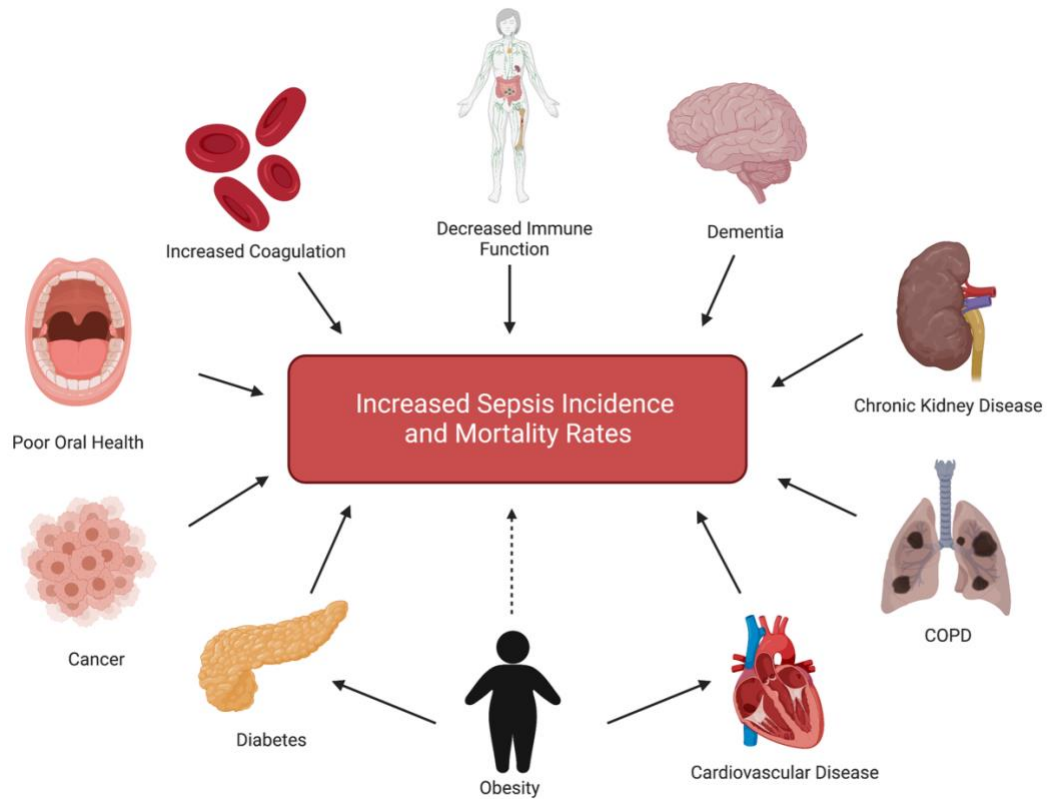
Figure 1-2 Age-associated comorbidities increase sepsis vulnerability. Shown by the solid arrows, decreased immune function, cancer, chronic obstructive pulmonary disease (COPD), chronic kidney disease, dementia, increased rates of coagulation, poor oral/ health, cardiovascular disease, and diabetes all increase sepsis risk and mortality. Further, obesity serves as a comorbidity and risk factor for several conditions, notably diabetes and cardiovascular disease. Although obesity's role in sepsis is still unclear, it may have a negative impact on incidence and mortality rates in older adults (dashed line). All of these conditions occur more frequently with age, thus contributing to higher rates of sepsis incidence and mortality in older populations (≥65 years old) and emphasizing the need to use at least middle-aged animals in experiments.

1.1.2   Sepsis epidemiology

Worldwide, sepsis affects 48.9 million individuals and accounts for over 11 million deaths annually (11). Despite 37% and 52.8% decreases in incidence and mortality worldwide since the turn of the century (11), top grossing countries such as the United States, Japan, and Germany have seen an alarming trend, recording marked increases in sepsis incidence over the same period of time (2, 11-15). This creates a phenomenon in which decreased mortality pairs with increased incidence to lead to more and more individuals being afflicted with and surviving sepsis annually, with the latter largely being due to advances in modern medicine and increased overall sepsis awareness. Over 2.2 million individuals in the US alone were diagnosed and treated at the hospital for sepsis in 2018, up from fewer than 500,000 individuals in 2004 (2). Thus, due to increasing incidence and decreasing mortality, there are well over 1.9 million *new* sepsis survivors in the US, annually (2, 13, 14, 16). Together, this underscores not only the need for sepsis treatment during the acute in-hospital event, but also the great need for effective therapeutics relating to chronic post-sepsis complications. Further, sepsis is the most costly hospital-treated condition in the US, with annual estimates ranging from $23.7 to $62 billion (2), excluding long-term costs of post-sepsis complications which would only further increase sepsis's economic impact.

Sepsis disproportionately impacts aged individuals, with incidence rates nearly 100-fold higher in those ≥85 years of age (0.2/1000 in children, 5.3/1000 in those aged 60-64, and 26.2/1000 in patients ≥85) (2). Mortality rates are much higher for older patients as well. While patients ≤50 years of age have an in-hospital rate of 25.2%, those ≤80 years old have an in-hospital mortality rate of 49.8%. More alarming, for those patients suffering from severe sepsis, patients >80 years old had a mortality rate of 78.9% (2).

1.1.3   Post-sepsis syndrome

Post-sepsis complications affect most sepsis survivors (17-20). Long lasting sepsis complications include, but are not limited to, chronic infections, brain fog,

PTSD, depression, fatigue, and, as it relates to this project specifically, chronic skeletal muscle weakness. These symptoms are collectively referred to as "Post-Sepsis Syndrome" (PSS) and affect as many as 95.5% of all sepsis survivors (18). After sepsis, nearly 1/3rd of sepsis survivors get discharged to assisted living facilities due to complications of PSS, and these individuals also have much higher 1-year mortality rates (2).

1.1.4 *Experimental Sepsis*

A major key to this study was picking an appropriate animal model that would enable study of post-sepsis skeletal muscle weakness. It was critical to use a model of sepsis that caused severe disease that induced long-term muscular changes while yielding a high number of survivors. Noting that most models had significant flaws preventing them from being optimal for post-sepsis research, Dr. Allison Owen created and optimized the cecal slurry (CS) model of sepsis induction whereby a high number of severe sepsis survivors could be studied for at least one month following recovery. Through this model, Dr. Owen discovered mitochondrial abnormalities are associated with skeletal muscle weakness, though no causative effect was found (42).

The cecal slurry (CS) injection model of sepsis induction was therefore chosen for my project due to it being a model that (a) reflects human sepsis pathophysiology, (b) is suitable for long-term study, and (c) is highly reproducible, and (d) is user-friendly.

1.2 **Post-sepsis skeletal muscle weakness**

1.2.1 Skeletal muscle

1.2.1.1   *Structural basis of skeletal muscle*

Skeletal muscle function and structure are tightly linked. Muscle strength relies upon total muscle mass and the actual force-generating capacity of that muscle, the latter of which is a key factor in post-sepsis skeletal muscle weakness

(21). Muscle fibers, nervous tissue, blood, and connective tissue come together to make up what enables locomotion, breathing, postural support, and heat production in situations of cold stress. Each muscle fiber is made up of myofibrils that contain the contractile proteins actin, myosin, and titin. Together with multiple nuclei, mitochondria, and innervation points where motor nerve fibers come together with neuromuscular junctions, muscle fibers are able to create the contractile force that enables daily function.

Muscle contraction occurs based on the sliding filament model of muscle contraction wherein a nerve impulse triggers the release of calcium which then binds to troponin, enabling the exposure of myosin binding sites on actin. Myosin then latches onto actin and pulls the latter filament across it to shorten the distance between the two filaments and produce movement (22, 23). As long as the process is provided with a neural stimulus and enough energy to enable the power stroke wherein myosin attaches to actin and utilizes ATP (releasing ADP and Pi), repeated and sustained muscle contractions can be carried out through this cross-bridge cycling fashion (24).

1.2.1.2   *Energetic basis of skeletal muscle*

As mentioned above, contraction requires energy. ATP, a majority of which is provided by oxidative phosphorylation and secondarily through glycolysis, serves as this energy source. Therefore, mitochondria are critical organelles to proper skeletal muscle function. Skeletal muscle mitochondria can be divided into two clear subpopulations: intermyofibrillar (IMF) mitochondria found near contractile proteins and subsarcolemmal (SS) mitochondria located just under the sarcolemma (25, 26). IMF mitochondria function to provide energy critical to producing the force required to sustain muscle contractions, while SS mitochondria have key roles in moving ions across the sarcolemma through active transport (24, 27). As such, mitochondrial health is closely linked to skeletal muscle health, and regulatory pathways often overlap. Skeletal muscle transcription factors regulate mitochondrial processes, with stimuli that enhance skeletal subsequently

7

promoting mitochondrial health (27). Further mechanisms of regulation of mitochondria are separate from skeletal muscle processes and include mitochondrial biogenesis and mitophagy (autophagy specific to mitochondria). While processes to build skeletal muscle (i.e., resistance exercise), promote mitochondrial expansion, increasing mitochondrial content and mass (mitochondrial biogenesis) are not enough to support high oxidative energy metabolism (28). As such, mitochondrial quality control—the interplay of mitochondrial dynamics, biogenesis, and mitophagy—is critical to proper skeletal muscle function. Further, issues with mitochondria, either structural or functional in nature, are linked to serious muscle dysfunction, with muscular dystrophies (29), cachexia (30, 31), and other myopathies (32) all suggesting mitochondrial abnormalities play a role in decreased function.

This interplay of metabolism and muscle function has led to fiber-type specific metabolic processes. Type I fibers, or those that are typically called slow-twitch fibers, are heavily reliant on oxidative metabolism, while type II fibers, or fast-twitch fibers, can take preference to glycolytic processes. Like type I fibers, type IIa fibers rely on oxidative processes that are slower to fatigue and can sustain being under tension longer, while type IIx and IIb fibers utilize glycolytic metabolism to produce faster, stronger, and quicker fatiguing contractions (33). Additionally, since muscle is a dynamic tissue, these fibers can shift from type I → IIa → IIx→IIb, making muscle metabolism flexible in turn (33-35). Indeed, muscle's great amount of metabolic flexibility allows other metabolically inflexible organs to use their required substrate first. This comes into play significantly in disease states, such as sepsis, which will be discussed later.

1.2.1.3   *Mechanisms of muscle weakness in post-sepsis dysfunction*

Muscle weakness occurs via a few routes: atrophy (muscle wasting), polyneuropathy (electrophysiological abnormalities), or myopathy (structural abnormalities), either individually or in combination. When there is a protein turnover imbalance in which protein degradation is greater than protein synthesis,

muscle atrophy can occur (21, 36-38). Common causes of atrophy include inactivity, aging, starvation, cancer, chronic illness, and loss of neural input. Typically type I (slow) fibers are less sensitive to atrophy, as are type IIa fibers, likely due to their frequent use to sustain contractions (39, 40) Type IIx (and IIb in rodents) fibers are highly susceptible to atrophy, and quickly change when nutrient or nervous supply are cut off (39). However, while occurring up to 4% each day during acute sepsis (41), atrophy resolves within two weeks in our murine model of sepsis (42). In patients with muscle weakness lasting at least 6 months after an ICU stay, atrophy status had little relationship to muscle weakness, and individuals demonstrating resolution of atrophy still had persistent muscle weakness (43).

Myopathy can have many causes (outlined in **Figure 1.3**), with persistent inflammation, structural alterations, bioenergetic failure, circulatory disturbances, ion channel dysfunction, and genetic disorders all being possible sources. Persistent inflammation can cause atrophy during acute illness, as can excessive oxidative damage. However, both inflammation and excess free radicals, reactive oxygen species, and toxic lipid species can induce long-term structural damage to the myofibers themselves, altering the contractile proteins and undermining contraction strength (44). Problems in the neuromuscular junction can prevent proper contraction as well (45). Lack of calcium prevents cross-bridge cycling (46), as does a lack of ATP (47). Mitochondrial abnormalities can create a vicious cycle in which damaged mitochondria release free radicals and reactive oxygen species which induce even more damage, all while possibly causing an energy crisis (48).
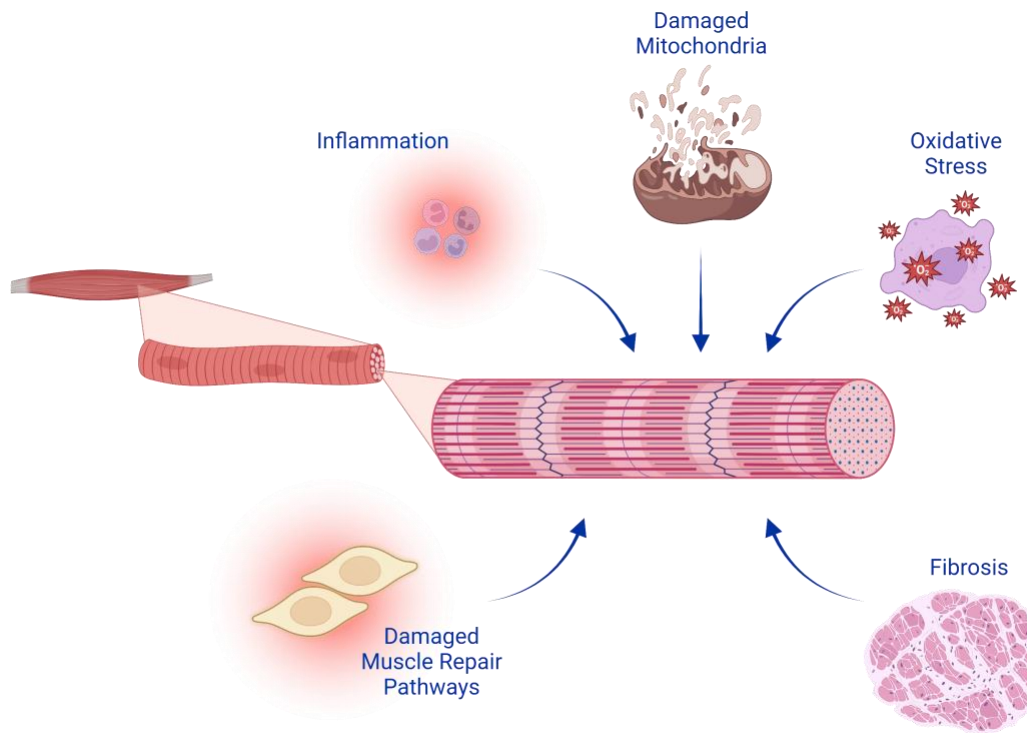
Figure 1-3 Common causes of myopathy.

Common causes of myopathy include prolonged oxidative stress that induces both damage to the contractile proteins and can trigger an energy crisis. Fibrosis, or the scar tissue that forms when muscle does not heal properly, can prevent proper function by negatively impacting muscle regeneration (49). Damaged muscle repair pathways, including defective satellite cells and ineffective differentiation, can also lead to limited function and myopathy. Like prolonged oxidative stress, inflammation can cause damage to the contractile proteins (50) while also inhibiting proper satellite cell function (51, 52). Notably, damaged mitochondria can undermine a number of these processes. Not only can abnormal mitochondria cause an energy crisis (53, 54), they can also produce free radicals and reactive oxygen species to drive prolonged oxidative stress (55) and alter muscle repair pathways.

Muscle weakness is one of the most reported symptoms of sepsis survivors and is directly associated with 5-year morality (21, 56, 57). Both skeletal muscle and diaphragm dysfunction have been identified as predictors of mechanical ventilation need (48), with the former also being linked to extubation failure. As such, muscle weakness is associated with worsened short-term outcomes (58) and one-year mortality (48), as muscle weakness is associated with lower likelihoods of live ICU discharge, earlier live hospital discharge, and live weaning from mechanical ventilation (48). While in the ICU, atrophy is the largest contributor to muscle weakness. However, even after recovery of muscle mass, weakness persists in both human and experimental sepsis. This indicates that post-sepsis muscle weakness is caused by a mechanism or mechanisms beyond atrophy alone. Further indicating this trend is the accompaniment of dysfunctional and damaged mitochondria in post-sepsis skeletal muscle after the resolution of atrophy (42).

1.2.2 *Mitochondria in post-sepsis skeletal muscle weakness*

As previously mentioned, skeletal muscle and mitochondrial health are tightly linked. Accordingly, mitochondrial dysfunction in skeletal muscle has been found in several diseases and disorders related to decreased muscle function.

It is well documented that mitochondria are significantly altered following sepsis. In both human and experimental sepsis, muscle biopsies have revealed decreased ATP/ADP ratios (59), reduced complex I activity (42, 59), depressed complex IV activity (60), increased reactive oxygen species (59), and disrupted mitochondria structure (42).

1.3 Lack of treatment for sepsis-induced skeletal muscle weakness

Since muscle weakness is a known complication of post-sepsis syndrome and is linked to short- and long-term outcomes, therapeutic interventions have been recognized as necessary. However, there are no successful interventions for

chronic post-sepsis skeletal muscle weakness. Nutritional supplementation during sepsis has not had any beneficial effect, as catabolism during acute illness is unavoidable (61). Instead of being used in protein synthesis to prevent a protein turnover imbalance where protein degradation outweighs protein synthesis (thus causing atrophy), the delivered amino acids are shuttled to ureagenesis (62, 63). Therefore, nutritional supplementation during acute sepsis may actively contribute to weakness. Atrophy status, as previously mentioned, has little relation to long term muscle weakness. Therefore, attempts at exercise and increasing muscle mass have not shown significant breakthroughs. Additionally, most therapeutic studies focus on surviving the initial sepsis event, not treating chronic complications.

1.4   Study rationale

1.4.1   Critical barrier to progress in the field

While chronic sepsis-induced skeletal muscle weakness affects a majority of sepsis survivors, there is no effective therapy to prevent or treat this complication. This is largely due to the lack of understanding of post-sepsis muscle weakness's cellular and molecular bases. Further, treatments that have attempted to mediate this complication have had limited and even negative effects. Intensive insulin therapy during sepsis may reduce muscle weakness incidence, but it can also lead to hypoglycemic episodes and worsen overall sepsis pathophysiology (21, 64, 65). Parenteral nutrition has been tried as a way to avoid early muscle catabolism. However, catabolism during acute illness is not avoidable, and once again, treatment in this way could actually prove dangerous (66). Instead of being used in muscle protein synthesis, amino acids delivered through nutritional modulation are shuttled to ureagenesis after being broken down (67, 68) while also suppressing skeletal muscle autophagy and actively contributing to weakness (58).

1.4.2 Central hypothesis

Sepsis-induced skeletal muscle damage is largely driven by mitochondrial dysfunction. If this mitochondrial damage can be mitigated during the acute sepsis event, then it is likely that muscle weakness will not occur. Further, mitochondria can be targeted via therapeutics to prevent and treat this devastating sepsis complication.

1.4.3 Specific aims

To test my central hypothesis that mitochondria are drivers of and therapeutic targets in post-sepsis skeletal muscle weakness, I carried out the following specific aims:

Specific Aim 1: To elucidate when mitochondrial damage induces skeletal muscle myopathy as a result of sepsis. Under this aim, I identified that mitochondrial damage is progressive, increasing from day 4 of sepsis pathogenesis to day 14, after recovery from the acute sepsis event. I identified this trend by utilizing *in vivo* function testing, western blotting, bulk mRNA sequencing, and histological analyses, all of which revealed worsened outcomes at day 14 as compared to day 3-4 and day 0.

Specific Aim 2: To evaluate if endogenous protection of mitochondria prevents the development of post-sepsis skeletal muscle weakness. To confer endogenous protection, I used a strain of transgenic mice overexpressing MnSOD, a mitochondria-specific antioxidant enzyme, and compared the MnSOD-TG animals to their wildtype littermates in functional and molecular analyses. MnSOD overexpressing mice were less susceptible to mitochondrial abnormalities following sepsis, despite equivalent sepsis severity when compared to wildtype sepsis controls. This translated to significantly less chronic muscle weakness.

Specific Aim 3: To identify treatments that confer mitochondrial protection and prevent/treat skeletal muscle weakness resulting from sepsis. Multiple therapeutic approaches known to target mitochondria were utilized including exercise and drug administration with nicotinamide mononucleotide (NMN) or SS-31. The exercise study demonstrated that muscle weakness persists at least two months after sepsis, though voluntary exercise did not yield positive results. Though in low numbers (n=3 per group), drug treatment with NMN following the resolution of sepsis yielded restoration of function following sepsis. SS-31 administration in conjunction with resuscitation fluids after sepsis development completely protected against muscle weakness development, as confirmed in multiple drug studies.

CHAPTER 2. METHODS

2.1 Animals and Husbandry

C57BL/6 and transgenic MnSOD-TG and WT mice were used in this dissertation study. Young mice were obtained from The Jackson Laboratory and used to prepare cecal slurry stock solutions. Late-middle-aged C57BL/6 mice were obtained from the National Institute on Aging and sepsis was induced when mice were between 16 to 17 months of age. Aged mice were obtained from the National Institute on Aging, and sepsis was induced when mice were between 24 to 25 months of age. Animals were acclimated for at least 7 days in the University of Kentucky Division of Laboratory Animal Resources (DLAR) prior to the beginning of experimentation.

MnSOD-TG mice were gifted to us by Daret K St Clair who created the animal strain described previously (69). Human MnSOD was endogenously overexpressed, which translated to a significant increase in skeletal muscle MnSOD (**Figure 2.1**). Mice were bred and maintained in the University of Kentucky DLAR. Genotyping was performed after weening using either an ear punch or a tail snip.

Mice were housed 3-5 animals per cage in pressurized intraventilated (PIV) cages on a 14/10 hr light/dark cycle with controlled temperature (21-23°C) and humidity (30-70%) in DLAR. Animals were allowed ad libitum access to water and standard chow. All experimental procedures were approved by the Institutional Animal Care and Use Committee at the University of Kentucky and animal handling was in accordance with the National Institute of Health's guidelines for ethical treatment. All techniques were performed as detailed in our approved Animal Use Protocol #2009-0541.
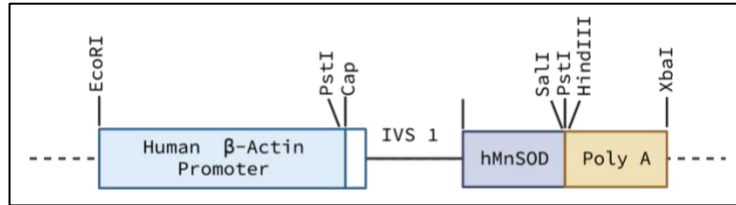
Figure 2-1 Construct of the overexpressed human MnSOD transgene.

Human MnSOD cDNA was flanked by EcoRI restriction sites and inserted into the human β-actin expression vector pHβAPr-1 (69). The transgene was then injected pronuclei of fertilized mouse eggs via microinjection. Mouse were produced using the progeny of C57BL/6 X C3H hybrids and then maintained by breeding MnSOD TG male mice with C57BL/6J female mice to produce heterozygous transgenic mice in a 1:1 ratio of WT to TG offspring.

2.2 Cecal slurry stock preparation

30 young male C57BL/6 mice (8-weeks) were obtained from The Jackson Laboratory, acclimated in the University of Kentucky Division of Laboratory Animal Resources, and aged to 16-weeks-old. The animals were weighed and monitored for any abnormalities and then separated into two cohorts (20 for making the cecal slurry stock and 10 for testing minimum lethal dose) where mice were housed at least 3 per cage. Upon euthanasia, ceca from the 20 donor mice were dissected. To resuspend the cecal slurry, the wet cecal content was obtained and for every 100mg of wet cecal content, 1mL of 5% glycerol-PBS was measured out. Using half of this stock, the cecal contents were resuspended. The remaining 5% glycerol-PBS was reserved for washing the cecal slurry through each mesh.

The slurry was then passed through six sterile meshes (1080, 860, 380, 190, 98, and 74 um). To help with flow through the strainers, a sterile pestle and 1/6 of the remaining 5% glycerol-PBS was used. After the last mesh, the cecal slurry was continuously stirred with a magnetic stir bar, and 1- and 2-mL aliquots were measured out into cryovials. The cecal slurry stock was then stored at -80°C until use. Samples were slowly frozen at -1°C/minute utilizing the CoolCell

Freezing System for Cyrogenic Vials (Corning, Mfr# 432000; Item # UX-04392-00). After two days in the CoolCell chambers, samples were moved to a pre-chilled sample box to enable easy storage.

To determine minimum lethal dose, CS was thawed and mixed thoroughly for intraperitoneal injection into the subject mice. For this 210615 CS, the minimum dose to obtain 100% mortality in 48 hours was 600uL. Since young mice were used to determine LD_{100}, a pilot study on late-middle aged mice was necessary to determine their LD_{100} since older animals are more susceptible to sepsis and exhibit a stronger response for the same CS dose. For the 210615 CS, the minimum lethal dose for 16-month-old male mice was 400 uL and 350uL for females. Aged mice (24 to 25 month old mice) had to have a further reduction in CS dose to achieve LD_{100}. A summary of CS stocks and their minimum lethal doses for experiments carried out as a part of this dissertation can be found in **Table 2.1**.

Table 2.1 Cecal Slurry Batch Characteristics

Batch	Minimum Lethal Dose (young animals)	Minimum Lethal Dose (16-months-old)
CS 170814	500 uL	400 uL male mice 350 uL female mice
CS 180808	550 uL	250 uL
CS 190705	650 uL	350 uL
CS 191206	550 uL	400 uL
CS 210615	600 uL	400 uL male mice 350 uL female mice

2.3   Induction of polymicrobial sepsis via CS injection

Upon selection of the correct cecal slurry dose and batch based on the age and sex of the animals, the CS stock was thawed in a water bath at 37°C prior to use. If multiple vials were being used, they were combined into a single container that was consistently agitated to prevent settling of the cecal contents. After mixture, the CS was injected into mice intraperitoneally (i.p.) using a 1mL syringe with a 25-guage needle. Each injection was the minimum lethal dose for the age and sex of the animals of the study. Body weight was monitored daily for five days and then again on days 7, 10, and 14 (and each week thereafter if studies were longer). Body temperature was monitored every 12 hours using a rectal temperature probe (RET-3 Physitemp Instruments, Clifton, NJ, USA attached to a Thermocouple Meter Model 20250-91, Davis Instruments, Clifton, NJ, USA) for five days. In some experiments, once mice had two or more timepoints at their pre-sepsis body temperature, rectal probe monitoring was ceased to prevent extra stress on the animal. **Figure 2.1** outlines the sepsis induction with late-stage resuscitation protocol (described below).
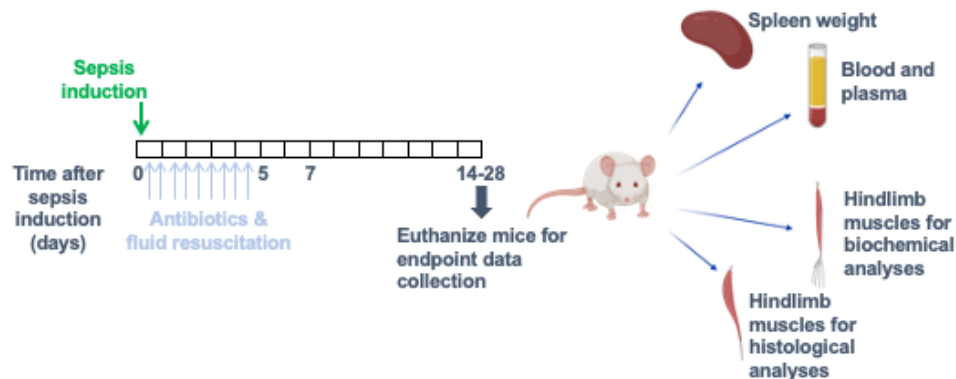
Figure 2-2 Sepsis induction with late-stage resuscitation timeline.

Prior to sepsis induction via CS injection, mice were weighed and body weight and temperature were recorded. Body weight was then monitored every day, with temperature being recorded every 12 hours in tandem with resuscitation administration. Starting at 12 hours, late-stage resuscitation with antibiotics (imipenem) and physiological saline were administered via intraperitoneal and subcutaneous injections, respectively. This was repeated 2x daily for 5 days as shown by the light blue arrows. Body weight was then monitored on day 7, 10, and 14. Mice were euthanized based on experiment at 14, 21, or 28 days.

2.4   Late-stage resuscitation protocol

Late-stage resuscitation was initiated at 12 hours after CS injection. Septic mice were given 0.3 mL broad spectrum antibiotics *i.p.* (imipenem, IPM; 1.5 mg/mouse) and 0.7mL sterile saline *s.c.* for resuscitation starting at 12h post CS injection and continuing every 12 hours thereafter for five days. IPM was reconstituted in sterile physiological saline as per manufacturer's instructions, aliquoted in appropriate volumes depending on the number of animals in each experiment and stored at either 4°C for up to 48h or -20°C for up to two weeks.

In select experiments, fluid administration with 0.7mL of sterile physiological saline was suspended once animals returned to 35°C and were able to drink and eat on their own. This prevented overloading the kidneys with fluid. Regardless of temperature status, i.p. antibiotic injections continued 2 times daily for 5 days after the start of CS injection. In select experiments, saline and antibiotic resuscitation was administered to non-sepsis controls to serve as true controls, despite previous evidence suggesting no differences arise from the resuscitation protocol's addition of antibiotics alone (42).

2.5   Evaluation of bacteremia

Following the development of severe sepsis prior to resuscitation beginning (12 hours after CS injection), a small amount of tail vein blood (10uL) was taken from each mouse and immediately diluted in 90uL of sterile saline for aerobic bacteria determination. Upon vortexing this solution, 10uL were added to a new sterile tube with another 90uL of sterile saline for anaerobic bacteria determination. The remaining 90uL of diluted blood from the aerobic bacteria tube were then plated on agar plates and stored at 37°C for 48 hours. The 100uL of diluted blood for anaerobic bacteria counting were spread on a different agar plate and placed into specialized pouches with the technology to absorb the oxygen remaining once they were sealed (GasPak EZ Anaerobe Gas Generating Pouch System with Indicator; Becton, Dickinson and Company; Sparks, MD, USA). These plates were then stored at 37°C for 24 hours. Upon completion of incubation, plates were sectioned into quarters and bacteria was counted for CFU analysis. Plates that did not have any colony growth were left another 24 hours and then noted as not displaying bacteria.

Agar plate preparation for 400-mL of agar (enough for 20 plates) consisted of adding 14.8g of BBL™ Brain Heart Infusion (BD211059) in 1-L glass bottle (orange cap) with a stirring bar. This was dissolved in 400-uL of deionized water on a heated stirring plate, after which 6.4g of granulated agar (Dfico 214530) was added. Next, the bottle of agar was autoclaved, and plates were poured in a

biosafety cabinet to prevent contamination. After the plates had set, they were packed into a plastic bag for storage upside down at 4°C until use.

2.6 Evaluation of severe sepsis

2.6.1 Splenomegaly

Upon euthanasia of sepsis survivors and their non-sepsis control counterparts, the spleen was carefully removed from the abdominal cavity and then weighed to help determine sepsis severity. Mice that did not have an enlarged spleen and underwent CS injection were excluded, as sepsis was not severe in those subjects. Splenomegaly is indicative of severe infection (70). While there has not been any study linking splenomegaly to sepsis, we use it as a marker of severe pathogenesis. Animals that have not undergone severe infection did not undergo severe sepsis. These animals would also not have large spleen sizes, allowing us to use splenomegaly as an exclusion criteria for animals that have not suffered from significant infection that would drive sepsis.
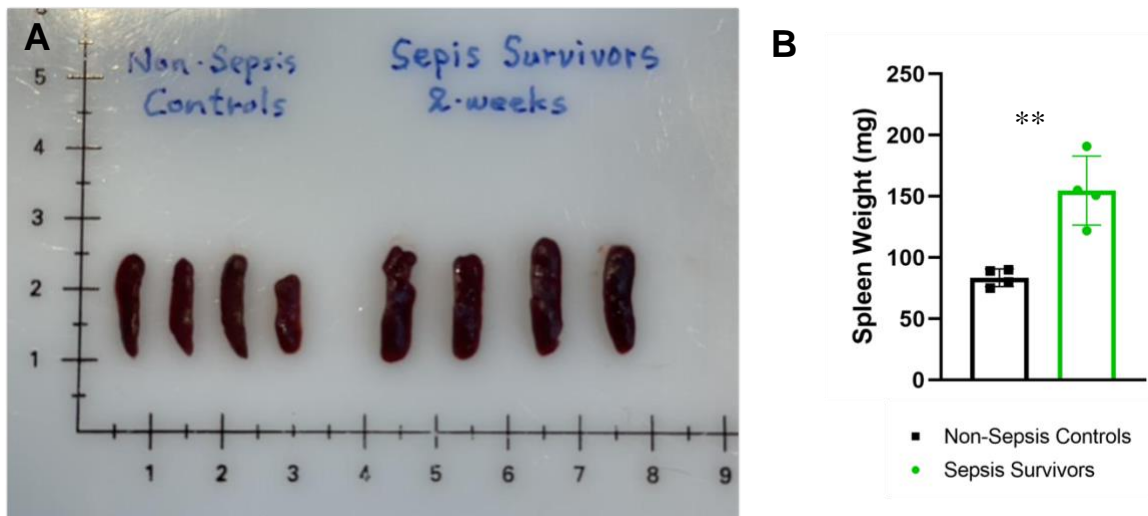
Figure 2-3 Splenomegaly is indicative of severe sepsis.

(A) Mice that have undergone CS injection induced sepsis have significantly larger spleens both visually and upon measurement of their weights. (B) Spleens from sepsis surviving mice are typically elongated and thicker upon comparison to those from non-sepsis control mice (shown left).

2.6.2 Weight loss

Body weight was recorded throughout sepsis pathogenesis for all animals in all sepsis experiments. To help determine sepsis severity, pre- and post-sepsis body weights were compared. Previous studies have shown that weight loss (~8% body weight loss, totaling more than 2.0g) at two weeks is from fat mass (and not lean mass) (42). This prolonged fat mass loss is indicative of sepsis severity. Further, if control mice exhibited significant weight loss (>1.0g), they were excluded, as they could not be counted as healthy controls. At 16-months of age, it is possible for mice to continue to gain weight, therefore non-sepsis mice that gained weight were still considered healthy controls.

2.6.3 6-hour IL-6 Levels

Cytokinemia is common in sepsis, with IL-6 serving as a pro-inflammatory cytokine that is elevated at six hours (88). Therefore, a small amount of blood (10uL) was taken from the tail vein at the 6h point after CS injection. Blood was added to 1uL of sodium citrate and then centrifuged at 12,000 RPM for 10 minutes. The plasma was pipetted off and stored in a 0.5mL Eppendorf tube at -80°C until use. Plasma was thawed on ice prior to use for an IL-6 ELISA kit to determine acute cytokinemia. Since IL-6 levels are extremely high at the 6h timepoint, blood was diluted at a 1:250 ratio to the manufacturers provided sample diluent. The manufacturer's instructions were followed for the ELISA itself (Mouse IL-6 ELISA Kit; Invitrogen,; Bender MedSystems GmbH; Vienna, Austria).

2.7 Treatment with SS-31

SS-31 was synthesized at GeneScript and gifted to us by collaborator Zoltan Ungvari at The University of Oklahoma Medical Center. SS-31 was reconstituted using 40 mL of sterile saline to obtain a concentration of 100 mg/kg of body weight per mouse (avg. mouse 35 g). SS-31 treatment was incorporated

into the resuscitation protocol described above, where 0.7 mL of SS-31-enriched-saline was injected s.c. every 12 hours for five days. The standard 0.7 mL sterile saline injection thereby acted as a sham/control for SS-31 so all mice received the same amount of fluid. Non-sepsis control mice received the same volume of SS-31-enriched-saline or standard saline following the same treatment paradigm.

2.8 Exercise Intervention

Sepsis was induced as previously described and animals were given standard resuscitation. On day 7, animals were divided into three cohorts: (1) non-sepsis control with access to a locked running wheel, (2) sepsis surviving control with access to a locked running wheel, and (3) exercise treated sepsis survivor with access to an unlocked running wheel. Mice were allowed access to their locked or unlocked wheels for six weeks whereafter they underwent both *in vivo* and *ex vivo* muscle function testing.

Mice underwent 6 weeks of wheel running. Animals were singly housed in running wheel cages with free access to the wheel that was locked or unlocked depending on treatment group. Running data (km/day and total km run) was recorded using ClockLab software (Actimetrics, Wilmette, IL, USA).

2.9 Hyperoxia intervention

Following standard sepsis induction, mice were sorted into two groups of similar sepsis severity based on equivalent temperatures and body weights at the 12-hour mark. Half of the mice were placed into a hyperoxia chamber that had 70% oxygen, while the other half of mice served as controls in the same room. Standard resuscitation with saline and antibiotics occurred every 12 hours for five days at which point the mice were removed from the chamber and returned to the University of Kentucky DLAR. Survival was monitored thereafter each day.

2.10 Treatment of established muscle weakness with NMN

Mice were subjected to severe sepsis and our standard late-stage resuscitation protocol. Following recovery from sepsis, mice were injected with NMN (s.c. injection 300 mg/kg; Sigma-Aldrich N3501) or saline vehicle once a day beginning on day 7 through day 14. Body weights were monitored daily to assess if there were any adverse effects. On day 28, mice were euthanized for *ex vivo* function testing.

2.11 Assessment of muscle strength using an *ex vivo* system

2.11.1 Muscle preparation

Immediately following euthanasia, the left hindlimb was skinned and placed in oxygenated (95%O_2-5% CO_2) Krebs-Ringer solution. Due to the need to place sutures in tendon on each side of the muscle to perform function testing, only two major hindlimb muscles are suitable for *ex vivo* testing: the soleus and the extensor digitorum longus (EDL). Due to previous success with the muscle in the lab and previous research indicating that fast twitch muscles are particularly susceptible to the effects of sepsis-induced muscle weakness, I utilized the EDL for most of these experiments. The muscle bath was continuously oxygenated while the EDL was dissected under a microscope and sutures were placed in the proximal and distal tendons using braided silk (4-0). After freeing the muscle from the leg, it was mounted with the distal end attached to a hook and the proximal end attached to the lever arm of an ASI 300C-LR Aurora Scientific signal transducer system. The platinum electrodes were moved into place around the muscle and the continuously oxygenated muscle bath was raised to allow the EDL to acclimate for five minutes at 25°C prior to finding optimal length (Lo). After obtaining Lo by adjusting the EDL length until the maximum force for the shortest muscle length at a 1 Hz stimulation was found, the EDL length was measured using digital calipers.

2.11.2 Protocol to determine maximum force

While at Lo, the muscle was subjected to a series of stimulations to find the force-frequency relationship. Frequencies used were 1, 15, 30, 50, 80, 150, 250, and 300 Hz. Between each stimulus, there was a 1 min break followed by a 300 Hz stimulus and another 1 min break, after which the next stimulus in the series would occur. Following conclusion of the protocol, the muscle was once again measured with digital calipers to ensure there were no changes in Lo during the protocol. The EDL was then carefully removed from the apparatus, and the sutures were removed to obtain the wet weight of the EDL. The EDL was then stored in a cryovial and frozen in liquid nitrogen for storage at -80°C. Force was then normalized to the physiological cross-sectional area, taking into the weight, tissue length, and pennation angle of the EDL.

2.12 Assessment of muscle strength using an *in vivo* system

Using an Aurora Scientific 1300A: 3-in-1 Whole Animal System-Mouse apparatus, I assessed plantar flexion function. After ensuring the 300D-300C-FP motor with the ankle flexion apparatus was attached to the 809C animal platform and the platform was heated to 37°C using an attached water pump, mice were anesthetized using 2.5% isoflurane. The right leg was then shaved to remove fur and the mouse was placed in a supine position on the platform with its head in the nosecone to continue isoflurane administration. The knee was clamped at 90°, and the foot was placed on the force plate, with the ankle creating a 90° angle as well. Then, a piece of tape was placed to secure the foot and prevent any compensatory movement. Two electrodes deliver the stimulus and must be placed 1-2 mm apart probing the peroneal nerve. To test for optimal placement, I placed the probes just distal to the knee joint and then delivered a single stimulus at 50 mA. Once optimal placement was obtained by moving one probe, testing torque, and then moving the other probe, optimal current was determined. To do this, I started with the current set at 50 mA and recorded the twitch torque with the baseline subtracted. Then I adjusted the current up or down 10 mA until the maximum twitch torque

was found with the lowest mA (similar to the procedure for finding optimal length in the ex vivo procedure). This lowest current at which maximum torque was achieved was recorded and then utilized throughout the rest of the torque-frequency experiment.

To assess the torque-frequency relationship and determine peak isometric torque, I selected the pre-programmed plantar-flexion protocol in the software. It delivered 0.35s stimuli in increasing frequency: 10 Hz, 40 Hz, 120 Hz, 150 Hz, 180 Hz, and 200 Hz with a rest period between contractions of 120s. Following completion of the protocol, I recorded the post-twitch stimulus using the original optimal current (which should not have changed throughout the experiment) to help assess fatigue upon comparison to the initial peak twitch. The electrodes were removed from the mouse and its knee was unclamped. The isoflurane was turned off and the mouse was placed back in its cage and monitored until it regained consciousness. Figure 2.4 shows the in vivo system setup.

Figure 2-4 In vivo system setup.

Mice were anesthetized in then placed in a supine position with a secured nosecone providing constant anesthetic. This procedure enabled testing of the same mouse over time in a minimally invasive manner.

2.13 Assessment of muscle mass

Upon euthanasia and dissection of hindlimb muscles, wet weights were recorded for the right TA, EDL, gastrocnemius, and soleus using a scale. Tissues were then stored at -80°C for future biochemical or histological use.

2.14 Muscle histology

2.14.1 Tissue preparation

Upon euthanasia and hindlimb muscle dissection, the left tibialis anterior was embedded in a layer of optimal cutting temperature (OCT) (Tissue-Tek, #4583). Pinned to a foil-covered cork at resting length, the muscle was frozen via submersion in isopentane prechilled by liquid nitrogen. Following freezing, the cork was placed on dry ice where the OCT embedded TA was removed and placed into a prechilled cryovial for storage at -80°C until sectioning. Frozen tissue was sectioned using a cryostat (HM525-NX, Thermo Fisher Scientific, Waltham, MA,

USA) in 7um thick sections, air dried on slides, and subsequently stored at -20°C for short-term storage, or -80°C for long-term storage.

2.14.2 Staining for electron transport chain complex enzymes
2.14.2.1 SDH staining

For SDH (succinate dehydrogenase) staining, thawed skeletal muscle cross-sections were incubated in 100mM sodium succinate salt and 1.2mM NBT in 0.2M PBS for 1 hour in an agitated water bath at 37°C. Tissues were then rinsed with DI water, washed in a series of acetone solutions (30% for 1 min, 60% for 1 min, 30% again for 1 min, all at RT, and finally 100% acetone at -20° for 20 minutes), rinsed again, and washed with 1x PBS twice for 3 minutes. Sections were then mounted with Vectashield mounting medium or incubated with primary antibody overnight for fiber-typing.

2.14.2.2 NADH staining

NADH (nicotinamide adenine dinucleotide) staining followed standard procedures. Thawed sections were incubated in 2.4mM NADH and NBT in 0.5M Tris buffer for 30 minutes on a plate rocker at 37°C. Prior to applying the NADH solution, sections were circled with a PAP sectioning pen to enable better coverage of the solution per individual tissue section. Sections were then rinsed, fixed, and mounted as described above for SDH staining.

2.14.2.3 Image quantification

After imaging, quantification was carried out using Aperio ImageScope software looking at the mean staining intensity of each individual fiber. This was then averaged for each section and compared across groups.

2.14.3 Fiber-type staining and evaluation of CSA

2.14.3.1 Staining

Sections were dried and rehydrated with PBS for three minutes prior to staining fiber-type-specific isoforms of MyHC unless coming immediately from SDH staining. Sections were incubated rocking at 4°C overnight in primary antibodies from Developmental Studies Hybridoma Bank (DSHB, Iowa City, IA, USA): type I (1:100; BA.D5-C; IgG2b), type IIa (1:50; SC.71; IgG1), type IIx (served as diluent, 6H1; IgM), with laminin for fiber borders (1:100; Sigma, Cat#L9393) and type IIb fibers remaining unstained. Slides were then washed 3 times for 3 minutes each time in PBS. Secondary antibodies from Invitrogen were diluted in PBS and incubated at room temperature for 1 hour: anti-mouse IgG2b, AF647 (1:250; #A21242), anti-mouse IgG1, AF488 (1:250; #A21121), anti-mouse IgM, AF555 (1:250; #A21426), and anti-rabbit IgG, AF350 (1:250, #A21068). Following 3 PBS washes for 5 minutes each, sections were incubated in Steptavidin-AMCA (1:200) in 1x PBS for 1 hour at room temperature and washed with PBS again. Slides were then mounted with Vectashield mounting media (Vector, cat#H-1000).

2.14.3.2 Image quantification using MyoVision

Entire muscle cross-sections were then imaged with a Zeiss M1 axioscanner fluorescent microscope. MyoVision 2.0 was utilized to quantify fibertype and assess cross-sectional area per each myofiber based on the intensity within the Cy5, GFP, and Texas Red filters for type I, IIa, and IIx fibers respectively, with type IIb fibers remaining unstained and myofiber borders being marked by laminin which showed blue. Images were captured at 20-200x magnification with a Zeiss upright microscope. MyoVision 2.0 (Lexington, KY, USA) software was used to assess fiber type distribution and fiber-type specific CSA.

2.15 Transmission electron microscopy

Upon euthanasia, a small section of the distal EDL was placed in TEM buffer (2% paraformaldehyde, 2.5% glutaraldehyde in 0.1M cacodylate buffer, pH 7.4;

Electron Microscopy Sciences; Hatfield, PA, USA). Samples were then sent to the Harvard University electron microscopy core for tissue sectioning and imaging.

2.16 Protein Isolation

Upon euthanasia and hindlimb muscle dissection, the gastrocnemius muscles were placed in cryovials and flash frozen in liquid nitrogen for storage at -80°C. Protein was isolated using dounce homogenizers. Gastrocnemius muscles were isolated individually in 1.5mL uL of protein isolation buffer and the lysate was transferred to 2 mL Eppendorf tubes. Samples were then heated in a water bath at 80°C for five minutes and subsequently centrifuged (12,000g for 10 min at room temperature). Protein concentration was assessed using the Bio-Rad *RC DC* (cat# 500-0120) assay as per manufacturer's instructions.

A secondary protocol was optimized to enable quicker protein isolation using metal beads. For this protocol, 700 uL of protein isolation buffer was added into round bottom 2 mL Eppendorf tubes with 2 metal beads. Samples were then added and a TissueLyser LT was used to break down the tissue. Homogenate was then collected and heated in a water bath as described above and aliquoted for quantification and storage at -80°C. This protocol provided a higher yield of protein with more consistency across samples, all while taking less time.

2.17 Western blot analyses

Samples (20g) were separated by SDS-PAGE electrophoresis (Mini PROTEAN TGX Stain Free Gels, cat # 4568096, BioRad) using pre-cast stain-free gradient (4-20%) gels, whereafter total protein was measured for later normalization via stain-free imaging. Samples were then transferred onto PVDF membranes (Trans-Blot Turbo Pack, cat # 17004157) (except for blots were 3-NT was the primary antibody, in which case nitrocellulose membranes were used; Trans-Blot Turbo Transfer Pack, cat # 1704158). Blots were blocked in 5% blotting grade blocker (BioRad cat # 170-6404) for 1 to 2 hours at room temperature. Blots

were incubated overnight at 4°C with primary antibody (3-NT ab 61392 1:3000; 4-HNE ab46545 1:3000; OXPHOS Rodent Antibody Cocktail STN-19467, 1:250). Blots were then washed and incubated with secondary antibody for 1 hour. The membranes were then treated with Clarity Western ECL substrate (BioRad cat# 170-5060) and detected by chemiluminescence. Band volume was detected using Image Lab software and normalized to total protein.

2.18 RNA sequencing

2.18.1 Tissue processing and RNA isolation

Upon euthanasia and hindlimb muscle dissection, the right tibialis anterior was flash frozen in liquid nitrogen and stored at -80°C. Samples were placed in 1.5mL tubes with 700uL of TRIzol and a metal bead for homogenization using a TissueLyser. RNA was then isolated using an RNA isolation kit (PureLink RNA Mini Kit; cat no. 12183018A; Invitrogen, Carlsbad, CA, USA) as per manufacturer's instructions. DNase treatment was conducted on-column using DNase (DNA-free Kit DNase Treatment & Removal; Invitrogen, Carlsbad, CA, USA) as per manufacturer's instructions. RNA concentration was assessed, and isolated RNA was sent to Novogene for library construction, sequencing, and preliminary bioinformatic analyses.

2.18.2 Bulk RNA-seq analysis

For the first set of analyses of the bulk sequencing data, Partek Flow was utilized to align the raw FASTQ files using the STAR aligner and then analyzed and normalized using DESeq2. P-values were adjusted using the Benjamini-Hochberg FDR step-up method. Initial pathway over-representation analysis was performed using gProfiler with up-or-downregulated genes with adj. p-value <0.05. Heatmaps were generated in R using the pheatmap package (available through Github).

Subsequent analyses utilized R 4.2.2+. The aligned counts were sent through differential analysis using DESeq2. The data was then normalized and DEGs were identified by a P-adj value <0.05. PCA plots and heatmaps were then generated in R packages available through Github. For specific code, see Appendix 2. Following identification of DEGs, pathway over-representation analysis was completed using gProfiler and the top up- and down-regulated pathways were noted. All reported GO: Cellular Component, GO: Molecular Function, GO: Biological Function, and Human Disease Phenotype pathways reported were calculated to include at least 3 genes implicated in the altered pathways and were filtered utilizing a Benjamini-Hochberg value of 0.05 to exclude false-positives. This change in processing occurred as I learned how to code during my dissertation studies and was able to utilize DESeq2 in its native platform.

2.19 Metabolomics

Metabolomics analysis was performed on both plasma and skeletal muscle in conjunction with the Gentry lab at the University of Kentucky. Plasma was collected from the IVC upon euthanasia of the animals for muscle force testing analysis. Skeletal muscles were snap frozen and cryopreserved for later use. Samples were pulverized into <5um particles in liquid nitrogen with a cyrogenic grinder (SPEX SamplePrep model 6875D) after which metabolites were extracted by adding 1mL of 50% methanol containing 20mL-norvaline. Samples were centrifuged at 4°C at 15,000 rpm to separate them into polar (aqueous layer) and protein/DNA/RNA/glycogen/protein (pellet) divisions. The pellet was washed four times with 50% methanol and then once with 100% methanol and subsequently hydrolyzed in 200 uL of 3N hydrochloric acid. Prior to drying, 200 uL of 100% methanol was added, and the polar and pellet fractions were dried at 10^{-3} mBar with a SpeedVac and then went through derivatization or hydrolysis (pellet) and subsequent derivatization.

The pellet was resuspended in deionized water whereafter an equal part of 2 N HCl was added and incubated at 95°C for two hours. The reaction was

quenched with 100% methanol and then incubated on ice for 30 minutes. Following centrifugation at 15,000 rpm for 10 minutes, the supernatant was collected and dried as previously described.

Samples were derivatized by adding 50uL of 20 mg/mL methoxyamine hydrochloride in pyridine. Following incubation at 30°C for 1.5h, 80uL of N-methyl-trimethylsilyl-trifluoroacetamide was added and the samples were incubated for another 30 mins at 37°C.

Following transfer into a V-shaped amber glass chromatography vial, samples were analyzed via GC-MS (Agilent 7800B GC coupled to a 5977B MS detector; Agilent, Santa Clara, CA, USA). GC-MS protocols were described in Drury et al., 2022. Mass spectra were converted to relative metabolite abundance using MassHunter MS quantitative software and relative abundance was normalized using the L-norvaline standard and protein input from the pellet.

For metabolite analysis, MetaboAnalyst version 5.0 (Xia Lab, McGill University, Montreal, QC, Canada) was used. PLS-DA and heatmaps were generated through this analysis. Transformed metabolomics data was used to generate bar graphs of the averages of altered metabolites.

2.20 ATP quantification

For experiments where ATP needed to be quantified from skeletal muscles, mice were anesthetized with 2.5% isoflurane and then the left leg was skinned. The gastrocnemius was quickly removed and snap frozen in pre-chilled cryovials for storage at -80°C. Samples were then shipped to Jeff Brault at the University of Indiana for nucleotide measurements. After weighing the TA, the muscle was then homogenized in a glass-on-glass tissue grinder with chilled 0.5N perchloric acid + 5mM EDTA. The homogenate was spun down and after the supernatant was collected, it was neutralized using1N KOH and centrifuged to remove the salts. The samples were subjected to separation by ultra-performance liquid chromatography (Waters Acquit UPLC H-Class system, HSS T3 1.8 um, 2.1 mm

x 150 mm column) and ATP, ADP, AMP, IMP, inosine, and hypoxanthine were quantified using UV absorbance at 210nm (71).

2.21 Overall statistical analysis

Previous power analyses indicated that 6 animals per group were sufficient to have a well-powered study. For my SS-31 study, power analyses concluded n=4 was enough. As a result, I tried to have at least 6 animals in each group for each study. Student's T-tests were applied when comparing two means from independent samples, and a one-way analysis of variance (ANOVA) was used when comparing the means of three or more data sets. Two-way ANOVAs were used to compare the effect of a treatment over time across different groups. Appropriate post-hoc analyses were conducted as needed. To align raw FASTQ files for sequencing, the STAR aligner was used, and quality control was checked, with reads being trimmed when necessary. Counts were then processed for differential analyses using DESeq2 and subsequently normalized. P-adj values of 0.05 or less were considered significant for subsequent over-representation analyses as previously described. In general, P-values of less than 0.05 were considered statistically significant. Analyses were carried out in GraphPad Prism and R 4.2.2+.

CHAPTER 3. MITOCHONDRIAL DYSFUNCTION DRIVES SKELELTAL MUSCLE WEAKNESS AFTER SEPSIS

3.1 Abstract

With 95% of sepsis survivors reporting some symptoms of PSS and more than 70% of severe sepsis survivors reporting muscle weakness years after sepsis, understanding the mechanism(s) of this post-sepsis complication is critical. Previous research in the Saito lab demonstrated muscle weakness in mice subjected to CS injection induced sepsis is associated with mitochondrial abnormalities. However, whether this combination of mitochondrial damage and dysfunction causes lasting weakness is not known.

To determine if there is a causative relationship between mitochondrial abnormalities and sepsis-induced muscle weakness, we carried out multiple time-course experiments. Functional analyses were conducted in the same mice throughout sepsis, and another time-course experiment enabled us to examine the molecular changes throughout sepsis progression and resolution. In utilizing bulk RNA sequencing we were able to evaluate transcriptome changes as they paired with protein expression level changes. Histological analyses for changes in fiber-type distribution, cross-sectional area, and NADH and SDH staining intensity gave us further insight into these changes across time. Altogether, these analyses revealed post-sepsis skeletal muscle weakness begins at day 4 and progressively worsens through at least day 14. Mitochondria-related transcriptomic changes persist while inflammation related gene elevation resolves, pairing with decreased Complex I, II, IV, and V protein expression, and lower NADH and SDH staining intensity. As such, we concluded that mitochondrial damage occurs progressively in tandem with progressive post-sepsis skeletal muscle weakness.

3.2 Introduction

One of the most prominent post-sepsis complications is prolonged skeletal muscle weakness and fatigue. Chronic skeletal muscle weakness affects 70-100% of severe sepsis survivors and contributes to a diminished post-sepsis quality of

life. Further, muscle weakness after sepsis is directly linked to both short-term and long-term outcomes, with higher 1-year and 5-year mortality rates (21, 56, 57) in individuals reporting the post-sepsis syndrome symptom. Despite the condition's prevalence, relatively little is known about what drives sepsis-induced skeletal muscle weakness. Reports attribute possible causes to muscle wasting (i.e., atrophy), damage within the muscle fibers (i.e., myopathy), damage in the neuro-muscular junction (i.e., polyneuropathy), and the combination of myopathy and polyneuropathy called neuromyopathy. Regardless, there are very few studies characterizing sepsis-associated skeletal muscle weakness over time, nor are there any effective interventions to treat this sepsis complication.

During acute sepsis, patients are typically bedridden and suffer from muscle wasting. Septic individuals requiring ICU stays commonly suffer from atrophy as much as 4% per day during acute illnesss (21). However, in sepsis surviving patients, atrophy status has little relationship to muscle strength recovery (42), indicating causes other than atrophy alone are largely contributing to prolonged muscle weakness. This medical issue can be reproduced in laboratory animals that have survived severe sepsis. The Saito lab previously developed a murine model of sepsis survival in which survivors exhibit chronic muscle weakness for at least one month after recovering from sepsis. In this study, atrophy was clearly present in the acute phase of sepsis, but it resolved within two weeks, further suggesting atrophy is not primarily responsible for sustained post-sepsis skeletal muscle weakness (42).

In the same study, we also demonstrated that sepsis survivor skeletal muscle had profound mitochondrial abnormalities and increased nitro-oxidative protein modification (42). It is also well established that mitochondrial abnormalities occur with stress, particularly during sepsis (42, 72-75). These findings have led us to two theories on the development of chronic post-sepsis skeletal muscle weakness: (1) mitochondrial damage, protein modification, and muscle weakness occur simultaneously as a result of significant inflammation during the acute phase of sepsis, and (2) mitochondrial damage occurs in the early phase of sepsis thereby

inducing protein modification and further mitochondrial damage through free radical and reactive oxygen species production, all leading to muscle weakness that develops gradually. To examine these possibilities, it was essential to evaluate skeletal muscle weakness, as well as mitochondrial abnormalities and protein modification, prior to, throughout, and after sepsis.

3.3   Experimental Approach

The primary goal of this aim was to conduct a kinetic study in which I would characterize the chronological changes in skeletal muscle weakness, mitochondrial abnormalities, and protein damage throughout sepsis and after recovery. To assess functional changes over time, we repeated *in vivo* muscle function testing on the same mice at days -1, 3, and 14 to evaluate when function deficits were greatest. After confirming that transcriptome differences persist through at least day 14, we performed a secondary time-course study to look at the molecular underpinnings of chronic post-sepsis skeletal muscle weakness. This study was designed to compare changes at three different phases: pre-sepsis (Day 0), during sepsis (day 3-4), and post-sepsis (Day 14). For this, we euthanized animals on Days 0, 4, and 14 and collected hindlimb skeletal muscle tissue to evaluate how skeletal muscle weakness changes over time. The left TA was taken for RNA isolation and subsequent bulk sequencing. The right TA was used for histological analyses, while the gastrocnemius muscles were cryopreserved for biochemical analyses. To confirm sepsis severity, spleen weights were also obtained. Both studies used age-matched middle-aged mice and sepsis was induced using cecal slurry (CS 210615).

3.4   Results

3.4.1   Sepsis surviving mice demonstrate transcriptome differences.

To extend the lab's work and better understand what molecular changes are occurring two weeks after sepsis, we performed a pilot bulk mRNA sequencing experiment. For this study, we injected mice with CS (400 uL, CS 210615) to induce severe sepsis as shown in **Figure 3.1**. Sepsis severity was confirmed by

(1) a significant decrease in body weight due to sepsis (2) severe hypothermia during acute sepsis 6, 12, and 24h post CS injection, and (3) marked splenomegaly, in addition to an overall survival rate of 56% (**Figure 3.1 B-E**). Pre-sepsis body weights, and only mice undergoing sepsis demonstrated weight loss over the two-week study. Mice that did not develop severe sepsis (n=2) as noted by a lack of severe hypothermia at the 6h and 12h timepoints were eliminated from the study and did not undergo late-stage resuscitation or tissue collection. TA samples were flash frozen for subsequent RNA isolation and sent to Novogene for library creation and sequencing. Other hindlimb muscles were also collected for subsequent analyses including Western blotting for markers of oxidative phosphorylation protein complexes I-V and histological analyses.
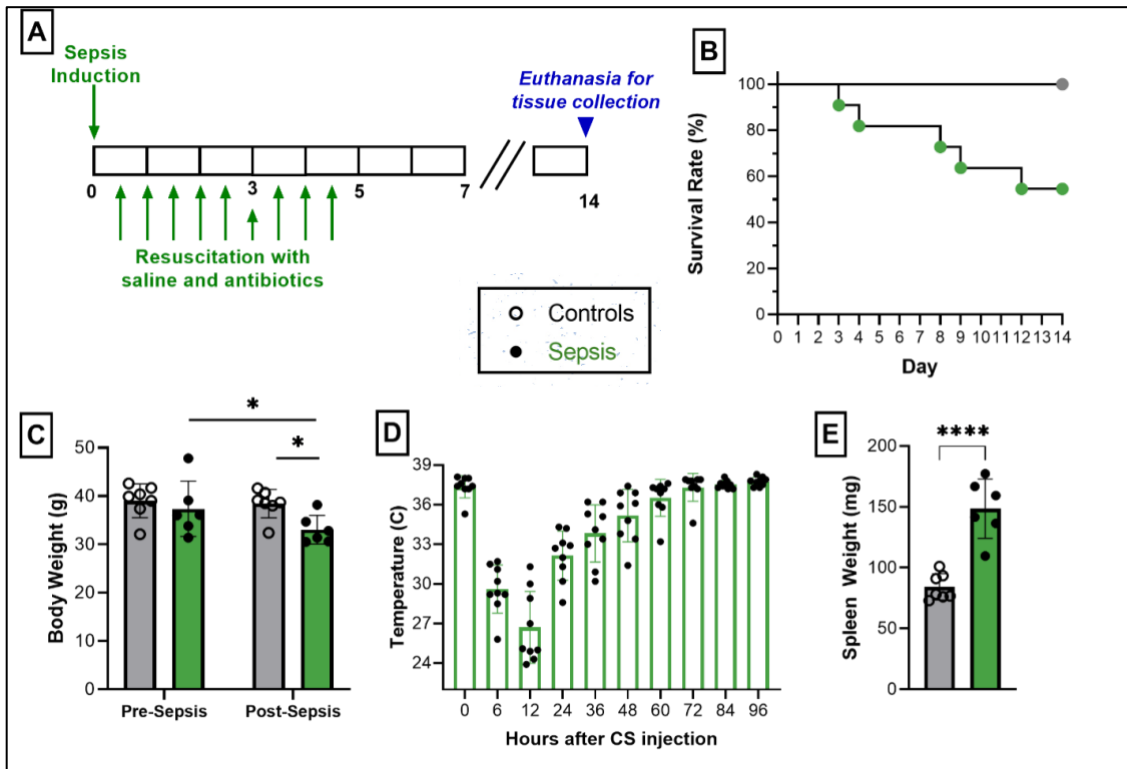
Figure 3-1 Cecal slurry induced severe sepsis in mice prior to euthanasia for bulk RNA sequencing.

(A) Sixteen-month-old C57BL/6 male mice were injected with cecal slurry to induce sepsis and 2x daily resuscitation began at 12h. Two weeks after sepsis induction, hindlimb skeletal muscles, spleens, and blood were harvested. (B) Survival curve showing 58% of mice survived sepsis (C) Sepsis survivors suffering 5% average body weight loss and non-sepsis controls exhibiting no change. (D) Sepsis survivors suffered severe hypothermia but recovered to baseline body temperatures as measured with a rectal probe within 96h. (E) Sepsis survivors demonstrated severe splenomegaly with significantly larger spleens than non-sepsis controls. * indicates p≤0.05, **** indicated p ≤ 0.0001

Upon principal component analysis (PCA) to evaluate correlation across the samples, it was clear that sepsis significantly altered the transcriptome. Samples clustered based on sepsis or non-sepsis status as shown in figure **3.2**. After DESeq2 analysis, there were 85 differentially expressed genes (DEGs) (p-adj < 0.05), 57 of which were upregulated and 28 of which were downregulated. Heatmap analyses revealed a clear clustering of mitochondria-related genes being limited after sepsis. Out of the 28 downregulated genes, 11 were mitochondrially encoded (**Figure 3.3**). While 37 genes are encoded by the mitochondrial genome, only 11 were probed for and detected by Novogene during library creation and sequencing. Upregulated genes related to glycolytic processes and muscle tissue itself, a trend that was confirmed through pathway analyses.

To better visualize post-sepsis transcriptome changes, DEGs were subjected to pathway analysis to see which GO: Biological Processes (GO:BP), GO: Molecular Function (GO:MF), GO: Cellular Component (GO:CC), and KEGG, pathways were up- and downregulated after sepsis (**Figures 3.4-3.7**, details in **Table 3.1**). Notably, processes related to mitochondria, the TCA cycle, and oxidative phosphorylation were all significantly downregulated. Countering this, glycolytic processes were upregulated. Most of the upregulated pathways relate to muscle function, indicating that damage occurs early during sepsis as expected. Out of the top 10 downregulated pathways, 5 relate directly to mitochondria, with the top downregulated GO: Cellular Component (GO:CC) term being the organelle itself ("mitochondrion"). Top upregulated GO:CC pathways favored muscle related terms (**Figure 3.5**). Notably, none of the upregulated pathways related to persistent inflammation, oxidative stress, or altered neuromuscular junction function. GO:BP (**Figure 3.4**) and GO:MF (**Figure 3.6**) analyses confirmed these trends with oxidative metabolism and mitochondria related terms being downregulated and muscle function, myofilament regulation, and glycolytic processes being upregulated.

A

B
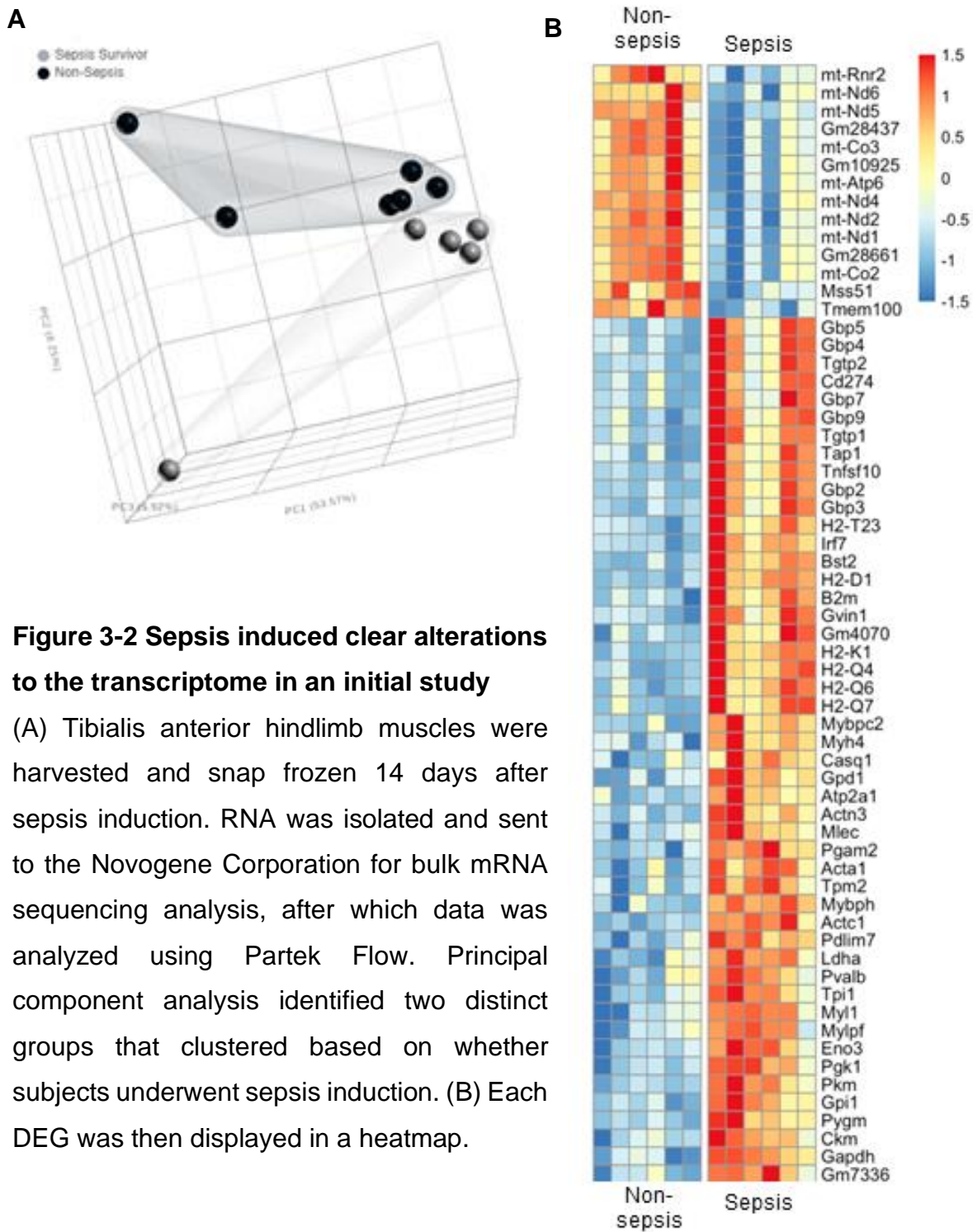
Figure 3-2 Sepsis induced clear alterations to the transcriptome in an initial study

(A) Tibialis anterior hindlimb muscles were harvested and snap frozen 14 days after sepsis induction. RNA was isolated and sent to the Novogene Corporation for bulk mRNA sequencing analysis, after which data was analyzed using Partek Flow. Principal component analysis identified two distinct groups that clustered based on whether subjects underwent sepsis induction. (B) Each DEG was then displayed in a heatmap.

41
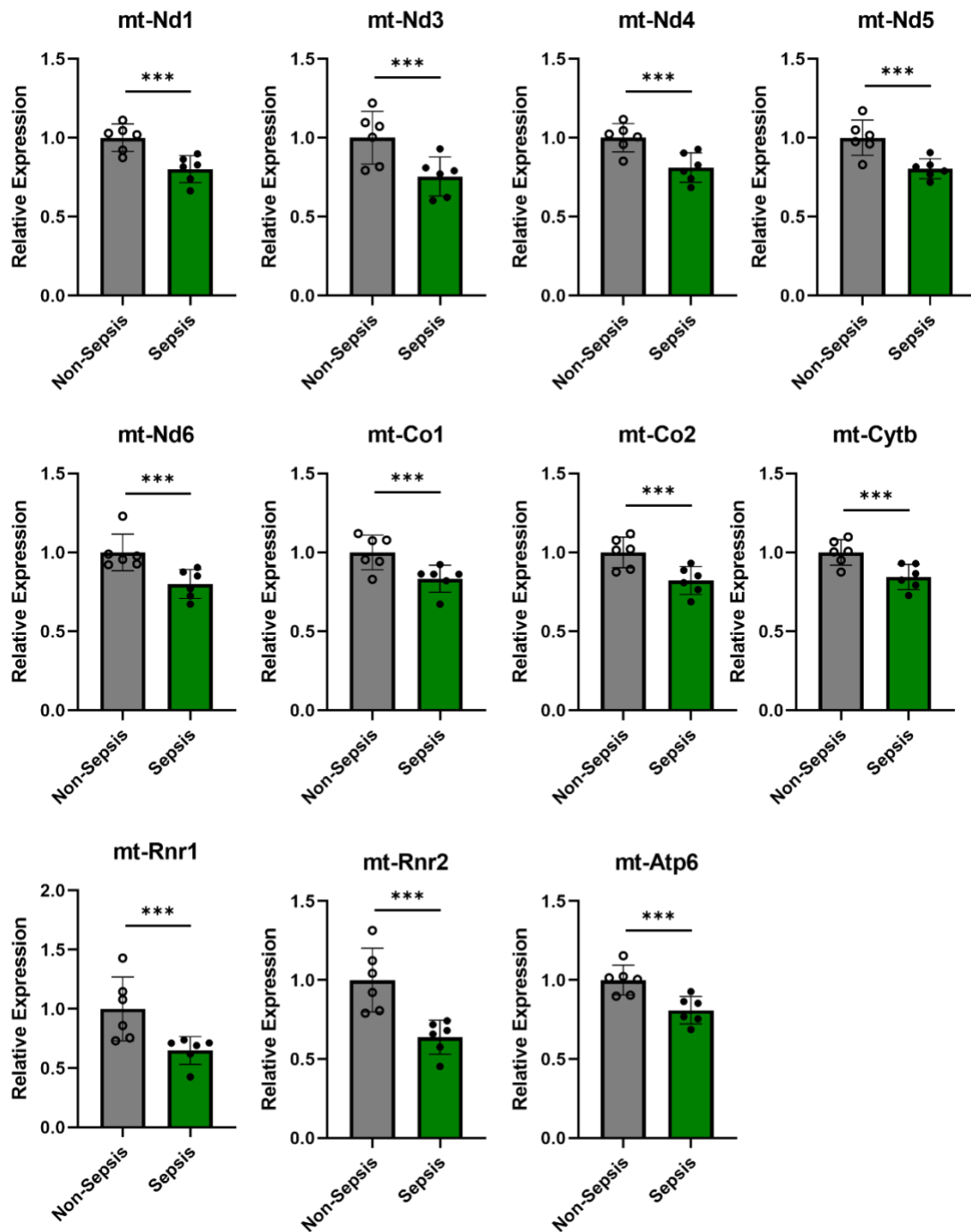
Figure 3-3 Mitochondrial encoded genes are downregulated in the tibialis anterior following sepsis recovery. Out of the 11 probed mitochondrially encoded genes, all were downregulated following experimental sepsis. *** indicates adj p-value ≤0.001

GO: Biological Processes pathways
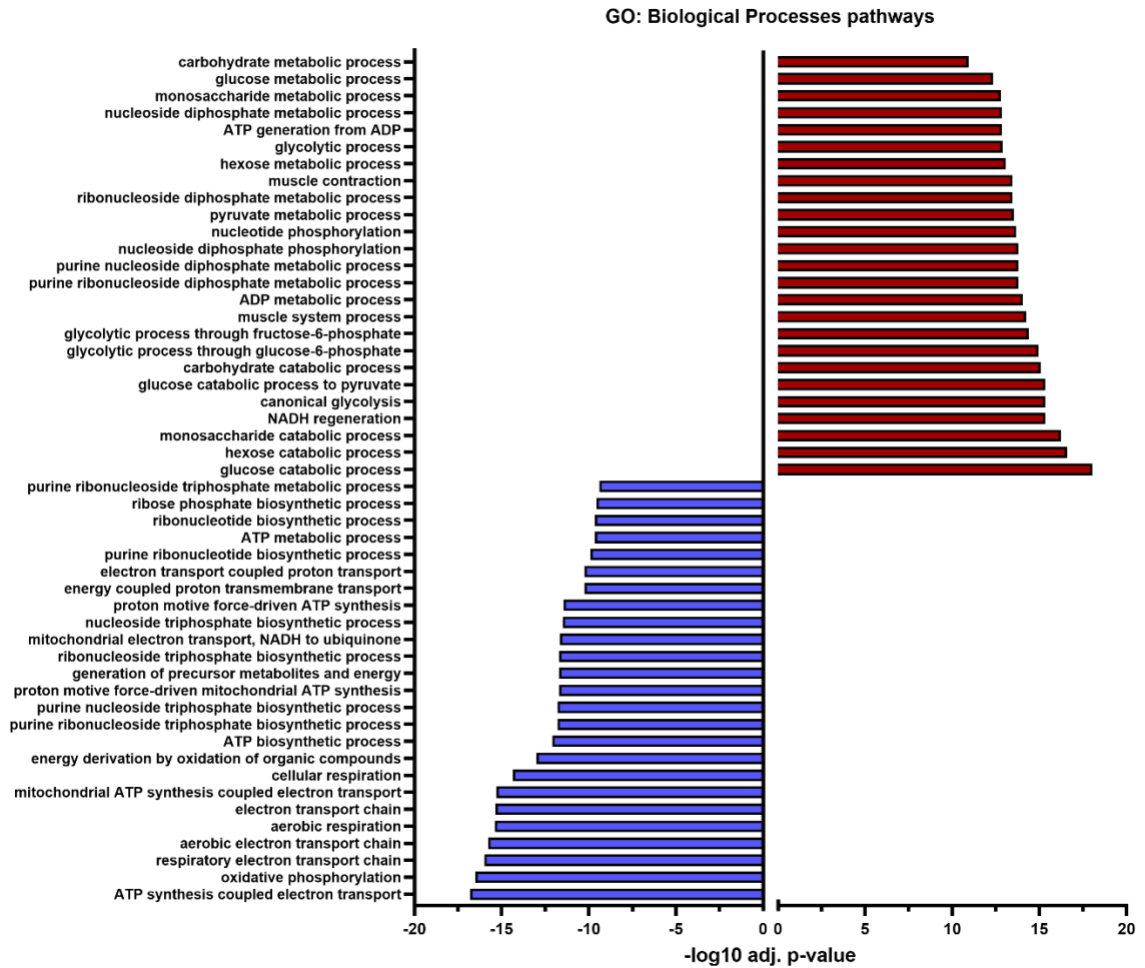
Figure 3-4 Top 25 up/down-regulated GO: Biological Processes Pathways.

All up/down regulated genes were entered into gProfiler for pathway analysis. Significant threshold for altered pathways were set based on a Benajmini-Hochberg FDR value under 0.05.
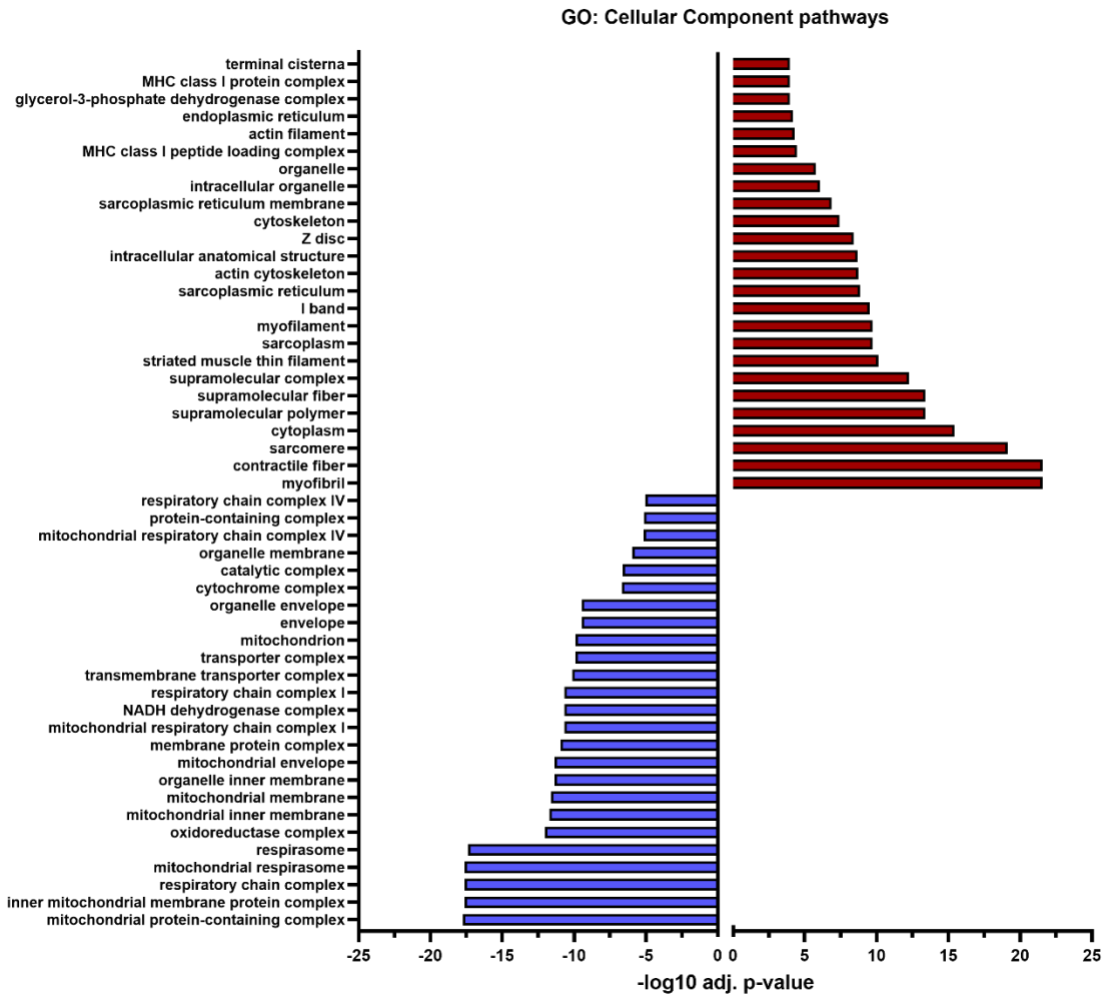
Figure 3-5 Top 25 up/down-regulated GO: Cellular Component Pathways.

All up/down regulated genes were entered into gProfiler for GO:CC pathway analysis. Significant threshold for altered pathways were set based on a Benajmini-Hochberg FDR value under 0.05.

GO: Molecular Function Pathways
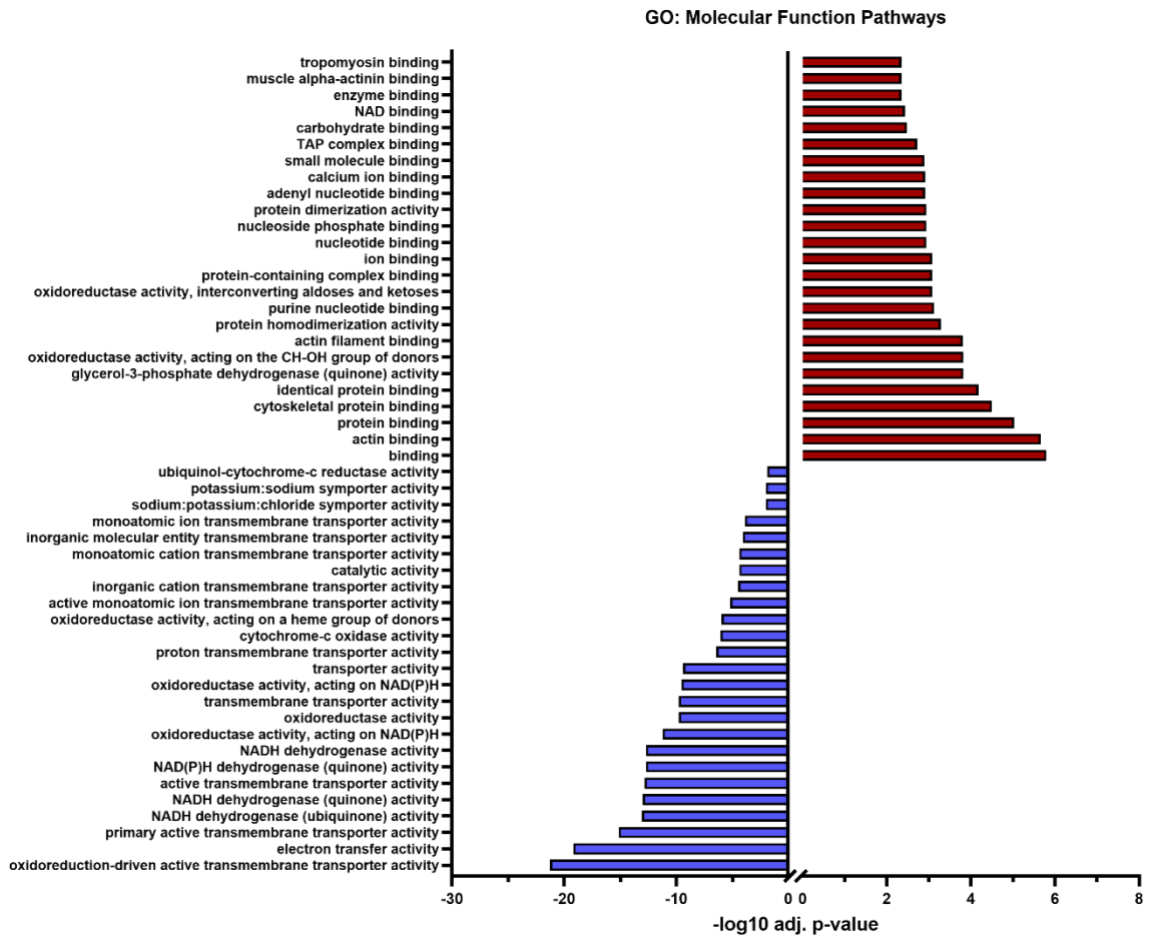
Figure 3-6 Top 25 up/down-regulated GO: Molecular Function Pathways.

All up/down regulated genes were entered into gProfiler for GO:MF pathway analysis. Significant threshold for altered pathways were set based on a Benajmini-Hochberg FDR value under 0.05.
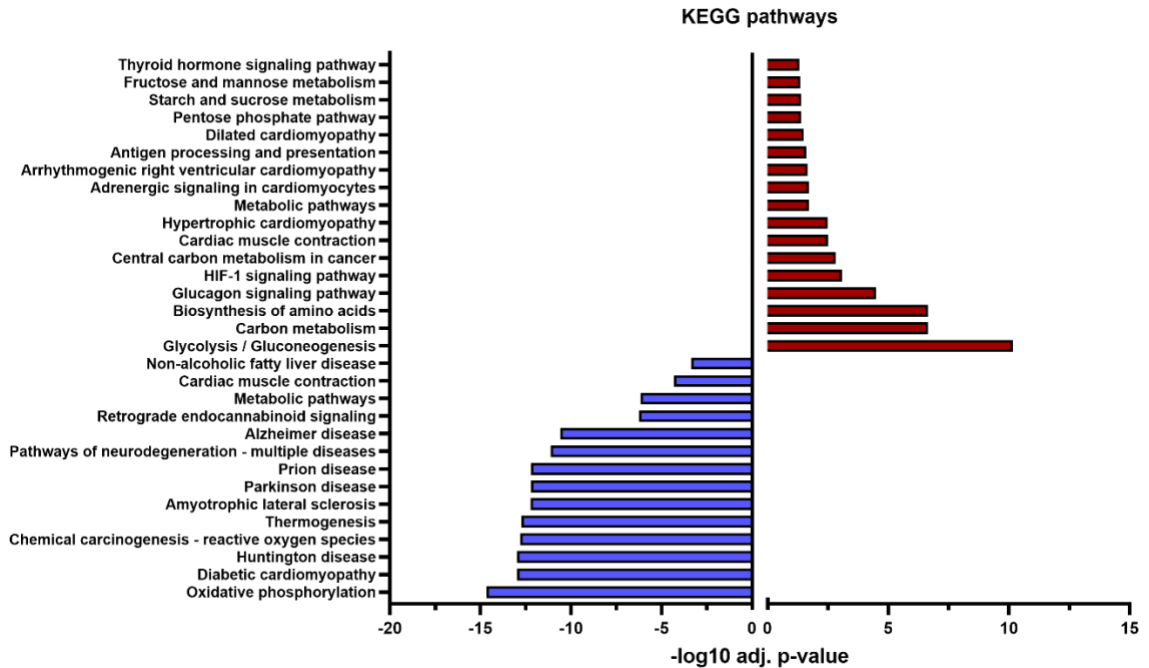
KEGG pathways

Figure 3-7 Top 25 up/down-regulated KEGG Pathways.

All up/down regulated genes were entered into gProfiler for KEGG pathway analysis. Significant threshold for altered pathways were set based on a Benajmini-Hochberg FDR value under 0.05.

Table 3.1 GO: Cellular Component pathways altered by sepsis

		Pathway	Term ID	Adj P-value	Neg. Log10 Adj P-value
Day 14 Post-Sepsis: GO:CC pathways	UPREGULATED	myofibril	GO:0030016	3.64E-22	21.43900858
		contractile fiber	GO:0043292	3.84E-22	21.41572757
		sarcomere	GO:0030017	9.44E-20	19.02482714
		cytoplasm	GO:0005737	4.01E-16	15.39711932
		supramolecular polymer	GO:0099081	3.57E-14	13.4473189
		supramolecular fiber	GO:0099512	3.57E-14	13.4473189
		supramolecular complex	GO:0099080	4.80E-13	12.31906613
		striated muscle thin filament	GO:0005865	8.10E-11	10.09147391
		myofilament	GO:0036379	2.16E-10	9.665962078
		sarcoplasm	GO:0016528	2.16E-10	9.665962078
	DOWNREGULATED	mitochondrial protein-containing complex	GO:0098798	1.92E-18	17.71660477
		inner mitochondrial membrane protein complex	GO:0098800	2.76E-18	17.55970007
		mitochondrial respirasome	GO:0005746	2.76E-18	17.55970007
		respiratory chain complex	GO:0098803	2.76E-18	17.55970007
		respirasome	GO:0070469	4.77E-18	17.32161726
		oxidoreductase complex	GO:1990204	1.09E-12	11.96384405
		mitochondrial inner membrane	GO:0005743	2.21E-12	11.65483361
		mitochondrial membrane	GO:0031966	2.65E-12	11.57642281
		organelle inner membrane	GO:0019866	5.13E-12	11.2901475
		mitochondrial envelope	GO:0005740	5.13E-12	11.2901475

To evaluate if transcriptional changes led to protein expression changes, I carried out a Western blot probing for complexes I-V of the electron transport chain. After normalizing to total protein, complexes I and II demonstrated significant decreases 14 days after sepsis in these samples (**Figure 3.8**). Expression was reduced more than 50% after sepsis survival, indicating the illness induces significant mitochondrial abnormalities.
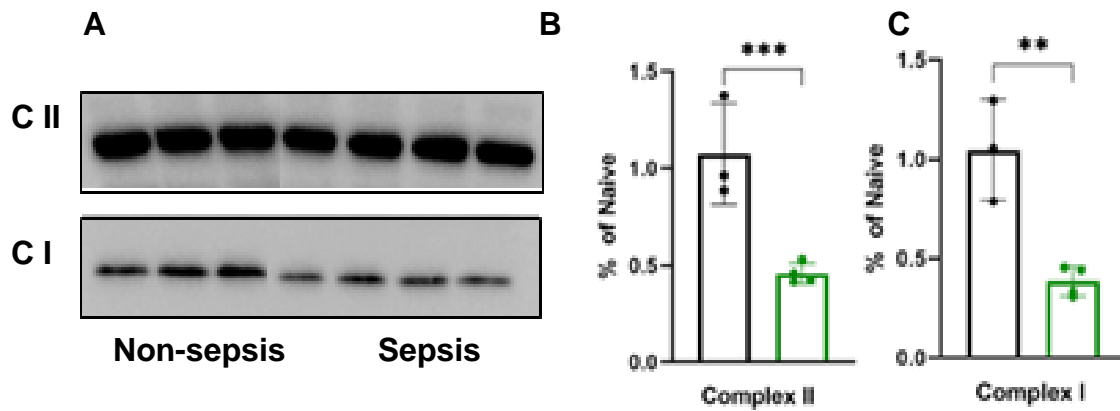
Figure 3-8 Complexes I (bottom) and II (top) were reduced following sepsis.

(A) Western blot of Complexes III (top) and (I) bottom were evaluated in non-sepsis samples (left four lanes) and sepsis survivors (right four lanes). Following normalization total protein, quantification of the relative expression as compared to non-sepsis/naïve samples is shown for complex II **(B)** and complex I **(C)**.

3.4.2 Muscle function progressively worsens as a result of sepsis.

To determine how sepsis alters skeletal muscle function over time, we utilized an *in vivo* plantar flexion function testing protocol before, during, and after sepsis (**Figure 3.9A**). After ensuring all animals had equivalent pre-sepsis body weights (**Figure 3.9B**), mice were subjected to baseline testing prior to sepsis induction. Following sepsis induction (i.p. injection with 350uL of cecal slurry (CS 210615)), mice developed severe hypothermia within 6 hours which persisted through hour 24 prior to returning to normal, pre-sepsis level body temperatures (**Figure 3.9C**). Mice received resuscitation with saline and antibiotics beginning at 12 hours after CS injection which continued 2x daily through hour 108. During acute sepsis (day 3-4), mice were again subjected to function testing, and peak isometric tetanic plantar flexor torque was 44.1% less than the pre-sepsis baseline levels (p=0.005) (**Figure 3.9E**). This finding was expected, as atrophy is severe at this stage and likely contributes to significant muscle weakness during the acute

phase of sepsis. Upon completion saline and antibiotic resuscitation, all the mice had recovered from sepsis as noted by a lack of hypothermia (**Figure 3.1C**).

After recovery from sepsis, mice were subjected to another round of function testing on day 14. Opposite of my hypothesis that function would increase from day 4 to day 14 without returning to pre-sepsis levels, peak torque had further decreased another 46.4% ($p = 0.033$) (**Figure 3.1E**). This means function deficits increased *after* resolution of sepsis and acute phase associated atrophy. Further, upon long-term testing, function had not recovered even 10 weeks after sepsis (day 70), with average peak torque was still being decreased 48.8% compared to pre-sepsis function. Progressive weakness occurs from day 3 through at least day 14 and persists for another two months thereafter, imparting significant chronic deficits to sepsis survivors. These data demonstrating decreasing function at day 3 after sepsis and further functional decline at day 14 indicate sepsis-induced muscle weakness begins during acute sepsis and progressively worsens through at least day 14.
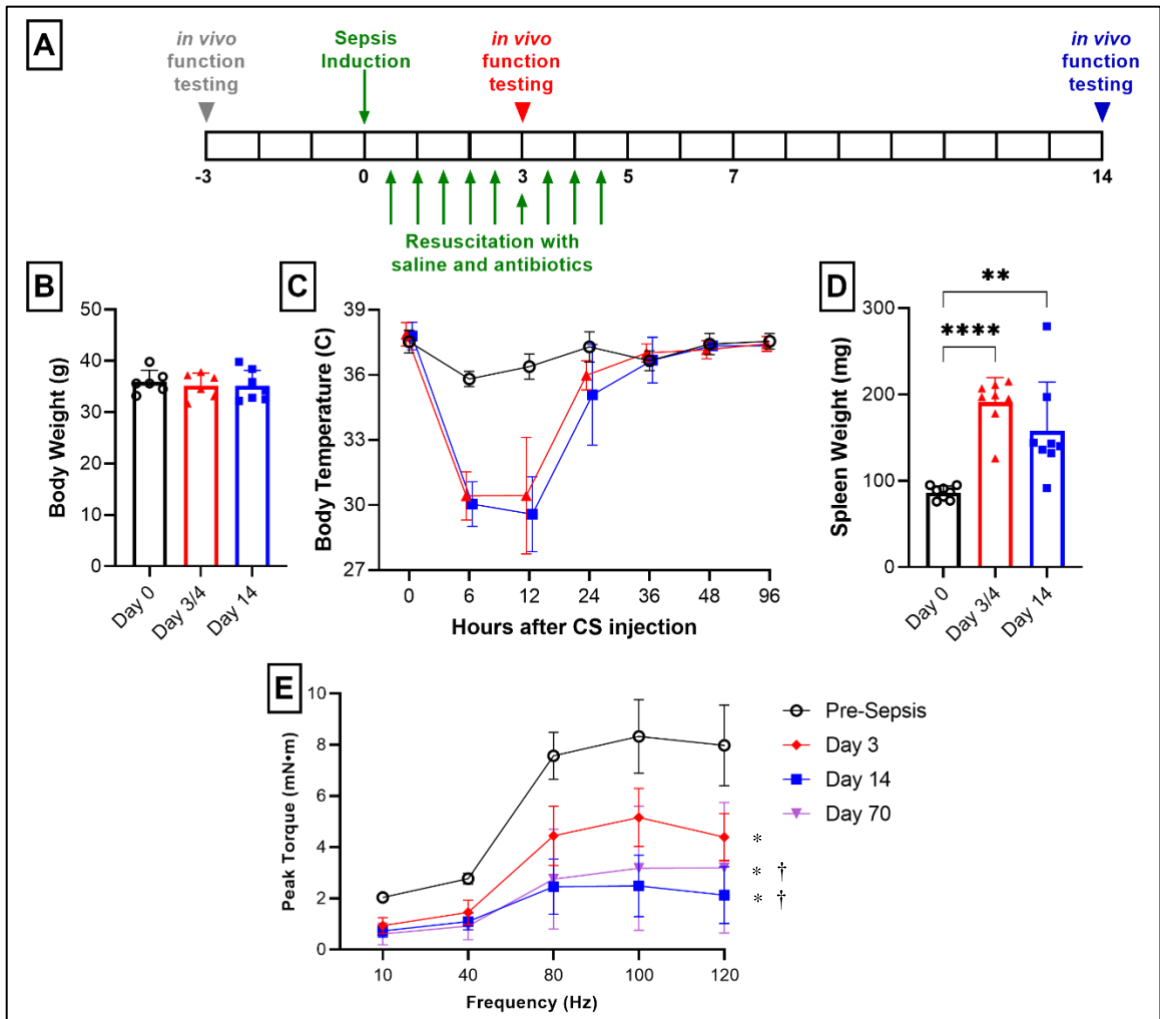
Figure 3-9 Muscle weakness develops in a progressive manner after sepsis.
(**A**) Function testing throughout sepsis paradigm. (**B**) Body weights of all mice were equivalent prior to sepsis induction. (**C**) Mice injected with CS developed severe hypothermia within six hours and remained lower than normal through at least hour 24 prior to returning to their pre-sepsis body temperatures. (**D**) Upon euthanasia, spleen weight was collected to evaluate sepsis severity. Sepsis mice suffered severe splenomegaly that did not resolve by day 14. (**E**) *In vivo* function testing revealed function deficits appear by day 3 post-sepsis and increase through at least day 14. Despite long term recovery from sepsis, functional deficits persist at day 70 after CS injection. The mice tested were the same across each timepoint. * indicates significant difference from pre-sepsis levels, † indicates difference from day 3 function levels.

3.4.3 Histological and biochemical changes occur progressively after sepsis.

Mice were subjected to severe sepsis and euthanized on days 0, 4, and 14 as outlined in **Figure 3.9A**. Hindlimb muscles were collected for histological and biochemical analyses to evaluate changes over sepsis pathogenesis. TA muscles were sectioned and stained for fiber-type distribution and fiber-type specific cross-sectional area (CSA). Mice demonstrate a decrease in mean CSA during acute sepsis (day 4), though by day 14, CSA was no different from pre-sepsis levels (day 0) (**Figure 3.10**).
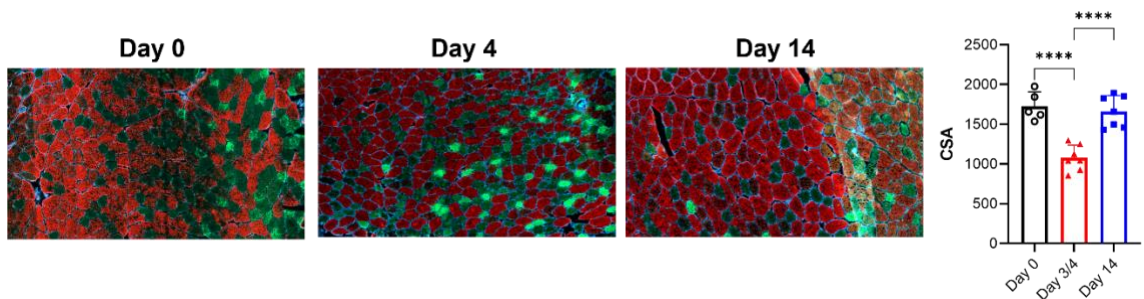
Figure 3-10 Sepsis induces atrophy during the acute phase that resolves in tandem with sepsis resolution.

Serial sections of the tibialis anterior were stained for fiber type and then run through MyoVision 2.0 for cross sectional area analyses. There were no differences between days 0 and 14, while atrophy was apparent at days 3-4. CSA of each individual fiber type was not obtained, though these samples could be run again for fiber type specific distribution.

Histological staining was also performed on these timepoint samples. NADH staining for mitochondrial complex I and SDH staining for mitochondrial complex II revealed progressive decreases in staining intensity from day 4 to 14 as shown in **Figure 3.11**.
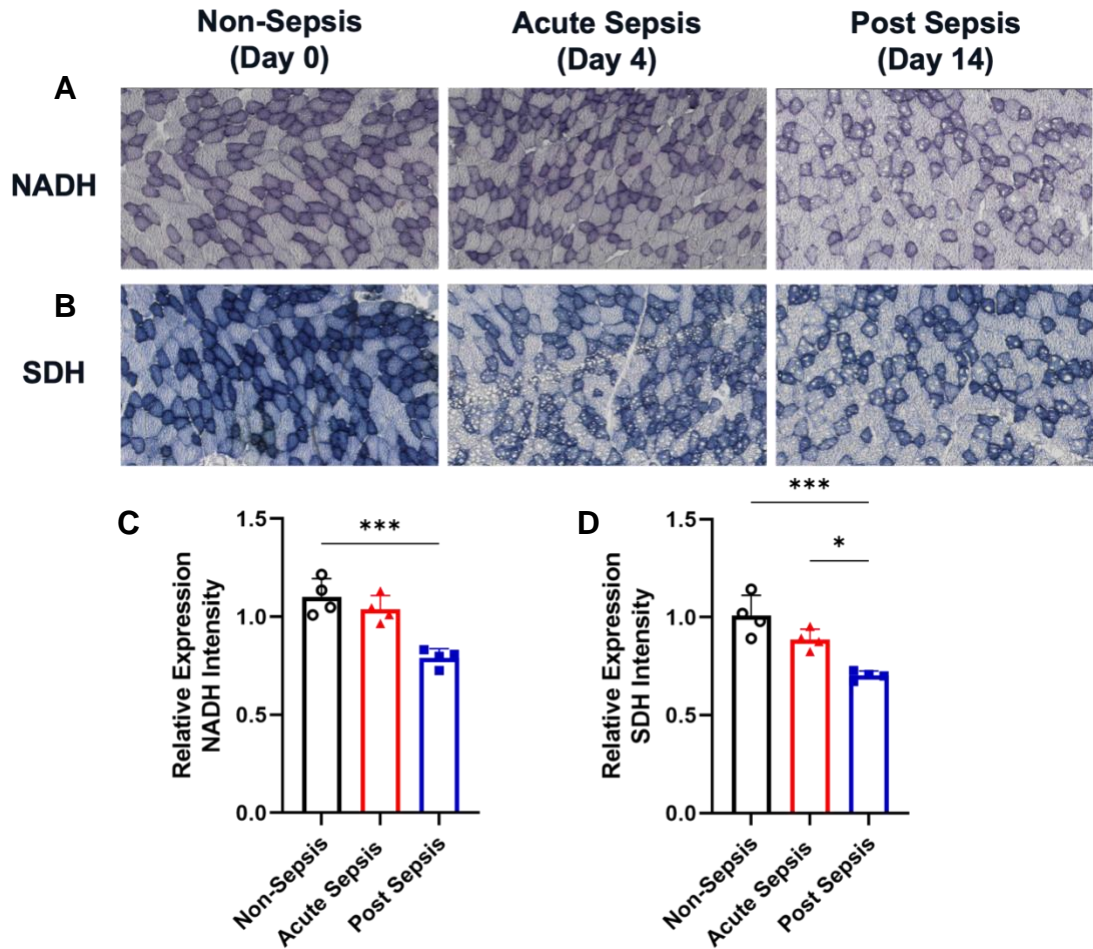
Figure 3-11 Histological changes occur progressively throughout sepsis.
NADH (**A**) and **(B)** SDH staining for enzyme activity of complexes I and II are shown at days 0, 4, and 14 in representative images. Quantification (n=4 per group) of NADH staining intensity **(C)** reveals staining intensity does not decrease until day 14, while SDH staining intensity quantification **(D)** indicates a progressive change in intensity after sepsis.

Protein markers of mitochondrial complexes I-V revealed time dependent changes as a result of sepsis, as well. While protein levels for markers of complexes I, II, IV, and V were depressed at day 4, they were just as low, if not lower, by day 14, with exception to complex IV (**Figure 3.11**). Complex I demonstrated an 49.4% decrease at day 4, which further increased 5.5% by day 14 yet still remained 46.6% decreased compared to day 0. Complexes II had no significant changes, matching up with a lack of change in bulk RNA sequencing for complex II related proteins. Complexes III, IV, and V demonstrated decreases as a result of sepsis, dropping 32.7%, 48.4%, and 29.2% by day 4 and a total of 37.0%, 17.1%, and 31.2% by day 14, respectively. This indicates mitochondrial abnormalities occur by day 4 and remain through at least two weeks after CS injection, possibly developing in a progressive manner.
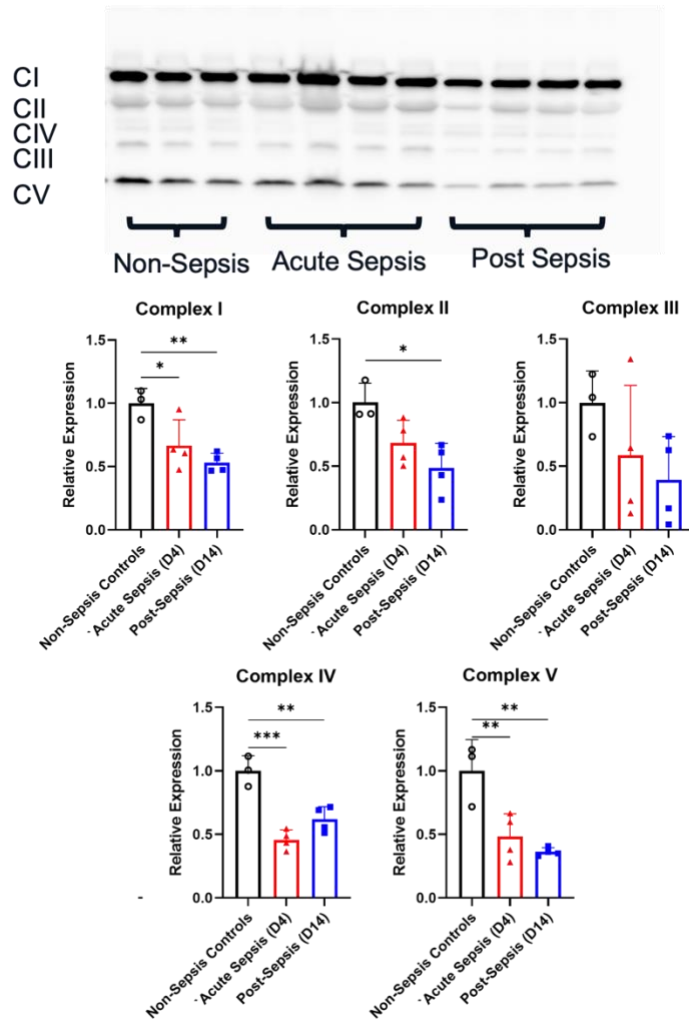
Figure 3-12 A time-course study revealed protein markers for complexes I-V follow similar trends to sequencing.

Similar to RNA sequencing trends, protein markers for complexes I, III-V reveal damage occurs by day 4. This damage that causes a decrease in protein expression does not resolve following the resolution of acute sepsis, meaning mitochondrial abnormalities persist long after sepsis. This also follows the decrease in function seen through *in vivo* function testing on days 0, 3, and 14.
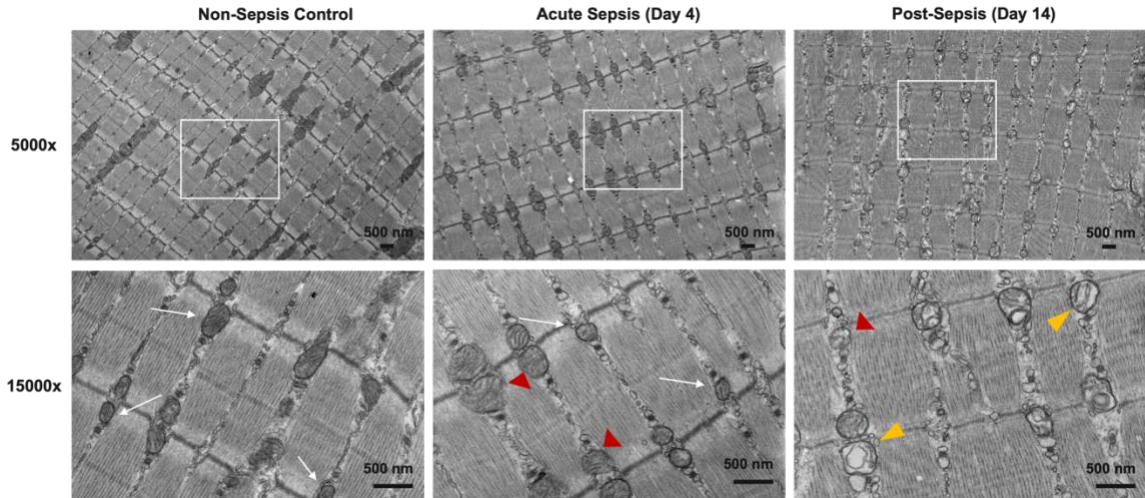
Figure 3-13 A time-course study revealed mitochondrial damage appears to be progressively developing.

While quantification was not able to be completed due to obtaining the images two days before my defense, representative images appear to show that mitochondrial damage accumulates progressively. White arrows indicate normally appearing mitochondria which are present in abundant numbers at days 0 and 4. Red arrowheads noting mitochondria with ruptured membranes begin to appear at day 4 and persist at day 14. Yellow arrowheads marking empty mitochondrial or organelles that have taken on a vacuole like structure (42) begin to appear at day 14. Together, these data indicate mitochondrial abnormalities appear to accumulate progressively, even after sepsis resolution.

To further investigate why function decreases from day 4 to day 14 after sepsis, we completed a second time-course study with euthanasia on days 0, 4, 14. Using the same animals from our sepsis experiment outlined in **Figure 3.8A**, we isolated RNA from the TA hindlimb muscle to evaluate transcriptomic changes over time. Initial principal component analysis revealed the samples clustered based on their groups (Day 0, 4, or 14) (**Figure 3.13**)

Day 4 sequencing indicated 2,318 genes were differentially expressed (adj P <0.05), with half (n=1160) of the DEGs being downregulated and the other 1,158 transcripts undergoing upregulation. These DEGs were then evaluated for pathway analysis as previously described. Day 4 analyses revealed mitochondrial downregulation is already occurring, as a majority of downregulated GO:CC terms related to mitochondrial cellular components.

Day 14 bulk mRNA sequencing was also performed, and at this timepoint, there were only 756 DEGs (368 upregulated, 359 downregulated) (**Figure 3.9)**. Out of these 756 DEGs, only 213 were common amongst days 4 and 14, indicating the resolution of 2,065 DEGs by the two-week mark. This also indicates that 513 DEGs appear after resolution of acute sepsis. These genes were then subjected to multiple pathway analyses. All 756 DEGs were subjected to pathway analyses as shown in **Figure 3.14** through **3.22**). Here, it is clear that mitochondrial downregulation remains at day 14 while inflammatory processes are downregulated.
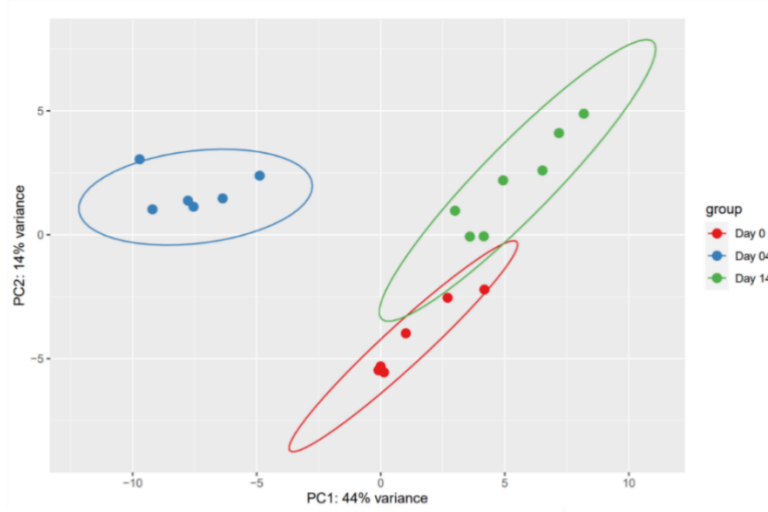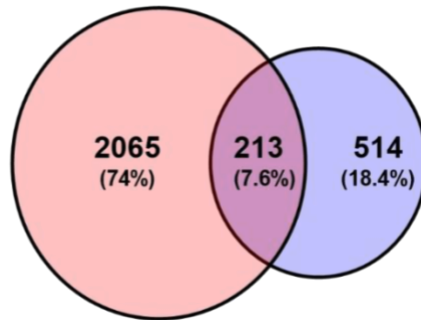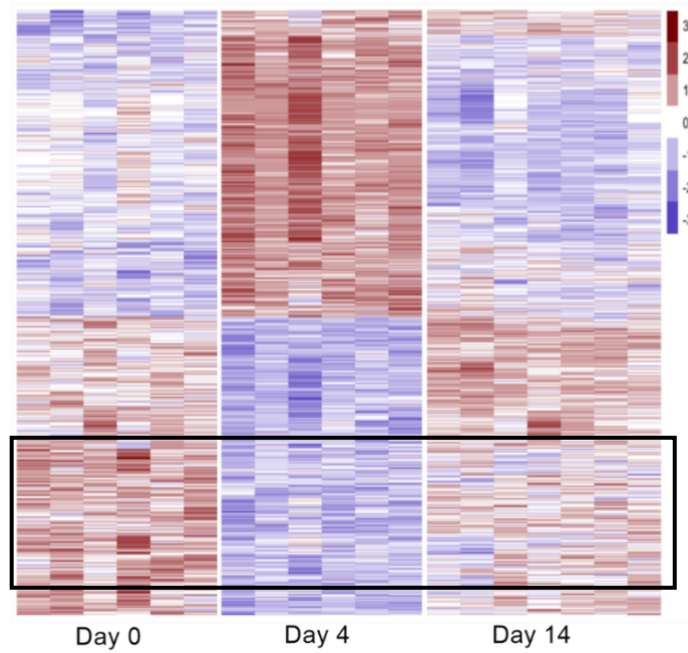
Figure 3-14 A time-course study revealed metabolism-related changes persisted after the resolution of inflammation-related alterations.

(A) PCA analyses revealed clear clustering of the different timepoints at days 0, 4, and 14, with days 0 and 14 appearing more similar than day 4. **(B)** Differentially expressed genes (DEGs) from days 4 and 14 are shown on the left and right, respectively, with DEGs overlapping across both timepoints being shown in the middle of the Venn diagram. **(C)** Heatmap of the DEGs indicates significant resolution of inflammatory and oxidative stress related genes. The box indicates that several mitochondria-related genes remained downregulated at day 14.
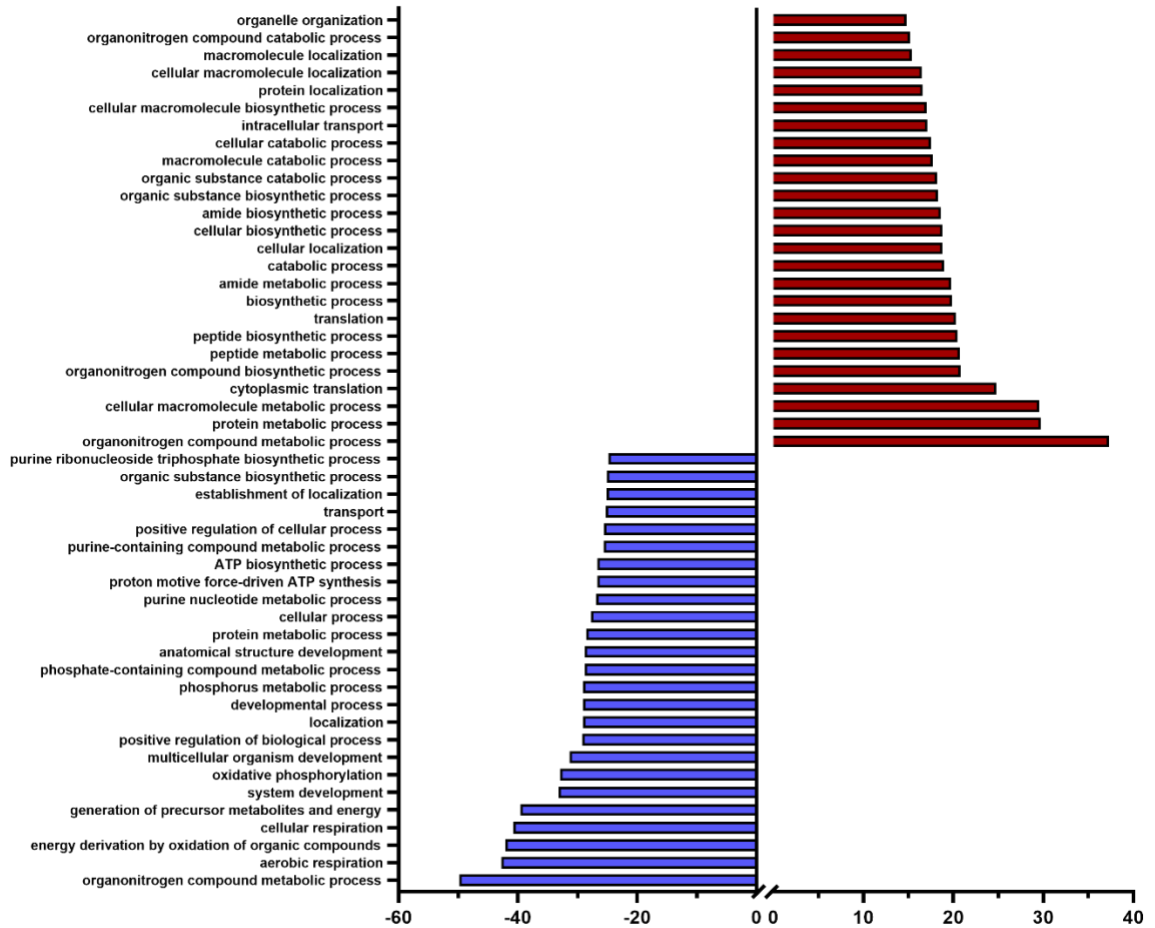
Figure 3-15 Altered GO: BP processes at day 4 of sepsis.

GO: Biological Processes pathways that were altered during acute sepsis emphasized that mitochondrial changes are already occurring as emphasized by the downregulated terms. Upregulated terms emphasize that catabolic processes are occurring, likely contributing to acute phase atrophy.
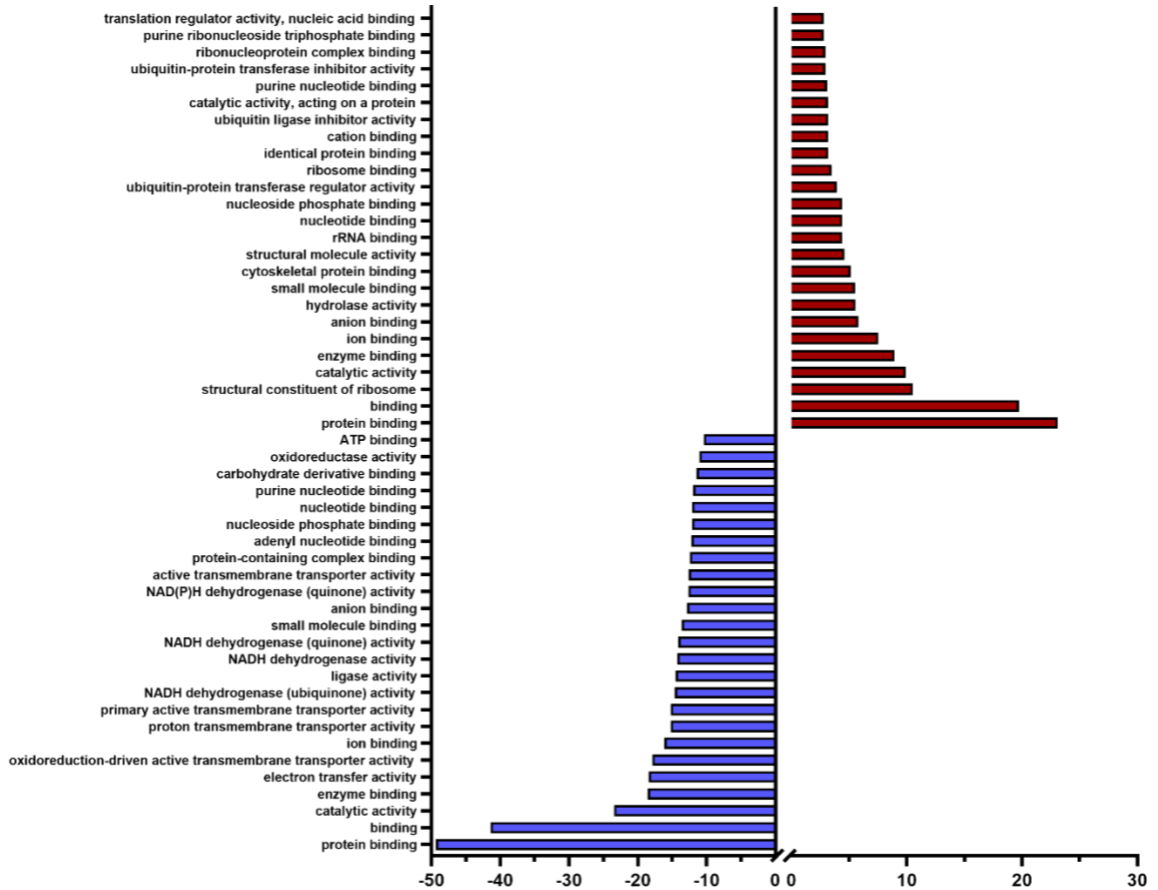
Figure 3-16 Altered GO: MF processes at day 4 of sepsis.

GO: Molecular Function pathways that were altered during acute sepsis emphasized complex I activity is significantly altered early on. This is indicated by all the downregulated terms containing NADH dehydrogenase related terms. Binding activity is significantly upregulated at this time as well.
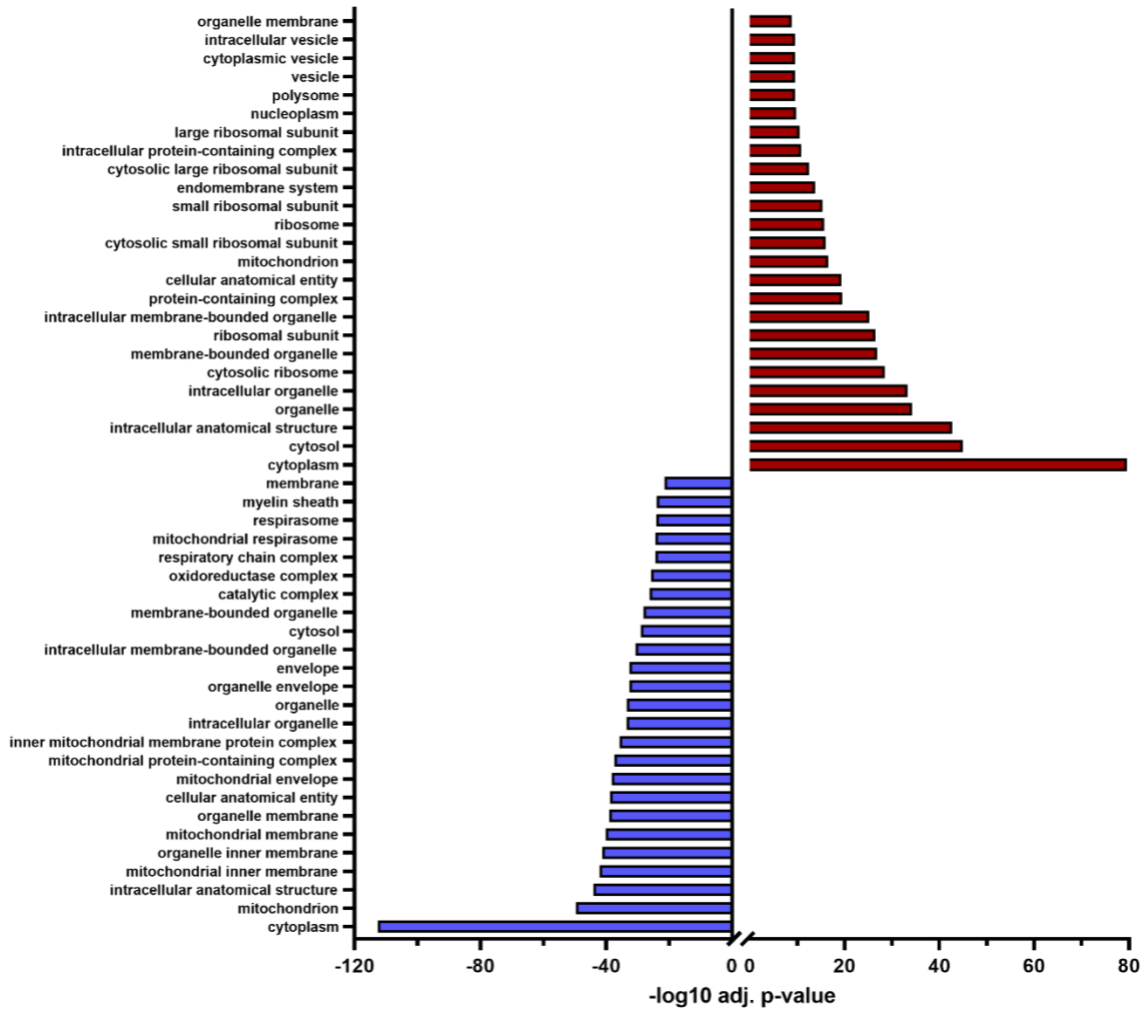
Figure 3-17 Altered GO: CC processes at day 4 of sepsis.

GO: Cellular Component pathways that were altered during acute sepsis emphasized significant mitochondrial alterations, as well as OxPhos related downregulation. Upregulated terms indicate significant changes to the cytoplasm and likely overall cell structure due to the large number of terms containing general organelle terms.
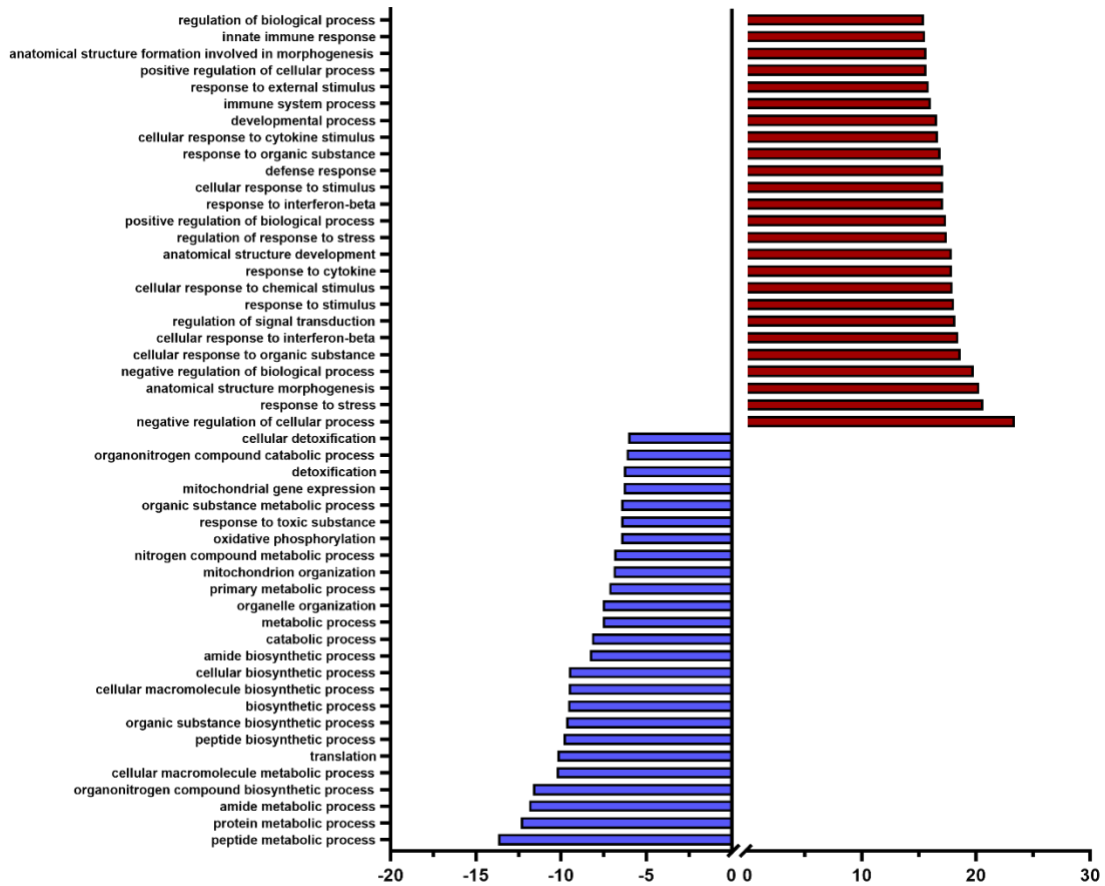
Figure 3-18 Altered GO: BP processes two weeks after sepsis.

GO: Biological Processes pathways that are altered two weeks after sepsis related overwhelmingly to metabolic processes, especially downregulated terms. Upregulated terms indicate lingering responses to external stimuli, though when looking at individual inflammatory and oxidative stress related genes, none are significantly upregulated.
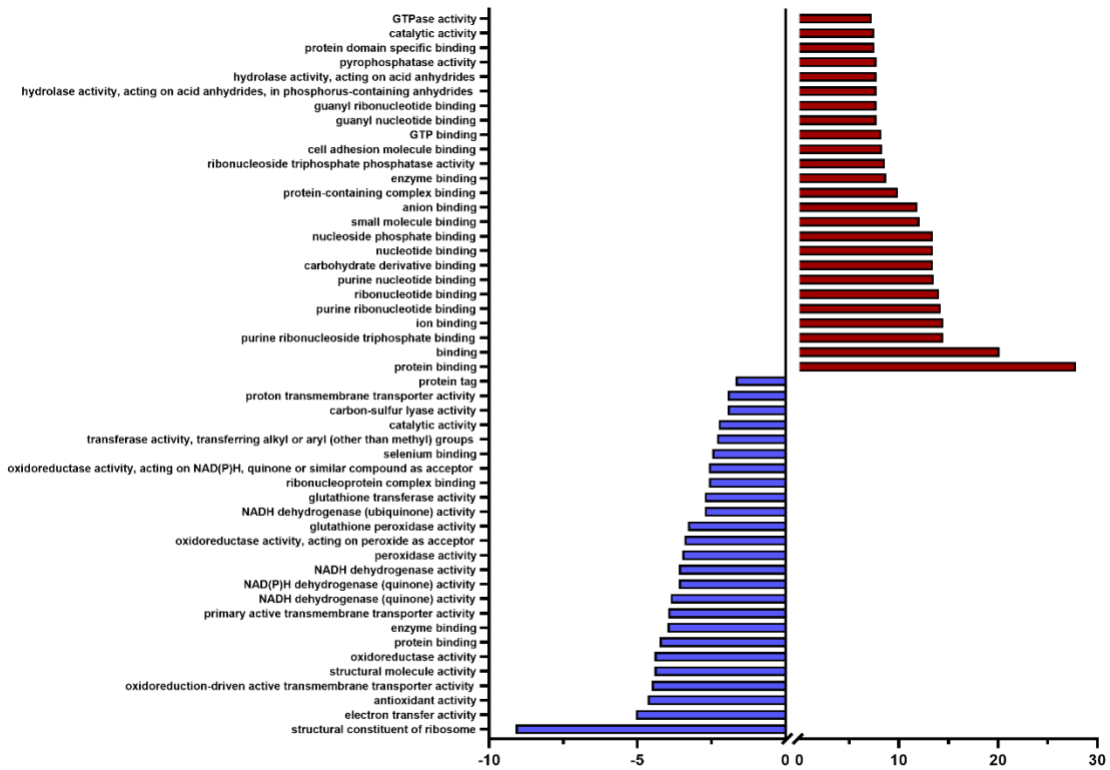
Figure 3-19 Altered GO: MF processes at 14 days after CS injection.

GO: Molecular Function processes two weeks after sepsis once again emphasize NADH dehydrogenase (and complex I) is significantly downregulated, similar to day 4. Upregulated terms emphasize GTPase activity and binding, as well as other binding processes, once again similar to day 4 changes.
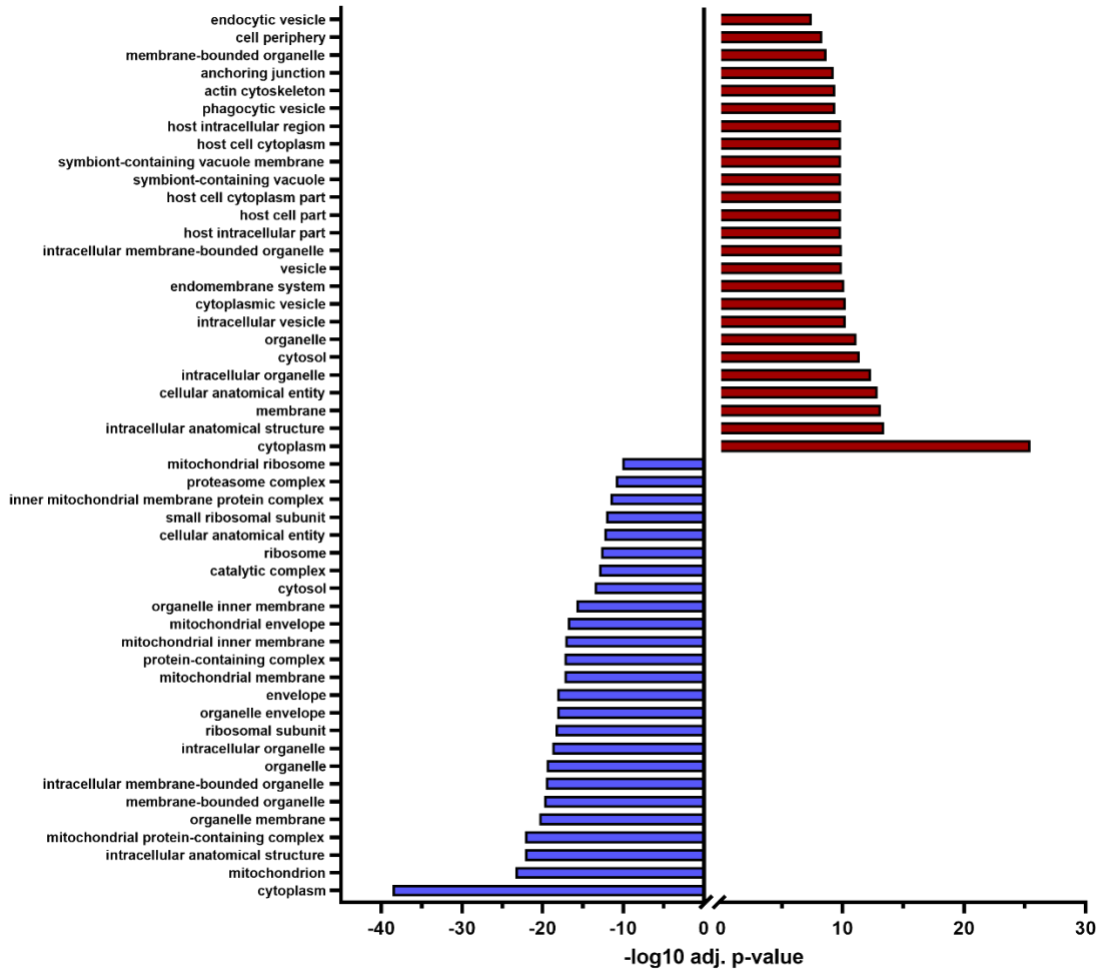
Figure 3-20 Altered GO: CC processes at day 14 of sepsis.

Downregulated GO: Cellular Component pathways 14 days after CS injection once again relate to mitochondrial processes. Upregulated pathways are similar to day 4 results.

Out of the day 4 and 14 DEGs, there were 213 altered transcripts that were common across both sequencing time points. These 213 common DEGs from days 4 and 14 were subjected to pathway analyses. Most of these terms related to mitochondria, emphasizing lasting changes occur at the transcriptomic level and do not recover in tandem with sepsis resolution. To investigate whether these 213 constant DEGs may be related to proteomic changes, trends from day 4 to 14 were evaluated. These genes followed one of four trends following sepsis: consistent downregulation (n=72), consistent upregulation (n=55), a change from up- to down-regulation (n=67), or down- to up-regulation (n=19). Genes that were constantly up- or down-regulated underwent pathway analyses (**Figure 3.20-3.22**).

For consistently upregulated genes, GO: BP pathways related mostly to regulation of metabolic processes and developmental pathways. Concurrently, GO:BP processes related to TCA related metabolism terms were consistently downregulated, emphasizing these changes occur early and persist throughout sepsis. GO:MF processes that remained upregulated throughout sepsis related to anhydrides and binding processes, while downregulated GO:MF pathways overwhelmingly contained terms related to NADH dehydrogenase activity. GO:CC terms that were always downregulated pertained to mitochondria for the most part, while upregulated terms related to synapses and neural processes. These data indicate mitochondria are significantly altered by sepsis, as emphasized by 10 of the 13 probed mitochondrial encoded genes were downregulated at day 4 and day 14, respectively.
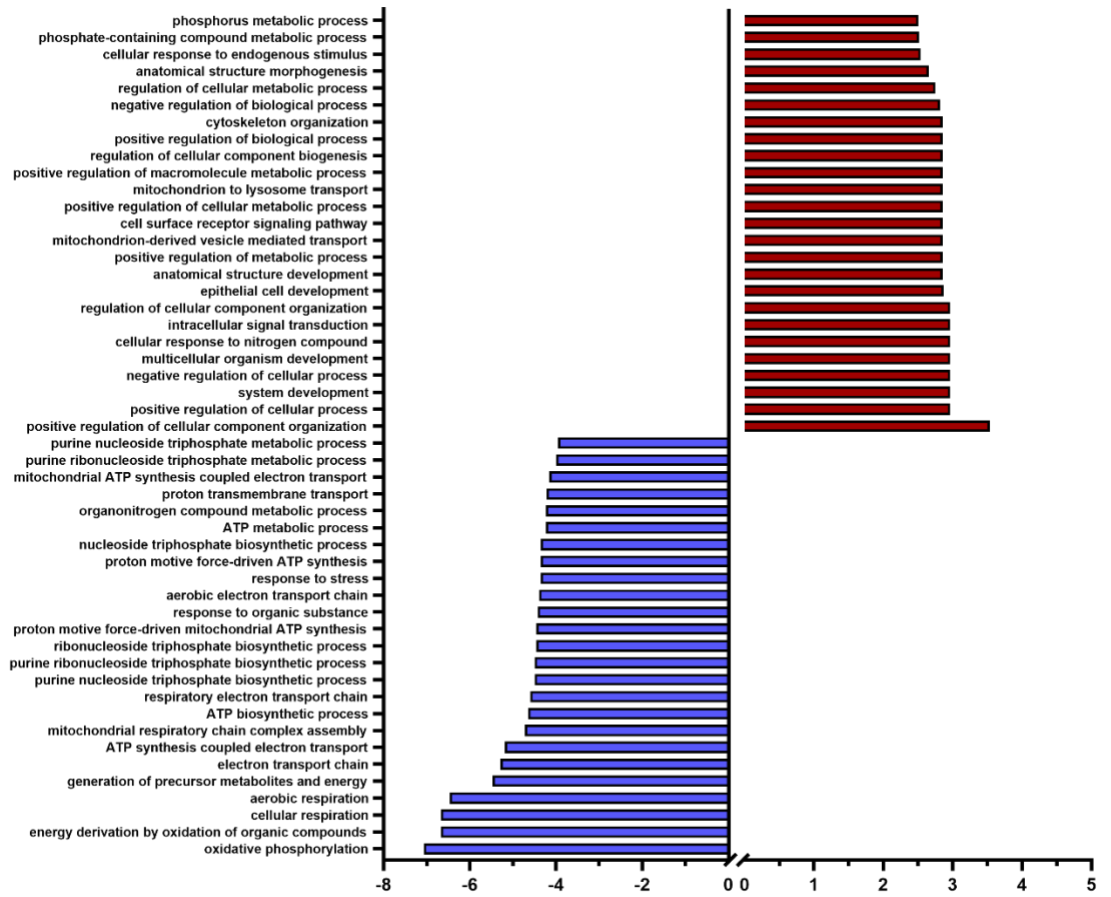
Figure 3-21 Consistently altered DEGs reveal metabolic changes persist throughout sepsis pathogenesis as indicated by altered GO:BP pathways.
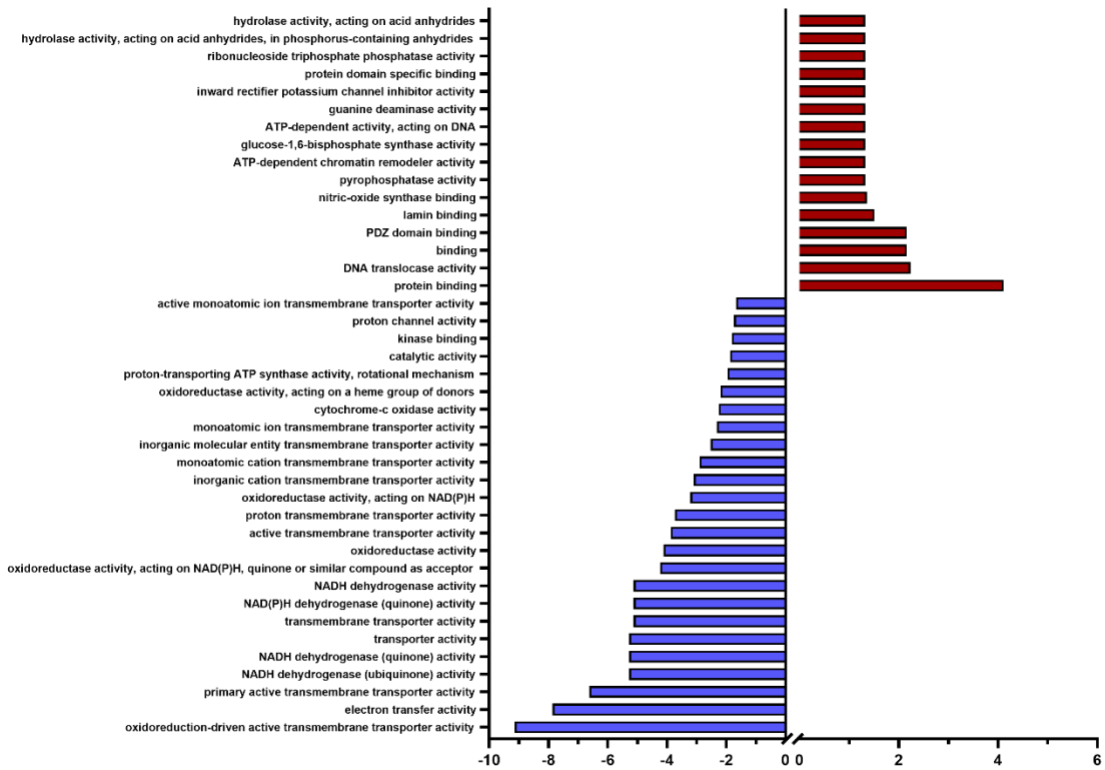
Figure 3-22 Constantly altered DEGs emphasize GO:MF changes relating to metabolic processes remain altered across sepsis induction and recovery.
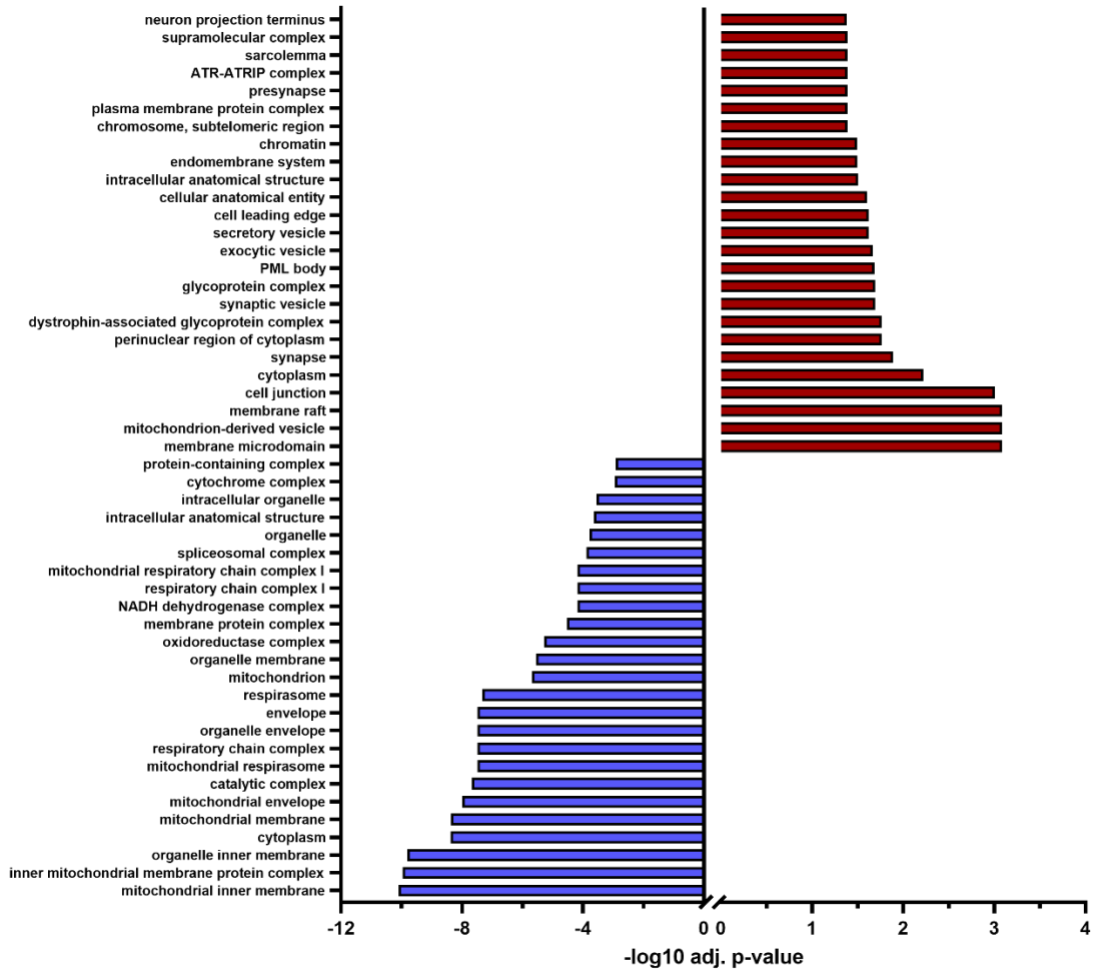
Figure 3-23 DEGs altered at days 4 and 14 reveal GO:CC pathways overwhelming relate to glycoproteins and mitochondria.

3.4.4 Sepsis induces metabolic changes in plasma

To evaluate if the changes we saw in the transcriptome matched up to changes in metabolite levels, we carried out metabolomics analysis on the major metabolites in glycolysis and the TCA cycle on the plasma of sepsis survivor and non-sepsis control mice (**Figure 3.23**). Nearly all the major metabolites were reduced in sepsis survivor plasma. Initial glucose input to split the molecule into two pyruvate molecules through glycolysis is significantly lower in sepsis survivors. Further, the output, either in the form of pyruvate or lactate, is decreased in sepsis survivors. As a result, input of pyruvate into the TCA cycle after conversion to Acetyl CoA is reduced, as are the major metabolites associated with the process (citrate, glutamate, fumarate, and malate). Together, these data indicate overall metabolic processes are blunted after sepsis.

Separate from analyses looking specifically at glycolysis and the TCA cycle, individual metabolites (**Figure 3.24**) that underwent significant change as a result of sepsis were subjected to pathway analyses. These analyses revealed both glycolysis/gluconeogenesis and the TCA cycle are significantly altered following sepsis, as are galactose metabolism, starch and sucrose metabolism, fatty acid biosynthesis, D-glutamine and D-glutamate metabolism, and nitrogen metabolism. The top 25 altered pathways are shown in **Figure 3.24**.
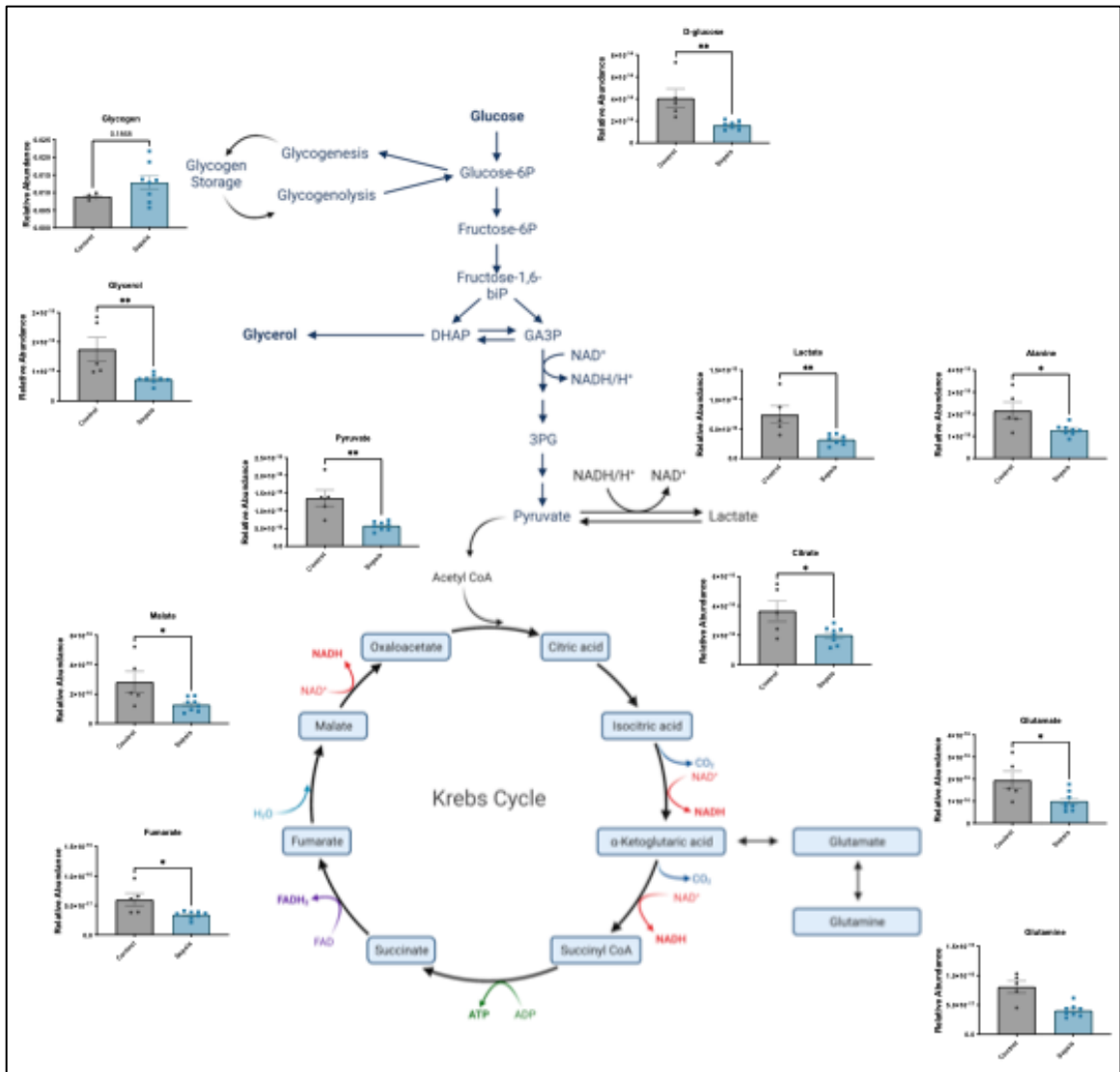
Figure 3-24 Sepsis causes changes in plasma metabolism up to two weeks after sepsis.

Following sepsis, plasma glucose was reduced, as were the end products of glycolysis pyruvate and lactate. Looking at the TCA cycle, sepsis caused reductions in plasma citrate, glutamate, fumarate, and malate. Glycogen was increased in sepsis surviving mice, and plasma glycerol, a byproduct of glycolysis, was decreased significantly.
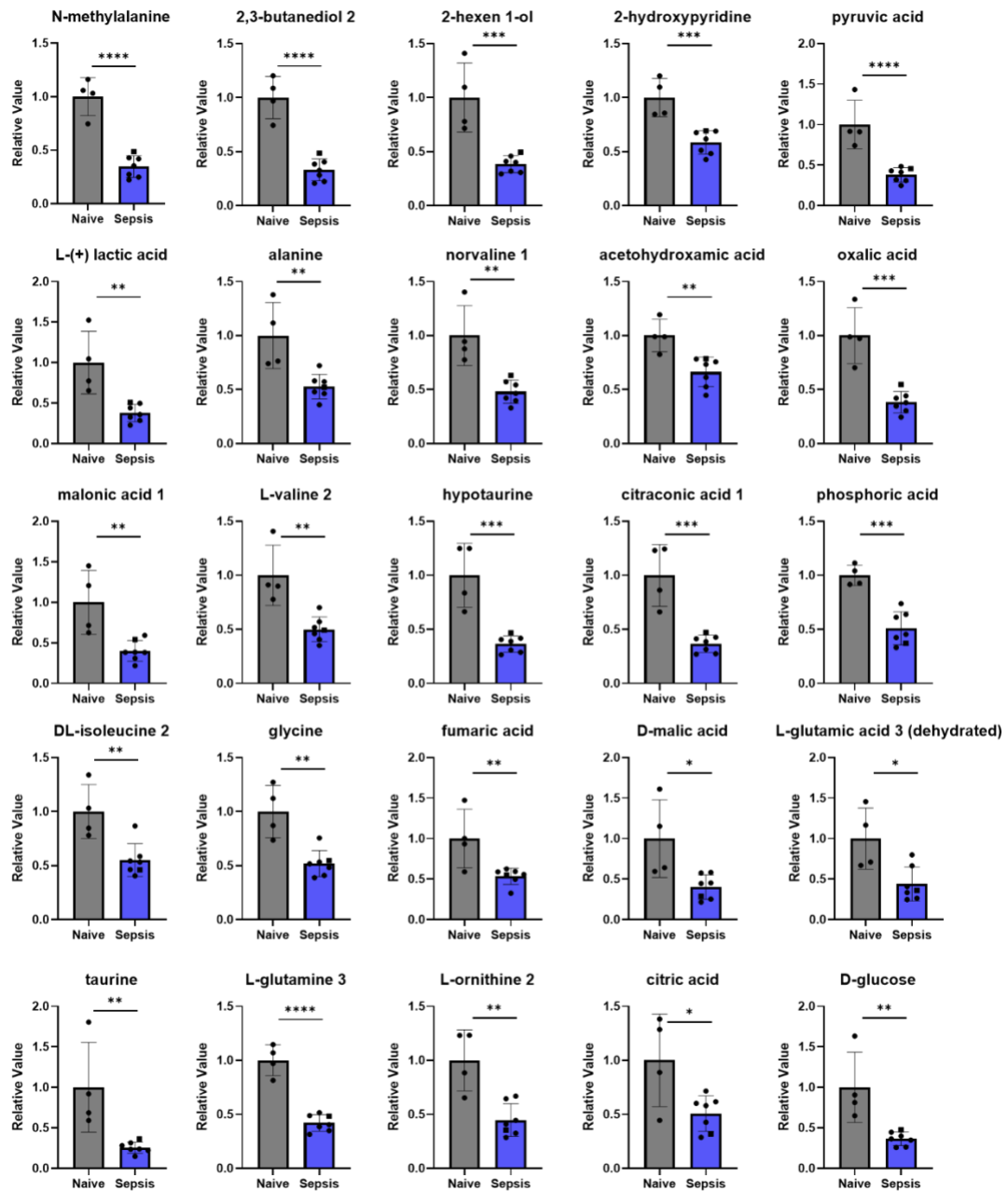
Figure 3-25 Plasma metabolites are downregulated after sepsis.

Individual metabolites indicate acute sepsis significantly alters long-term metabolic processes, even after recovery from the acute event. Metabolites with significant changes (as measured by student's t-test) are individually graphed.
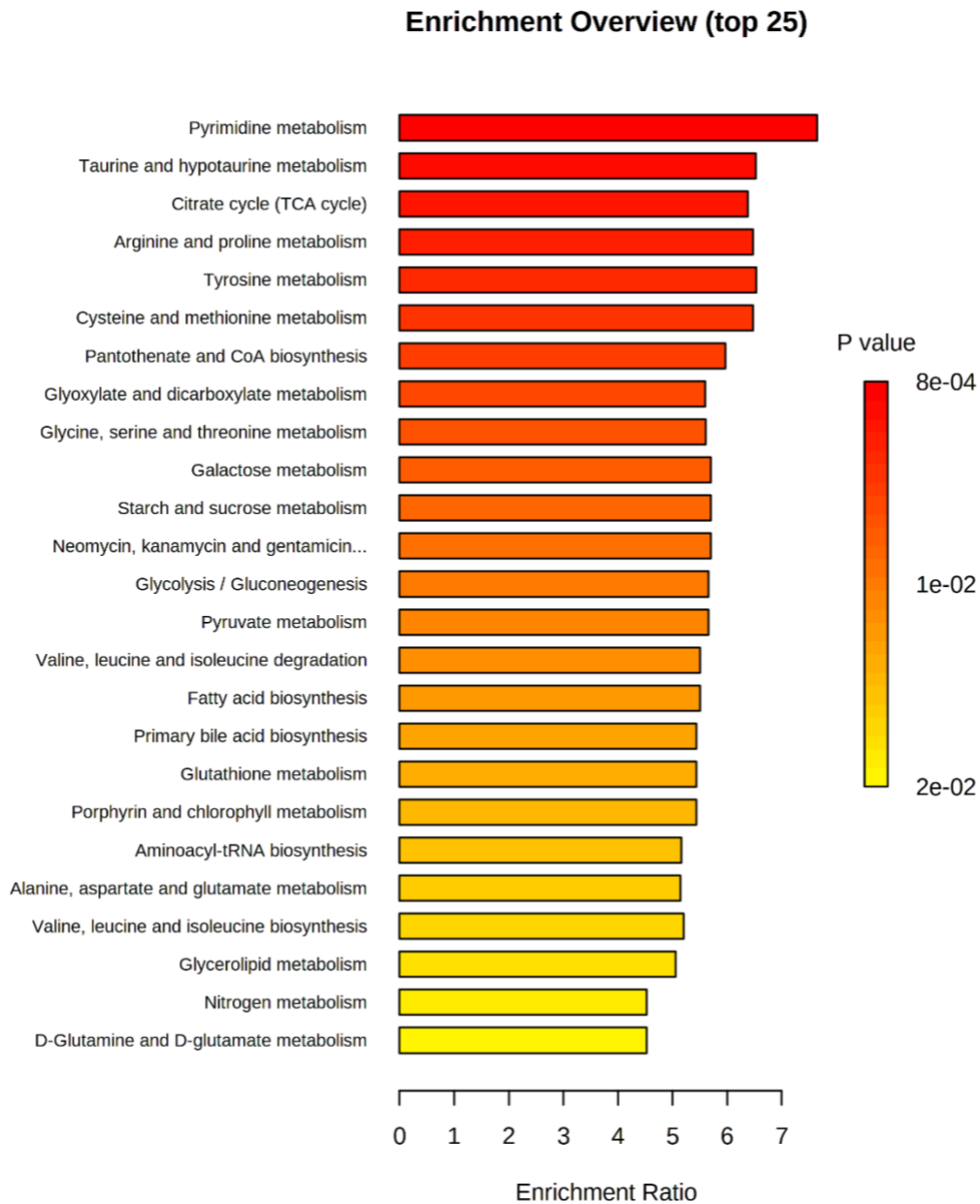
Figure 3-26 Metabolism pathways are significantly altered after sepsis.

Altered plasma metabolites were subjected to pathway analysis and the top 25 altered pathways are shown.

3.4.5 *Sepsis induces metabolic changes in skeletal muscle*

To identify if these changes were also occurring in skeletal muscle, we snap froze the TA of sepsis survivors which were then subjected to the metabolomics workflow (**Figure 3.26**). Glycogen was significantly higher in sepsis survivors. This result could also indicate glycogen storage issues. Glutamate, an intermediate metabolite in the TCA cycle, was significantly lower in sepsis survivors. However, no other metabolites involved in glycolysis or the TCA cycle were significantly altered in skeletal muscle after sepsis. All altered metabolites were subjected to pathway analysis, but no pathways were changed at a significant level (**Figure 3.27**). We carried out additional analyses looking at ATP levels following severe sepsis. There were no changes in gastroc or TA ATP levels as a result of sepsis.
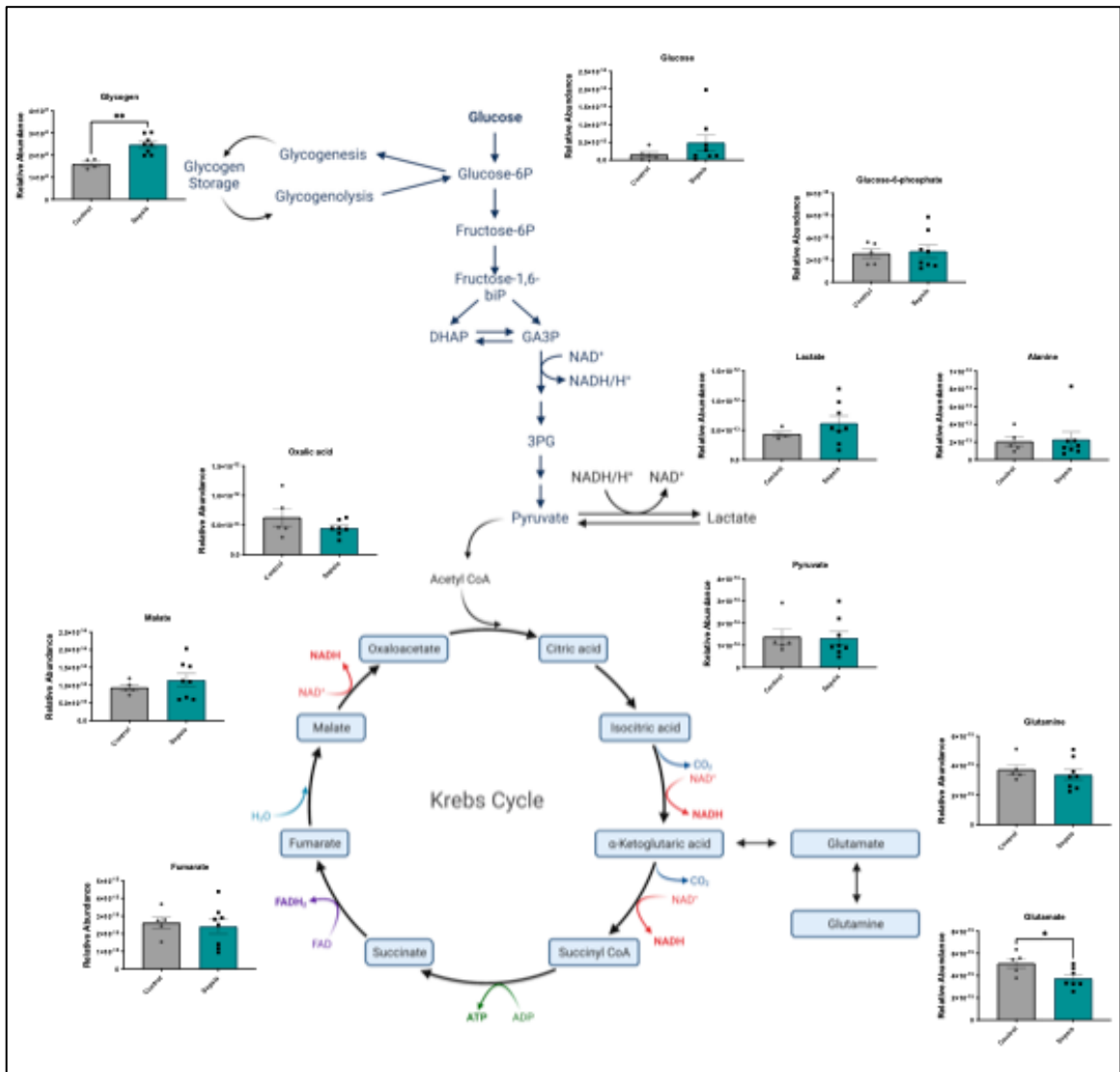
Figure 3-27 Muscle glycogen and glutamate are altered following sepsis.
Sepsis imparts metabolomic changes on skeletal muscle, including an increase in stored glycogen and a decrease in glutamate.

Enrichment Overview (top 25)
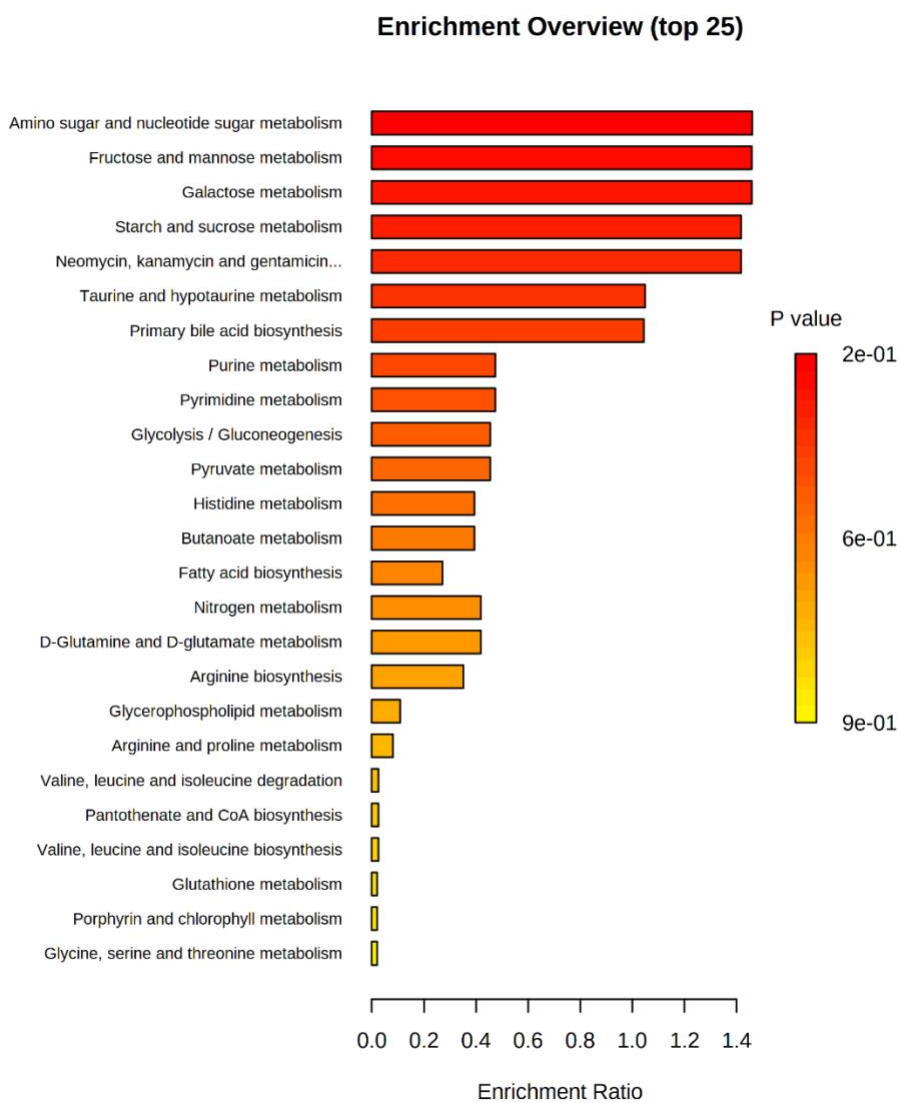
Figure 3-28 Metabolism pathways in skeletal muscle were not significantly altered following sepsis.

Altered muscle metabolites were subjected to pathway analysis and the top 25 altered pathways are shown

3.5 Discussion

Sepsis is a highly disruptive event that occurs when the body fails to contain a local infection and instead induces significant organ damage. However, with successful intervention, survival is possible, though most patients are left with significant long-term complications. Skeletal muscle, in particular, is greatly affected by sepsis and is linked to short- and long-term outcomes. Therefore, the first focus of my dissertation work was to elucidate when and how muscle weakness occurs. Accordingly, Aim 1 was designed as a time-course study. Knowing that muscle weakness and myopathy are contributors to weakness at the 4d mark, I hypothesized that weakness would be greatest at this time point. This work is the first to find that post-sepsis skeletal muscle weakness develops in a progressive manner, worsening even after the resolution of atrophy. These findings were unexpected, as we know atrophy resolves from day 4 to day 14 (42). Despite this, muscle weakness increased over the same period of time, further evidencing our earlier findings that there is another major cause of muscle weakness outside of atrophy.

When performing initial sequencing analyses, we discovered mitochondria-related terms are significantly altered two weeks post sepsis in skeletal muscle. Genes encoded be the organelle were significantly downregulated, as were genes related to the TCA cycle. Countering this, glycolysis-related genes were significantly upregulated. Pairing with these results, were increases in pathways relating to muscle damage and myopathy. Sequencing also revealed that inflammation- and oxidative damage- related genes were unaltered at day 14, indicating neither persistent inflammation nor oxidative stress cause lasting muscle weakness. Individual genes for polyneuropathy were examined and found to have no changes as compared to non-sepsis controls, and pathway analysis for neuromuscular junction related terms confirmed that neural connectivity issues are not significantly contributing to post-sepsis weakness. I also looked for genes relating to atrophy to further rule out the most obvious cause of muscle weakness. At day 14, no genes related to atrophy were altered, further confirming our previous

findings (42) that atrophy resolves by the two-week mark after sepsis. This is emphasized by no differences in CSA at day 14.

To further evaluate how the transcriptome is altered after sepsis and how these changes pair with progressively decreasing muscle function from 4 days to 14 days, we carried out a time-course study. Here, we sacrificed mice on days 0, 4, and 14 of sepsis pathogenesis and once again carried out sequencing analyses. As expected, there were more DEGs at day 4 as compared to day 14. These DEGs followed one of a few trends from day 4 to day 14: (a) resolution to levels insignificant compared to baseline, (b) sustained upregulation, (c) sustained downregulation, (d) a transition from up- to down-regulation, or (e) a change from down- to up-regulation. Out of the 2278 DEGs at day 4, 2065 genes returned to normal levels compared to non-sepsis controls by day 14, while 213 genes remained altered. I then evaluated whether each of the 213 DEGs changed regulation patterns from day 4 to 14.

Out of the 213 DEGs, 127 maintained their up- or down-regulation status from day 4 to day 14. Out of the top 10 altered GO: Cellular Component terms, 6 related to mitochondria. Upon individual gene analysis, mitochondrial-encoded genes remained downregulated at day 14, indicating significant mitochondrial abnormalities occur during sepsis and do not resolve following resolution of sepsis itself. Top GO: Biological Processes pathways further implicate mitochondrial abnormalities persist at day 14. The remaining 86 DEGs demonstrated a change from downregulation to upregulation or vice versa—that is, the transcript abundance flipped from its initial day 4 level to be the opposite at day 14. These changes are likely due to compensation from altered protein levels at day 4. In initially downregulated genes that are upregulated by day 14, transcription likely increased to produce more protein that resulted from depressed levels during acute sepsis (at day 4). Similarly, protein levels may have increased in genes significantly upregulated at day 4. To return protein levels to normal, transcript levels may be up at day 14 as a compensatory mechanism. Upon subjecting these genes to pathway analysis in gProfiler, the top 25 implicated GO: Cellular

Component terms included the cytoplasm, cytosol, ribosomal subunit, cytosolic ribosome, small ribosomal subunit, cytosolic small ribosomal subunit, intracellular organelle, proteasome core complex, ribosome, and organelle. Combined, these data indicate that genes that are significantly downregulated at day 4 and remain downregulated by 14 should be focused on and likely drive lasting post-sepsis complications. Indeed, inflammation markers resolve in turn with the return of inflammatory genes to non-sepsis control levels from day 4 to 14. To confirm that these changes are compensatory for genes swapping up- or down-regulation trends and evaluate if DEGs that remain constantly altered translate to increased protein level changes from day 4 to day 14, proteomic analyses should be carried out.

In addition to the 213 genes that remained altered from day 4 to 14, 515 additional DEGs appeared by day 14. Most of these genes related to metabolism, mitochondria, and/or muscle pathways upon pathway analyses using gProfiler to evaluate GO:CC and GO:BP pathways. The *P*-adj value for mitochondria related terms decreased (i.e., became more significantly altered) upon adding these genes into pathway analysis with the 213 consistently altered genes. Terms related to muscle abnormalities and damaged myofilaments also emerged as significantly altered pathways at the day 14 mark. Combined with no upregulation of genes related to persistent neurodegeneration, inflammation, atrophy, or oxidative damage at day 14, it is clear that muscle weakness at day 14 is likely driven my mitochondria related issues, with abnormalities there causing skeletal muscle structural damage. Adding support to the theory that initial mitochondrial abnormalities drive subsequent issues is that SOD2, or MnSOD, a mitochondrial enzyme protecting against oxidative damage was downregulated at day 4 though not at day 14. This could explain why initial mitochondrial damage is able to accumulate and drive further, increased mitochondrial abnormalities later on after sepsis recovery as emphasized by our TEM results. Further, it is possible that there is an energy crisis, as glycolysis related genes are upregulated, while TCA cycle related genes are depressed following sepsis resolution.

To further investigate if bulk sequencing findings relating to altered metabolic pathways led to altered metabolites, we carried out GC-MS metabolomic analyses. Plasma glucose levels were lower post-sepsis, while at the transcript level, glycolysis related genes were upregulated. Paired with a trending increase in glycogen storage and a significant increase in muscle glycogen storage after sepsis, it is possible that glucose is down not because it inhibited, but rather because it is being utilized. Rather than going all the way through glycolysis, though, it enters the pentose phosphate pathway (PPP) after being converted to G6P. When looking at genes related to the PPP (GO Term: 0006098), almost all are upregulated by day 4, indicating that the pentose phosphate pathway machinery is being used. This could explain why other glycolytic metabolites are decreased (glycerol via DHAP, pyruvate, lactate via pyruvate, and alanine). Increased use of the PPP can occur under mitochondrial stress (76, 77), emphasizing that this shift may be occurring following sepsis.

Plasma metabolites, however, differed from those in skeletal muscle following sepsis. It is well known that fatty acid metabolism increases following sepsis. Current research indicates that instead of utilizing glucose, the liver shifts to preferentially utilizing fatty acids. The change in muscle glycogen could be explained by this, wherein glucose is increasingly stored in favor of a shift to FA metabolism and B-oxidation. Further providing evidence for this theory is an increase in genes related to fatty acid metabolism and B-oxidation at 4 days and 14 days after sepsis. In addition, malate trends higher in sepsis survivor muscle and is higher in plasma, indicating that FFA may be serving as fuel for the TCA cycle at that point. A shift to utilizing lipids can lead to the production of toxic lipid species (78) that, in a fashion similar to the production of free radicals and ROS, can damage mitochondria and further alter metabolism. A decrease in glucose may further be explained by its mutually competitive regulation in relation to FA oxidation in the glucose-fatty acid cycle (79, 80). Here, acetyl-CoA (from beta-oxidation of FA) inhibits the activity of pyruvate dehydrogenase complex (PDC) while citrate (TCA cycle) inhibits PFK (glycolysis) (79, 80). Together, this may help

explain why function decreases from day 4 to day 14, despite the resolution of atrophy.

Decreased plasma glutamate during early sepsis serves as an independent predictor of survival (81). Two weeks after sepsis, glutamate, formed through a deamidation reaction with glutamine, remains decreased in both plasma and skeletal muscle. However, glutamine levels are normal in both tissues. Overall low glutamine levels would negatively impact the body, as glutamine is a major source of nitrogen for purine and pyrimidine synthesis, as well as amino sugars. Therefore, it is possible that the low levels of glutamate are due to an increased conversion to glutamine to prevent further detrimental metabolic changes that would drive immunosuppression as a result of decreased glutamine (82). Further research is necessary to test this thought, however, as maintaining muscle glutamine levels in a disease state is usually accompanied by severe atrophy (83).

While most of these changes were seen in plasma metabolites, muscle metabolites demonstrated relatively little change. Further investigation is required to determine if this lack of change is due to poor isolation and snap freezing in which the metabolites degraded too quickly for proper analyses, or if it is truly that muscle metabolites are not changing following sepsis. The lack of overall changes in muscle ATP do not provide further insight into one of these theories, as switching to alternative pathways could explain a lack of overall change. However, significant changes in metabolism-related genes both 4 days and 14 days after sepsis indicate that alternative pathway use may be likely. Regardless of which metabolic machinery is being preferentially utilized at day 14, it is clear that mitochondrial abnormalities occur after sepsis. Evidence for abnormal mitochondria and altered function is emphasized not only by gene expression analyses, but our previous mitochondrial stress tests (42), decreases in OxPhos protein expression from day 4 to 14, and increasing mitochondrial damage in TEM images. Paired with function data, it provides reason that the two are connected, and it is possible that mitochondrial protection may prevent the development of subsequent post-sepsis skeletal muscle weakness.

3.6 Conclusions

Sepsis induced muscle weakness progressively worsens until at least day 14 and persists for *at least* 2 months thereafter in experimental sepsis. This negative functional change is accompanied by downregulation of mitochondrial encoded genes. Pathway analyses also point to mitochondrial pathway alterations as occurring in tandem with declining muscle function post-sepsis. When examining mitochondrial morphology, a majority of organelles are significantly altered at day 14 (42). This damage is accompanied by decreased protein levels for proteins encoding complexes I, II, IV, and V. Therefore, it is possible that mitochondrial damage is also a progressive process after sepsis, with increasing dysfunction pairing with worsening muscle weakness from day 4 to day 14. With resolution of atrophy, a lack of polyneuropathy markers, and no signs of other major drivers of myopathy, we can conclude that mitochondrial abnormalities drive post-sepsis skeletal muscle weakness and that the organelle serves as a likely therapeutic target.

CHAPTER 4.MnSOD OVEREXPRESSION AND
SKELETAL MUSCLE WEAKNESS

4.1 Abstract

Mitochondrial abnormalities accumulate in post-sepsis skeletal muscle weakness which progressively worsens in sepsis survivors over time. In this second aim, I investigated if mitochondrial protection could limit sepsis induced skeletal muscle weakness using a transgenic strain of mice overexpressing manganese superoxide dismutase (MnSOD). This would help to establish a causative relationship between mitochondrial abnormalities and post-sepsis muscle weakness. As demonstrated in Chapter 3, sepsis alters metabolism related genes, several of which are mitochondrial encoded or related to mitochondrial function. SOD2 (MnSOD) specifically, was reduced during acute sepsis, indicating mitochondria's ability to reduce superoxide to hydrogen peroxide was reduced after sepsis. After experimental sepsis, mice overexpressing the mitochondrial localizing enzyme MnSOD were significantly protected from skeletal muscle weakness and exhibited less mitochondrial damage despite similar sepsis severity. Taken together, these findings further indicate that mitochondrial damage during sepsis pathogenesis is a major driver of skeletal muscle weakness, and protection of mitochondria confers protection against this complication. Therefore, therapeutic interventions aimed at protecting mitochondria may provide clinical benefit to sepsis survivors, and early intervention during acute sepsis may prevent chronic weakness altogether.

4.2 Introduction

After determining mitochondrial abnormalities are major contributors to post-sepsis skeletal muscle weakness, it became clear that the organelle may be targetable in a therapeutic fashion. This aim was designed to provide further evidence for mitochondrial abnormalities as causative drivers of this sepsis complication, hypothesizing that mitochondrial antioxidant overexpression

protection could decrease this chronic issue. I therefore utilized a strain of mice overexpressing MnSOD that has previously been shown to protect against mitochondrial damage in multiple models (69, 84, 85).

MnSOD is an essential antioxidant enzyme localized in the mitochondria that functions to detoxify superoxide and has been shown to protect against drug-induced mitochondrial damage when overexpressed in mice (69, 84, 85) without increasing their lifespan (86).

4.3   Experimental Approach

Noting that MnSOD is embryonic lethal (87), our lab first attempted to use heterozygous MnSOD (+/-) knockdown mice, though these mice proved to be too sensitive to sepsis and yielded a low number of survivors. Therefore, I used mice overexpressing human MnSOD (MnSOD-TG) for this aim. With these MnSOD-TG mice, I was able to get a high number of sepsis survivors that suffered from severe sepsis. The next steps under this aim were to determine if TG mice experienced less functional deficits as a result of sepsis and if mitochondrial abnormalities were reduced as a result of the endogenous protection conferred by overexpression. I carried out three different studies as a result, with the first determining how skeletal muscle weakness was impacted by overexpression. Here, I compared non-sepsis control MnSOD-TG and WT mice to sepsis surviving TG and WT mice. We then allowed the mice to recover, and on days 21-22 we euthanized them for *ex vivo* function testing. In the second study, I euthanized mice in all four groups at 14 days to determine how mitochondria were affected by (1) sepsis, and (2) overexpression. To evaluate if overexpression protected against the initial sepsis event, I took blood at 6 hours to assess IL-6 levels. The third study evaluated female mice, looking at molecular changes from day 0 to day 14 in WT and TG mice. Once again, IL-6 levels were assessed at 6-hours post sepsis-induction to determine if overexpression mediated the dysregulated host response to CS injection-induced infection that causes sepsis. As with my previous studies, mitochondrial abnormalities were assessed through TEM, Western blotting, and

histological analyses. Mice were all subjected to otherwise lethal sepsis (CS 170616) and resuscitation followed our standard protocol starting at 12 hours. Mice that did not suffer severe sepsis as determined by (1) severe hypothermia, (2) lasting weight loss, (3) significant splenomegaly, and, when applicable, (4) high IL-6 levels were excluded from further testing and excluded from analyses.

4.4 Results

4.4.1 MnSOD overexpression has limited effects on sepsis severity.

First, we confirmed MnSOD overexpression in TG mice after genotyping and aging the animals up to 16 months of age. In skeletal muscle, MnSOD was overexpressed nearly 3-fold as compared to WT littermate control mice. Since MnSOD overexpression is endogenous, there was a concern that the increased mitochondrial protection may mediate the initial acute sepsis event. It was therefore critical to monitor body temperature, body weight loss, splenomegaly, and plasma IL-6 to assess overall sepsis severity in wildtype and overexpressing mice. For this, we carried out studies in male and female mice, subjecting both WT and TG mice to an otherwise lethal dose (LD_{100}) of cecal slurry (CS 190705; 400 uL males, 350 uL females) to induce sepsis prior to rescuing them with our late-stage resuscitation protocol. MnSOD overexpression did not change survival rates in male or female mice, nor did it alter sepsis severity (**Figure 4.1 and 4.2**). In female mice, survival was not significantly difference for MnSOD-TG mice (84%) compared to WT animals (92%). For male mice, 79% of TG mice survived, while 81% of WT mice did. Both WT and TG mice exhibited severe hypothermia, marked splenomegaly, and significant body weight loss. To assess acute sepsis severity, tail vein blood was taken at 6 hours to assess plasma IL-6 levels. 6h IL-6 levels were similar for all CS-injected mice, regardless of MnSOD expression status. Upon euthanasia, the spleens of mice were dissected and weighed to assess splenomegaly (**Figure 4.1E, 4.2 E**). Body weights were monitored throughout sepsis. As expected, while non-sepsis mice demonstrated no differences, sepsis surviving mice demonstrated significant weight loss (**Figure 4.1B and 4.2B**) that we have previously shown is due to decreased fat mass (42). Together, these

results indicate MnSOD overexpression does not alter acute sepsis in male or female mice, and WT and TG mice suffer equivalent sepsis severity.

Following euthanasia, wet weights of skeletal muscles were obtained to determine if sepsis and/or overexpression status were impacting muscle mass. Both male and female TA, EDL, GAS, and SOL muscle wet weights were obtained, none of which revealed any differences (**Figure 4.1 and 4.2**). Cross sectional area of the TA was also calculated for male mice and did not reveal any differences across groups (**Figure 4.3**). Together, these data indicate that any atrophy that may occur during acute sepsis has resolved by the two-week mark, just as we saw previously (42). MnSOD overexpression did not impact skeletal muscle size, as indicated by similar wet tissue weights across all WT and TG mice and emphasized by similar fiber type distributions in all the mice (**Figure 4.3**), regardless of sepsis/overexpression status.
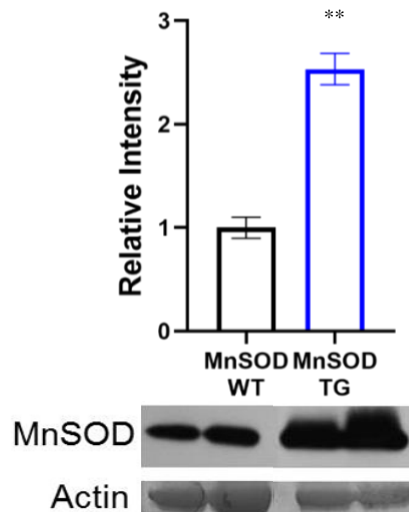
Figure 4-1 MnSOD is overexpressed over 2.5-fold in TG mouse skeletal muscle as compared to WT animals.
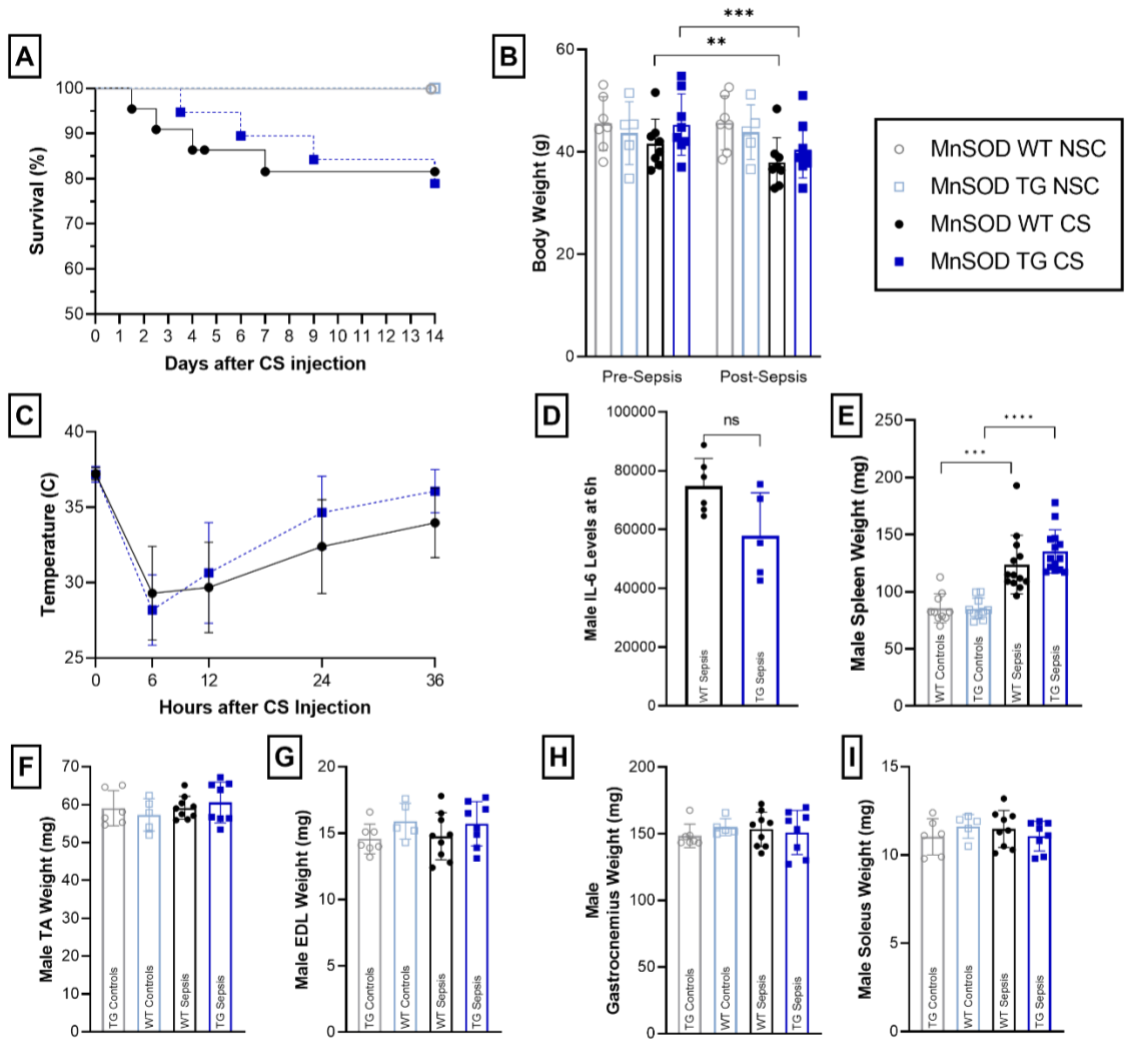
Figure 4-2 MnSOD overexpression does not alter overall sepsis severity in male mice.

(A) Survival curve analyses revealed no differences between WT and TG sepsis mice. (B) Pre-sepsis body weights were not different across groups. Post-sepsis animals suffered significant body weight loss. (C) Temperatures were recorded at 0h, 6h, 12h and every 12h until sepsis surviving mice returned to their pre-sepsis body temperature. Male TG and WT sepsis mice suffered profound hypothermia, but there were no significant differences due to MnSOD overexpression. (D) Tail vein blood was collected at 6h after sepsis induction from a randomized subset of CS-injected mice. Plasma was then collected for IL-6 ELISA analysis to determine sepsis severity. There were no significant differences in 6h IL-6 levels between WT and TG sepsis mice. (E) Upon euthanasia on day 14, spleen weights were recorded to determine sepsis severity. Mice subjected to sepsis had clear increases in spleen weights, while there were no differences between WT and TG mice within their respective non-sepsis control and sepsis survivor cohorts. Two weeks after sepsis induction, hindlimb muscles were collected from all mice to assess if atrophy could be driving long-term skeletal muscle weakness. Regardless of sepsis /non-sepsis and TG/WT status, there were no differences in the wet weights of the (G) tibialis anterior, (H) extensor digitorum longus, (I) gastrocnemius, or (J) soleus.
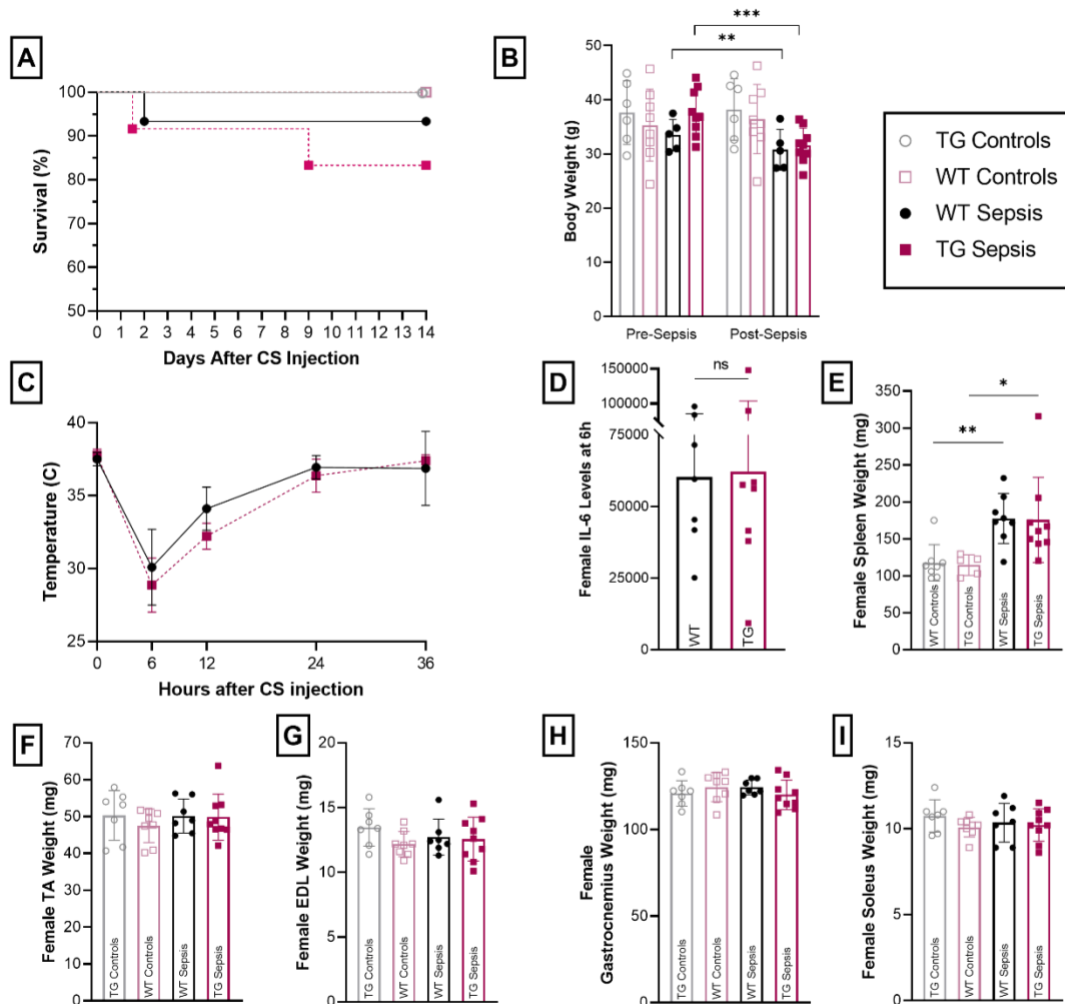
Figure 4-3 MnSOD overexpression does not alter sepsis severity in females.
(A) Survival curve. (B) Pre-sepsis body weights were not different across groups. Post-sepsis animals suffered significant body weight loss. (C) Temperatures were recorded at 0h, 6h, 12h and every 12h until sepsis surviving mice returned to their pre-sepsis body temperature. Female TG and WT sepsis mice suffered profound hypothermia, but there were no significant differences due to MnSOD overexpression. (D) 6h IL-6 levels revealed no differences between WT and TG sepsis mice. (E) Mice subjected to sepsis had clear increases in spleen weights, while there were no differences between WT and TG mice within their respective non-sepsis control and sepsis survivor cohorts. Regardless of sepsis /non-sepsis and TG/WT status, there were no differences in the wet weights of the (G) tibialis anterior, (H) extensor digitorum longus, (I) gastrocnemius, or (J) soleus.
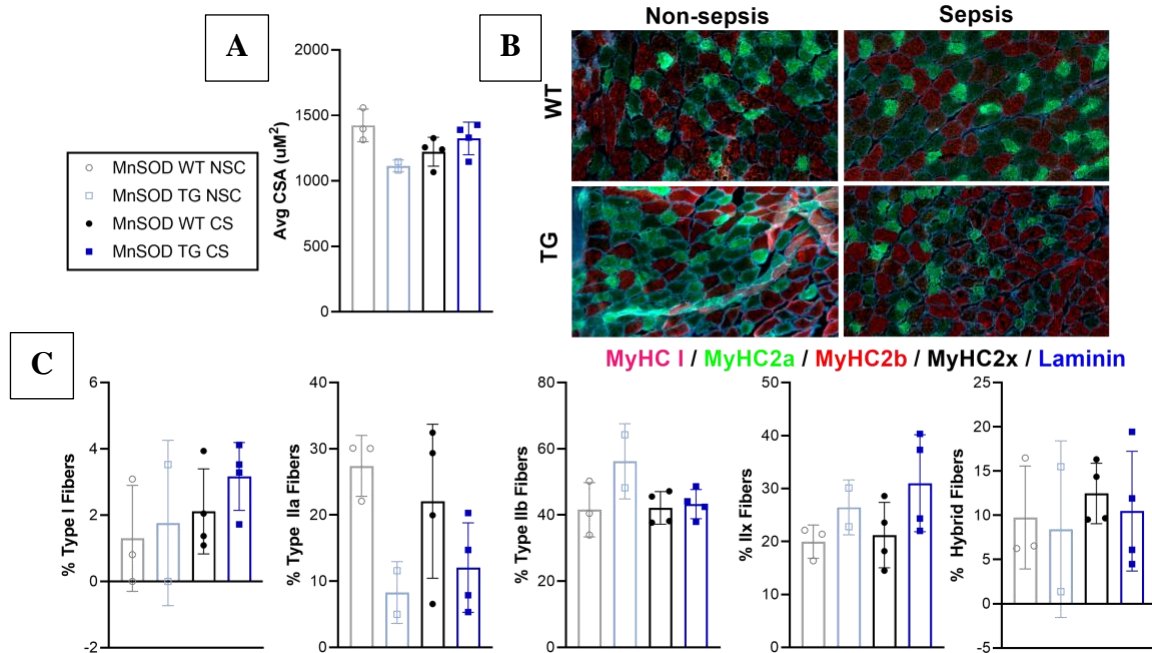
Figure 4-4 Niether MnSOD overexpression nor sepsis induction alters CSA or fiber type distribution in male mice.

(A) Average pooled CSA of the TA was measured after staining for fiber type borders and the different fiber types. There were no differences as a result of MnSOD overexpression status, nor did sepsis induce any changes at 14 days in sepsis survivors. **(B)** Representative images of MnSOD WT (top) and TG (bottom) TA sections for mice that served as non-sepsis controls (left) or survived severe sepsis (right). **(C)** When looking at individual fiber type distributions, there were no significant differences between groups. While MnSOD TG mice trended to have fewer type IIa fibers, this difference was not significant. With an increase in sample size, this result may change, as n=4 for each group.

4.4.2   MnSOD protects against sepsis-caused mitochondrial abnormalities.

Critically, sepsis severity was equivalent across MnSOD WT and TG mice. Therefore, we were able make conclusions on if mitochondrial protection through MnSOD overexpression protected against mitochondrial abnormalities throughout sepsis, as the protection did not blunt the acute sepsis event. To evaluate mitochondrial abnormalities, TA muscle sections were stained for NADH an SDH for complex I and II, respectively. While TG sepsis survivors showed less staining intensity than non-sepsis controls, they demonstrated stronger staining than their WT sepsis survivor counterparts. WT sepsis survivors exhibited a significant decrease in staining intensity as compared to their WT non-sepsis controls for both complex I and complex II (**Figure 4.5**). To further evaluate mitochondrial abnormalities, I performed a Western blot for OxPhos protein levels in protein isolated from female mice (**Figure 4.6**). There were no significant changes in any protein complex in MnSOD WT or TG mice as a result of sepsis. Further, there were no changes as a result of MnSOD overexpression in control mice, emphasizing MnSOD does not alter base level OxPhos protein content.
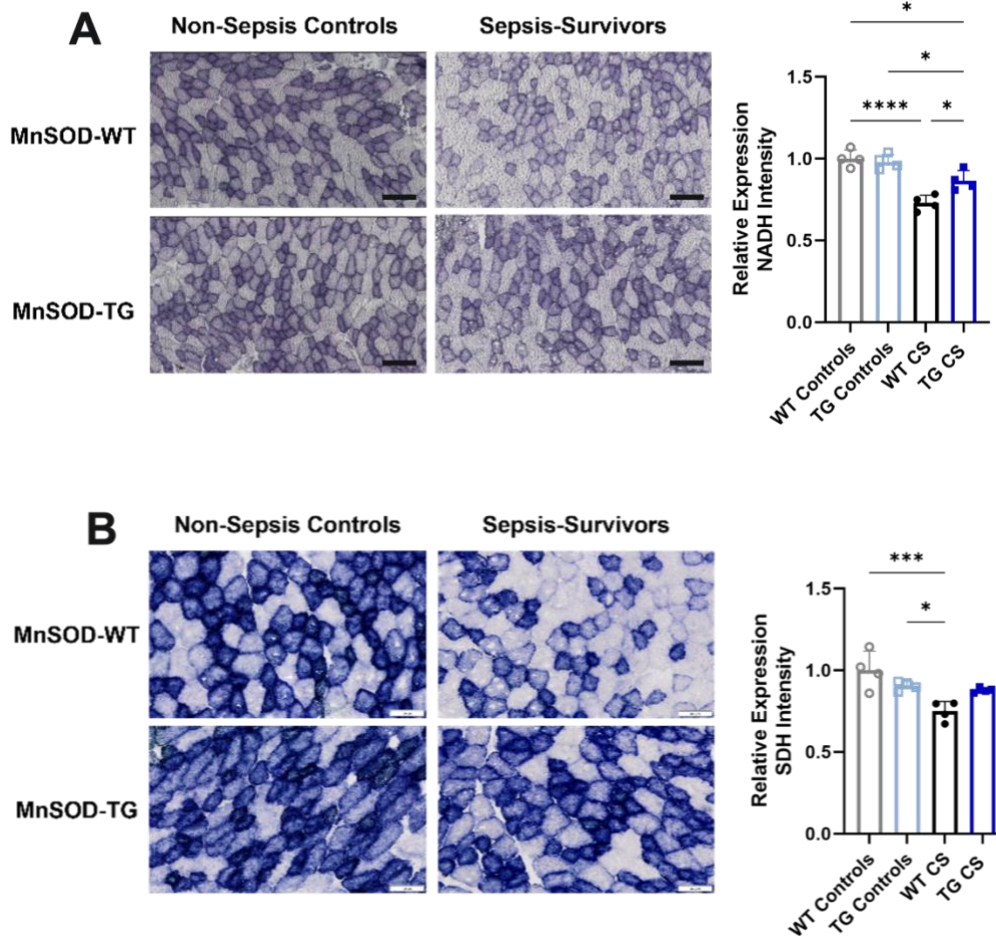
Figure 4-5 NADH and SDH staining revealed MnSOD has a protective effect on post-sepsis staining intensity.

(A) NADH staining and quantification revealed MnSOD-WT and TG mice suffer from complex I related issues after sepsis. However, sepsis surviving TG mice had significantly higher staining intensity than their WT counterparts, indicating MnSOD has some protective effect. This protective effect is further seen in the staining for SDH **(B)** where TG sepsis survivors do not demonstrate a difference in staining intensity while WT sepsis survivors do.
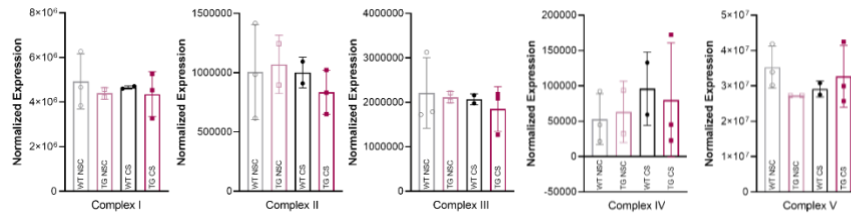
Figure 4-6 Niether MnSOD expression nor sepsis status affected protein markers for OxPhos complexes I-V in female mice.

After performing multiple blots using 15-well gels (n=3 each group), it became clear that MnSOD expression status did not affect OxPhos markers for complexes I-V in female mice.

Transmission electron microscopy (TEM) imaging revealed TG mice suffered significantly less mitochondrial damage as compared to WT mice after surviving sepsis (**Figure 4.7**). When comparing WT and TG mice, we saw that 76% of WT mitochondria were damaged on average, as compared to just 26% of TG mouse mitochondria. Since sepsis was equally equivalent between WT and TG animals, this difference was due to MnSOD overexpression.
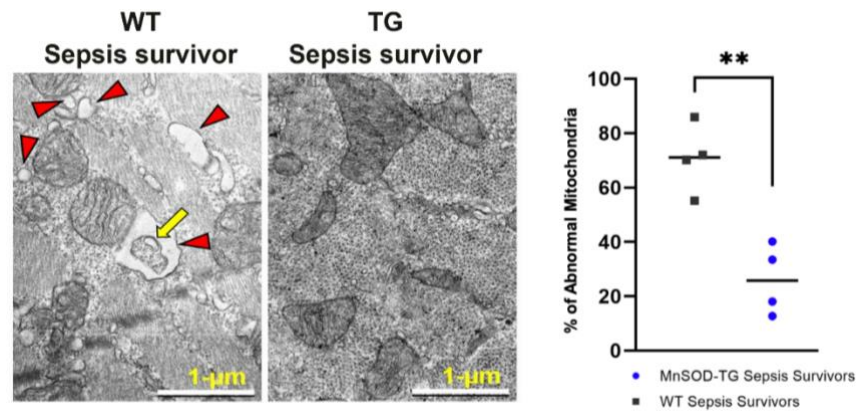
Figure 4-7 MnSOD overexpression confers strucutal protection to mitochondria during sepsis in male mice.

Following euthanasia, small sections of the EDL were collected for TEM imaging and quantification. Representative images of WT and TG sepsis survivors are shown on the left, with red arrowheads marking empty organelles, and the yellow arrow pointing out a mitochondrion that has centralized into a vacuole like structure. Abnormal mitochondrial were quantified (right, n=4 per group) and graphed, with TG animals having significantly less mitochondrial structural change after sepsis.

4.4.3 *MnSOD-TG mice do not exhibit skeletal muscle weakness after sepsis*

A subset of MnSOD mice underwent *ex vivo* function testing to evaluate the effectiveness of mitochondrial protection in preventing post-sepsis skeletal muscle weakness. Upon subjecting the extensor digitorum longus (EDL) to a force-frequency protocol, significant differences emerged between MnSOD-WT non-sepsis control mice and WT sepsis survivors (**Figure 4.8**). These data indicate sepsis imparts a functional deficit of 19.9% that lasts through at least three weeks (i.e., days 21-22, when these mice were subjected to function testing). However, TG sepsis survivors subjected to the same protocol demonstrated no differences from their TG non-sepsis controls and the WT non-sepsis controls. When compared to the WT sepsis survivors, the TG sepsis survivors were 18.3% stronger, indicating that mitochondrial protection prevented post-sepsis skeletal muscle weakness.
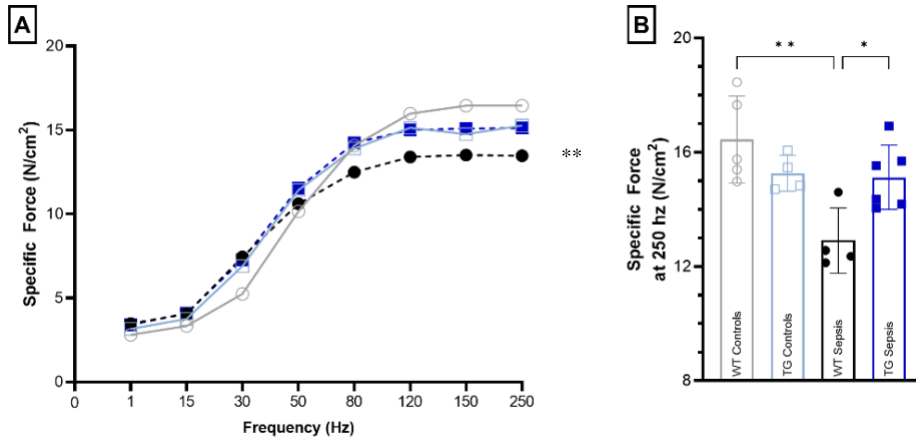
Figure 4-8. MnSOD overexpression prevents post-sepsis skeletal muscle weakness without affecting strength in non-sepsis control mice. EDL hindlimb muscles of non-sepsis control and sepsis surviving mice were subjected to ex vivo function testing to establish if there were differences in the force-frequency relationship across groups. Force was normalized to the physiological cross-sectional area of each individual muscle to eliminate the effects of size variation across individual muscles. (A) Force-frequency curves of non-sepsis WT and sepsis surviving WT mice were significantly different, with sepsis survivors having a great reduction in force production with increasing frequencies. However, TG mice demonstrated no differences based on sepsis status. (B) Maximum force analysis revealed again that WT mice suffered a significant decrease in function (19.9%) as a result of sepsis. TG sepsis survivor mice, however, displayed no differences from their non-sepsis counterparts indicating overexpression protects against muscle weakness. Further, TG sepsis survivors were 18.3% stronger than their WT counterparts.

4.5 Discussion

MnSOD overexpression prevented both mitochondrial abnormalities and muscle weakness that occurs following sepsis, further indicating mitochondrial damage and dysfunction drive this debilitating complication. Endogenous MnSOD overexpression conferred nearly 3-fold higher SOD2 in the skeletal muscle of TG mice as compared to WT controls. Since age is a critical component of sepsis severity and lasting complications, we aged male and female mice to 16-months old before inducing sepsis. We had three initial concerns to address with MnSOD overexpressing mice: (1) whether or not MnSOD overexpression would alter basic muscle function in non-sepsis animals, (2) if SOD2 (MnSOD) overexpression would mitigate the initial sepsis event, and (3) whether overexpression would alter post-sepsis muscle architecture between TG and WT mice.

First, we needed to establish if MnSOD overexpression had any differences on mitochondrial abnormalities and muscle function in non-sepsis mice. While MnSOD overexpression protected against sepsis-induced skeletal muscle function deficits, there were no changes in non-sepsis control muscle function as an effect of overexpression. This is consistent with findings in the cancer field, where MnSOD overexpression does not increase lifespan, only providing mitochondrial protection during insult (69, 84-87).

Our second concern with MnSOD overexpression was that it would alter acute sepsis. Since there is a known energy crisis and metabolism related issues during acute sepsis, we were concerned that TG mice would not develop as severe sepsis when compared to their WT sepsis controls. This would mean our muscle function results were due to a blunted acute sepsis event and less severe pathophysiology in TG mice. While this would be a welcome finding, as further decreasing sepsis mortality is never a bad thing, it would have altered the course of this project significantly. Upon analysis, overexpression did not impact sepsis severity. When analyzing 6h IL-6 levels, the field's standard way of marking acute phase sepsis severity in rodents (88), WT and TG mice had similar levels. Further, survival curve analysis, hypothermia, and overall weight loss were similar across

all sepsis survivors. Evaluation of splenomegaly, an indicator of severe infection and likely sepsis, revealed both TG and WT mice injected with equal doses of CS developed equivalent sepsis severity that conferred long term changes to their spleen weight as compared to their WT and TG non-sepsis controls. Thus, is it clear that overexpression did not alter the initial sepsis event, only lasting mitochondrial and muscular changes.

Muscle size, as assessed by wet tissue weight and fiber type cross-sectional area, was not altered by overexpression or sepsis. When evaluating post-sepsis wet weights of the TA, gas, sol, and EDL, there were no differences as an effect of sepsis or overexpression status for male or female mice. When evaluating cross-sectional area using MyoVision 2.0, sepsis survivors did not have altered fiber type distributions or diminished CSA. Together, these data indicate that atrophy has little, if any, role in lasting post-sepsis skeletal muscle weakness. Further, protecting mitochondria via endogenous MnSOD overexpression had no impact on size, indicating the weakness following sepsis in WT mice is due to changes outside of atrophy.

Mitochondrial morphology is normally altered following sepsis, as cristae are destroyed or altered, and mitochondria can even appear to look empty (42, 60, 72, 74, 89). However, MnSOD overexpression significantly prevents these issues. While a vast majority of WT sepsis survivor mitochondria are significantly damaged after sepsis, nearly three-quarters of TG mitochondria demonstrated normal morphology. Sepsis altered the morphology of 66% fewer mitochondria in survivors overexpressing MnSOD. When looking at protein markers for mitochondrial complexes I-V, there were no major differences in protein content. While this was an unexpected result, it indicates that mitochondrial dysfunction is likely occurring to cause lasting weakness. Confirming through high resolution respirometry would be a good subsequent experiment. Regardless, it is clear from these data that MnSOD overexpressing mice are significantly protected from some mitochondrial abnormalities and subsequent muscle strength deficits.

4.6   Conclusions

Endogenous overexpression of MnSOD conferred protection against post-sepsis mitochondrial abnormalities and subsequent muscle weakness, not against sepsis itself. Indeed, upon testing for *in vitro* function deficits after sepsis, we saw no functional changes in TG mice subjected to sepsis, while WT sepsis survivors exhibited more than a 15% decrease in maximum force production. Combined with our data demonstrating MnSOD overexpression protects against typical sepsis-induced mitochondrial structural changes, it is clear that mitochondrial abnormalities cause post-sepsis skeletal muscle weakness. Additionally, it is highly likely that we can recreate this protective effect utilizing mitochondria-targeting therapeutics.

CHAPTER 5. MITOCHONDRIA-TARGETING THERAPIES AND SKELETAL MUSCLE WEAKNESS

5.1 Abstract

Mitochondrial abnormalities appear to be the main causes of post-sepsis skeletal muscle weakness. To further evidence this causative role, we utilized a transgenic strain of mice overexpressing human MnSOD. After subjecting wild type (WT) and overexpressing (TG) mice to severe sepsis, we compared post sepsis function in an *in vitro* approach. Here, we found that mitochondrial SOD completely protected against muscle weakness development despite equivalent sepsis severity as confirmed by equal body weight loss, 6h IL-6 production, hypothermia, and splenomegaly across all sepsis survivors. Fewer mitochondrial abnormalities accumulated following sepsis. Together these data confirm that mitochondrial abnormalities cause post sepsis weakness, and that mitochondria may be able to be targeted in a therapeutic manner.

However, MnSOD overexpression is not a viable therapeutic strategy to treat human sepsis patients. Therefore, evaluating therapeutic strategies targeting mitochondria became the focus of this third aim. I utilized two pharmacological treatments and an exercise protocol as part of this aim in evaluating whether or not multiple strategies aimed at increasing mitochondrial quality could restore muscle function to levels comparable to non-sepsis control animals. Treatment with SS-31 after the development of severe sepsis showed significant improvement for both mitochondrial abnormalities and subsequent muscle weakness, with non-sepsis controls and SS-31 treated sepsis survivors demonstrating no differences *in vitro* muscle function testing. Here, mitochondrial damage was prevented, and structural integrity was significantly less compromised at 28 days after sepsis. Providing higher oxygen levels to promote efficient substrate use and energy production within skeletal muscle and other organs during acute sepsis had an unexpected negative result, causing a termination of this therapeutic intervention study. Treatment with the drug NMN did not yield significant results, though its promise in restoring already developed

muscle weakness (treatment began one week after CS injection), yields further study. While showing mixed results in the clinical setting, exercise did not show significant promise in treating post-sepsis skeletal muscle weakness. Altogether, data from this aim indicates pharmacological intervention will likely be necessary to prevent and/or treat post-sepsis skeletal muscle weakness in sepsis surviving human patients. The restoration of function and lack of mitochondrial abnormalities in SS-31 treated animals indicates that this drug specifically may have a benefit in preventing treatment if administered with fluid and antibiotics in the clinic, and it may have efficacy in treating already established muscle weakness.

5.2 Introduction

Despite the prominence of sepsis-induced muscle weakness, there are no current successful preventative or treatment interventions for chronic post-sepsis skeletal muscle weakness. Nutritional supplementation during sepsis has not had any beneficial effect, as catabolism during acute illness is unavoidable. Instead of being used in protein synthesis to prevent a protein turnover imbalance where protein degradation outweighs protein synthesis (thus causing atrophy), the delivered amino acids are shuttled instead to ureagenesis and aid in suppressing skeletal muscle autophagy, possibly actively contributing to weakness (58, 66-68). Other interventions have also proved to have no major positive effect, such as insulin control during sepsis (90) and post-discharge physical therapy (58). However, none of these strategies specifically target mitochondria, which are a main cause of chronic post-sepsis muscle weakness. Noting that mice overexpressing the antioxidant (and therefore mitochondria protecting) MnSOD did not suffer as severe mitochondrial abnormalities and subsequent muscle weakness after severe sepsis, utilizing therapies aimed at increasing mitochondrial quality was the major focus of this Specific Aim 3.

Septic patients often exhibit an increase in basal metabolism with oxygen and consumption levels increasing (74, 91). However, individuals that do not

exhibit these increases have worsened outcomes (92-94). Therapeutics aimed at improving sepsis survival have examined ways to restore oxygen delivery and increase proper oxygen consumption/oxygen utilization by the organs (95). In skeletal muscle specifically, oxygen utilization by the tissue decreased with worsening sepsis (96). To evaluate if providing animals with more oxygen during acute sepsis could be beneficial to survival and/or decrease chronic complications, we utilized a hyperoxia chamber in which mice were provided 70% oxygen. In providing more oxygen, energy issues that developed during acute sepsis and lasted through at least 14 days via RNA sequencing may be mediated. This would enable proper mitochondrial function and energy production, thereby helping not just skeletal muscle during severe sepsis, but all other organs. This approach could reduce the overall severity of sepsis, thus leading to less post-sepsis muscle weakness. While mitochondria are not specifically targeted with increased oxygen administration, they may benefit, as mitochondria consume a large amount of oxygen in the cells and play a central role in aerobic metabolism through which most of our energy is produced.

Exercise is another potential mitochondrial therapeutic, as it is well established that exercise training promotes mitochondrial biogenesis (97). Exercise has been shown to activate PGC-1α signaling (98-100). PGC-1α serves as the master regulator of mitochondrial biogenesis (101-104), thereby implicating exercise as a positive regulator of mitochondrial biogenesis. Fusion can also occur as a result of exercise, thereby increasing mitochondrial quality when combined with mitochondrial clearance via fission and mitophagy to eliminate damaged or dysfunctional organelles (105). Indeed, exercise has been shown to increase mitochondrial turnover to promote healthy a healthier overall mitochondria pool (103, 105-111). Resistance exercise has been shown to improve maximum coupled respiration without increasing mitochondrial mass or gene expression (98, 100, 112), indicating exercise may be able to have a restorative effect on less effective mitochondria. This is particularly notable, as we have previously shown significant mitochondrial dysfunction (42) separate from the altered gene expression I have found in this work. Therefore, exercise may help restore strength

after sepsis by increasing overall mitochondrial quality and mediating remaining dysfunctional organelles. Since exercise is a relatively easy intervention—there are no clinical trials that must be carried out to ensure its safety—we evaluated its efficacy in treating established post-sepsis skeletal muscle weakness.

Knowing that the prior interventions may not work, we also examined pharmacological alternatives. Nicotinamide mononucleotide, or NMN, is a rate limiting precursor to NAD+ synthesis and has been explored as a potent mitophagy inducer with promise in treating Werner syndrome (113) and Alzheimer's Disease (114). NMN's ability to increase mitochondrial respiratory capacity in skeletal muscle (115-117) and models of AD (113) and hemorrhagic shock (118), both of which exhibit significant mitochondrial damage, provide reason that the drug will have a positive effect in the context of sepsis-induced muscle weakness. NMN has the additional benefits of increasing mitochondrial quality by increasing the expression of proteins required for mitochondrial fission, fusion, and biogenesis, adding to this promise that the drug can increase mitochondrial function following recovery from sepsis (113, 119-121). Further, NMN supplementation drove increased expression of muscle remodeling genes in a human model (122).

SS-31 (D-Arg-Dmt-Lys-Phe-NH2), a small mitochondria-targeting synthetic tetrapeptide also known as Elamipretide™, and Bendavia™, and MTP-131, was discovered by Szeto and Schiller (121, 123-125). It can selectively target and concentrate roughly 5000-fold in the inner mitochondrial membrane through electrostatic and hydrophobic interactions (126-128). SS-31's dimethyl tyrosine residues provide the peptide with antioxidant features, as SS-31 can scavenge oxygen radicals (123, 124, 129-131) to make tyrosyl radicals (127) which can then further neutralize oxygen radicals (132) and inhibit low-density lipoprotein and linoleic acid oxidation (133). SS-31 also selectively binds to cardiolipin (CL) in the inner mitochondrial membrane, modulating the opening of the mitochondrial permeability transition pore by binding to CL and preventing its translocation and peroxidation, thereby conferring structural protection, promoting ATP synthesis (127, 128, 134), and decreasing electron leakage (126). It can also bind to subunits

in the electron transport chain protein supercomplexes, further stabilizing and protecting mitochondrial structure and function (127, 128). SS-31 is undergoing phase 1 and 2a clinical trials for treating severe atherosclerotic renal artery stenosis and altered renal function (135). It has had preclinical success in treating mitochondrial myopathy associated with cardiac disease, acute kidney injury, ischemia-reperfusion injury, and diabetic nephropathy (121, 124-131, 135). Since it is dissolvable in water, is completely excreted by the kidneys, does not target healthy mitochondria (135), and can be distributed to skeletal muscle (126, 129), we chose SS-31 as a possible post-sepsis therapeutic.

5.3   Experimental Approach

While experiments utilizing overexpressed MnSOD showed that antioxidant protection of mitochondrial prior to sepsis induction had positive effects, this is not possible in the human population developing sepsis. Therefore, it was critical that all these therapeutic experiments be carried out after sepsis had already developed. As such, severe sepsis was induced in 16-month-old C57BL/6 mice for each experiment, and we followed our late stage resuscitation protocol as is standard. The treatment paradigm is shown in **Figure 5.1**. For hyperoxia therapy, mice were sorted into groups and placed in the chamber at 12 hours, remaining there for up to three days. SS-31 treatment was incorporated into the saline of our resuscitation protocol, thereby enabling standard saline administered to untreated sepsis mice to serve as a control. SS-31 was administered 2x daily (dose) for 5 days and then once daily through day 10 (saline volumes were matched in sepsis surviving controls). This, however, was aimed at preventing weakness. To evaluate the efficacy of true treatments of already established chronic post-sepsis muscle weakness, NMN and exercise treatment began on day 7 and was continued for one week (NMN) or 6 weeks (exercise). All animals were euthanized for *in vitro* function testing and tissue collection for biochemical and histological analyses as described in Chapter 2.
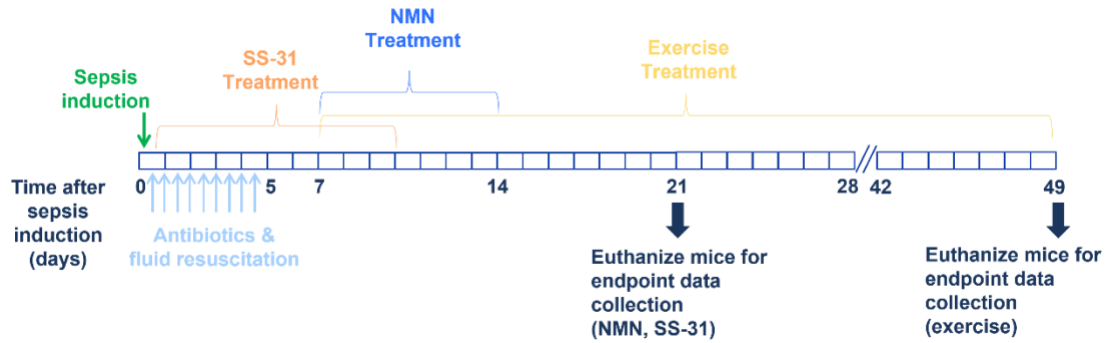
Figure 5-1. Treatment paradigm following sepsis development.

5.4 Results

5.4.1 SS-31

5.4.1.1 SS-31 had limited effects on acute sepsis

Mice were injected with 400uL of CS (CS 191206 through March 2021; CS210615 through December 2022) and then sorted into SS-31 or vehicle treatment groups based on pre-sepsis body weight and 6h body temperature. Late-stage resuscitation began at 12h after the development of severe sepsis, with all mice receiving broad spectrum antibiotics administered via *i.p.* injection. For the pharmacological treatment group, mice were injected with SS-31 added to their resuscitation saline. Thus, mice received SS-31 2x daily for 5 days via *s.c.* injection (0.7ml saline, 100mg/kg SS-31). To prevent possible adverse effects from administering too much fluid to sepsis surviving mice, SS-31 concentration was doubled to allow for only 0.35mL of saline to be injected once daily on days 5-10. Saline only was given to sepsis control mice. All resuscitation began at 12 hours, after the development of severe sepsis. Drug treatment had no effect on overall survival from otherwise lethal (LD_{100}) sepsis (**Figure 5.2A**).

To evaluate the impacts of SS-31 administration on acute sepsis severity, we collected blood at 6-hours to assess IL-6 levels. When compared to their saline-treated sepsis controls, sepsis survivors treated with SS-31 showed no differences in 6-hour IL-6 levels (**Figure 5.2E**), an inflammatory cytokine that increases during the acute phase of sepsis. Further indicating SS-31 administration did not alter

sepsis severity were similar mortality rates, degrees of acute hypothermia, and long-term weight loss amongst all the CS injected mice, regardless of SS-31 status (**Figure 5.2B-D**). When compared to non-sepsis control mice, SS-31 treated sepsis survivors and saline-treated survivors demonstrated marked splenomegaly that is not dependent on drug treatment status. Taken together, these results displayed in **Figure 5.2** indicate SS-31 administered after sepsis development did not have any impact on overall sepsis severity.
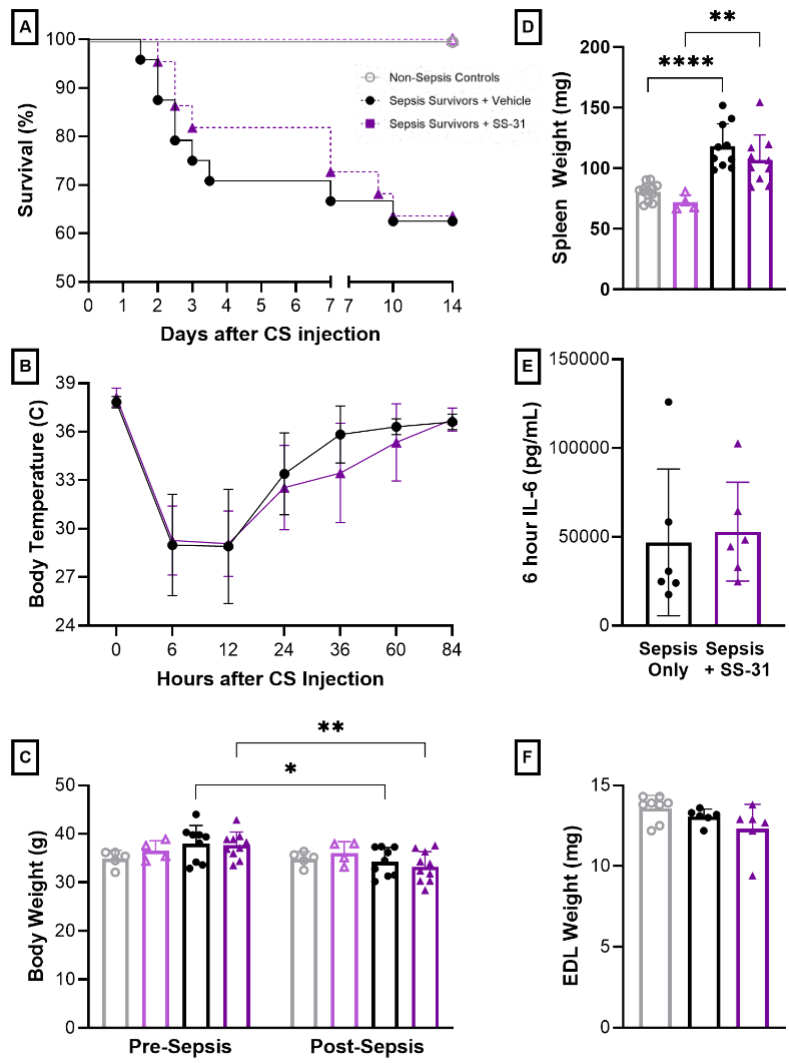
Figure 5-2. SS-31 treatment did not impact overall sepsis severity.

Mice were divided into groups based on pre-sepsis body weights and 6h body temperatures. (**A**) Both SS-31 and vehicle treated groups demonstrated ~65% survival from otherwise lethal sepsis. (**B**) Body temperatures were equivalently decreased as a result of sepsis. (**C**) Prior to sepsis, body weights were equivalent for all mice, and only sepsis survivors suffered from similar degrees of weight loss. (**D**) Splenomegaly was clear following sepsis in both treatment and vehicle groups, as were 6h IL-6 levels (**E**). Post-sepsis EDL weights were obtained upon euthanasia, and there were no group-based differences.

5.4.1.2   SS-31 reduced typical histological and biochemical alterations that occur after sepsis.

Following euthanasia, tissues were subjected to biochemical and histological analyses. RNA sequencing revealed that SS-31 significantly helped in preventing alterations to the transcriptome, as emphasized by the heatmap in **Figure 5.3**. At this day 28 timepoint, there were 58 DEGs (65 downregulated, 29 upregulated) for standard sepsis survivors and 94 DEGs (54 downregulated, 24 upregulated) for SS-31 treated sepsis survivors (**Figure 5.4**). Samples clustered clearly into saline treated sepsis survivors and naïve animals. SS-31 treated animals mixed with both groups upon principal component analysis (**Figure 5.4**). The two samples closer to the naïve mice are the middle two heatmap columns in the SS-31 samples emphasizing minimal changes occurred when compared to baseline (as emphasized by more similar shading patterns to naïve samples). DEGs were subjected to pathway analysis for implicated GO: Cellular Component pathways (**Figure 5.5**, **Table 5.1**). Out of the top 10 downregulated pathways for saline-vehicle treated survivors, 4 out of the top 10 terms were related to mitochondria. There were no significantly upregulated pathways, despite multiple upregulated genes for the saline treated sepsis survivors. SS-31 treated survivors did not contain any mitochondria-related terms in their top pathways. Downregulated pathways heavily related to myofibrillary processes and extracellular structures, while upregulated terms favored ribosomal subunits. Next,

I subjected the DEGs common to both groups to a separate pathway analysis using gProfiler (**Figure 5.6**). Out of the top 15 altered GO:CC processes, mitochondria were not implicated. This indicates that changes that are common in both SS-31 treated sepsis survivors and vehicle treated sepsis survivors are not related to mitochondrial abnormalities, as the term does not appear. Rather, cytoplasmic and myofibrillar changes persisted despite SS-31 treatment.
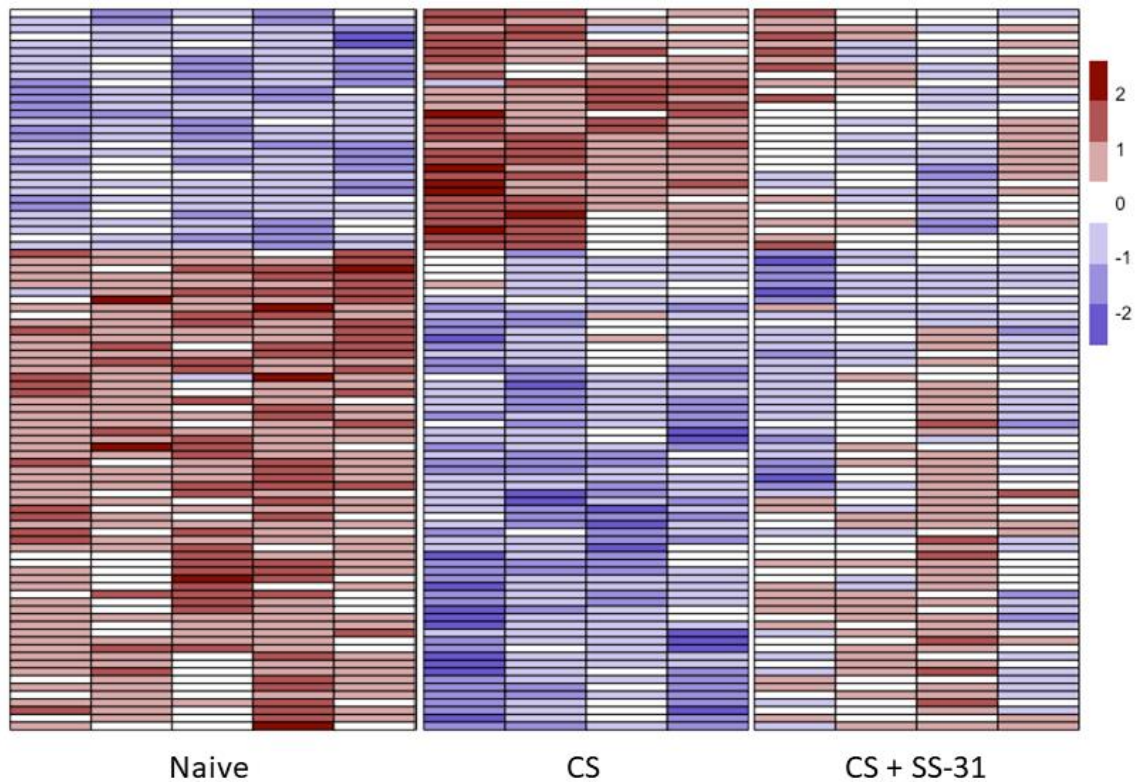
Figure 5-3. Heatmap of naïve mice, sepsis survivors, and sepsis survivors treated with SS-31.

Following euthanasia on day 28, TA muscles were utilized for bulk RNA sequencing. This analysis revealed SS-31 prevented as many changes to the transcriptome.
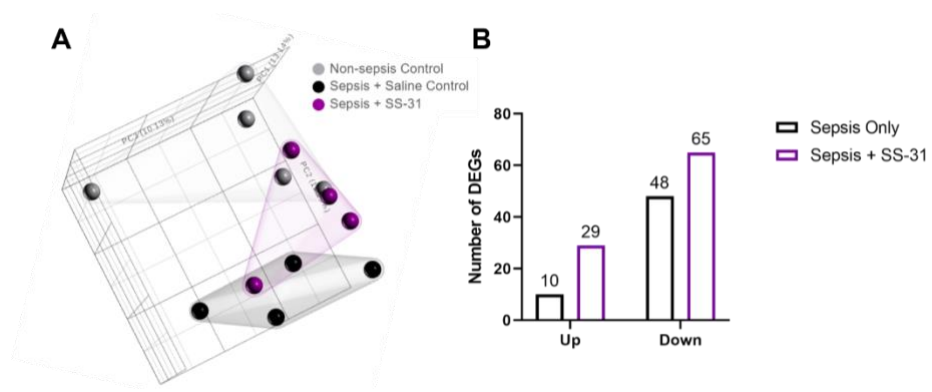
Figure 5-4. PCA and DEG analysis for saline and SS-31 treated sepsis survivors at day 28 post CS injection.
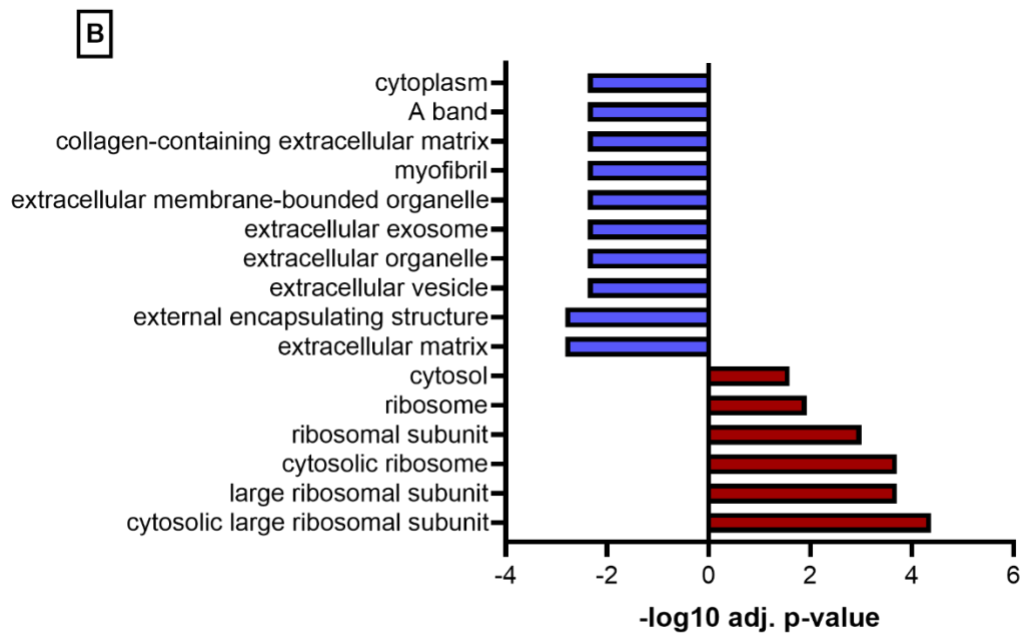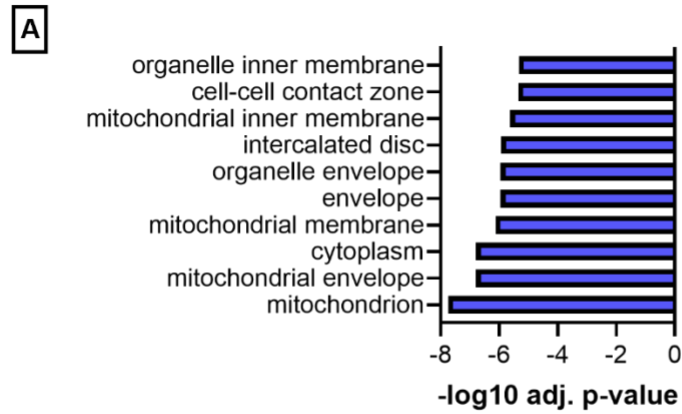
Figure 5-5. Altered pathways in saline and SS-31 treated sepsis survivors.
(**A**) Pathway analyses for saline treated sepsis survivors. (**B**) Pathway analyses
for SS-31 treated sepsis survivors.

Table 5.1 GO: Cellular Component pathways at 28 days post-sepsis with and without SS-31 treatment

		Pathway	Term ID	Adj P-value	Neg. Log10 Adj P-value
Day 28 Post-Sepsis: GO:CC Pathways	UP	N/A	N/A	N/A	N/A
	DOWNREGULATED	mitochondrion	GO:0005739	1.79E-08	7.747053051
		mitochondrial envelope	GO:0005740	1.63E-07	6.787221495
		cytoplasm	GO:0005737	1.63E-07	6.787221495
		mitochondrial membrane	GO:0031966	7.35E-07	6.133769596
		envelope	GO:0031975	1.11E-06	5.952993844
		organelle envelope	GO:0031967	1.11E-06	5.952993844
		intercalated disc	GO:0014704	1.15E-06	5.937443859
		mitochondrial inner membrane	GO:0005743	2.36E-06	5.627215103
		cell-cell contact zone	GO:0044291	4.44E-06	5.352713133
		organelle inner membrane	GO:0019866	4.69E-06	5.329064999
Day 28 Post-Sepsis +SS-31 Treatment: GO:CC Pathways	UPREGULATED	cytosolic large ribosomal subunit	GO:0022625	4.14E-05	4.382740718
		large ribosomal subunit	GO:0015934	0.00019741	3.704639458
		cytosolic ribosome	GO:0022626	0.00019741	3.704639458
		ribosomal subunit	GO:0044391	0.00098652	3.005892577
		ribosome	GO:0005840	0.01172355	1.930940971
		cytosol	GO:0005829	0.02591358	1.586472662
	DOWNREGULATED	extracellular matrix	GO:0031012	0.00151848	2.818589772
		external encapsulating structure	GO:0030312	0.00151848	2.818589772
		extracellular vesicle	GO:1903561	0.00416942	2.379923931
		extracellular organelle	GO:0043230	0.00416942	2.379923931
		extracellular exosome	GO:0070062	0.00416942	2.379923931
		extracellular membrane-bounded organelle	GO:0065010	0.00416942	2.379923931
		myofibril	GO:0030016	0.00416942	2.379923931
		collagen-containing extracellular matrix	GO:0062023	0.00416942	2.379923931
		A band	GO:0031672	0.00416942	2.379923931
		cytoplasm	GO:0005737	0.00416942	2.379923931
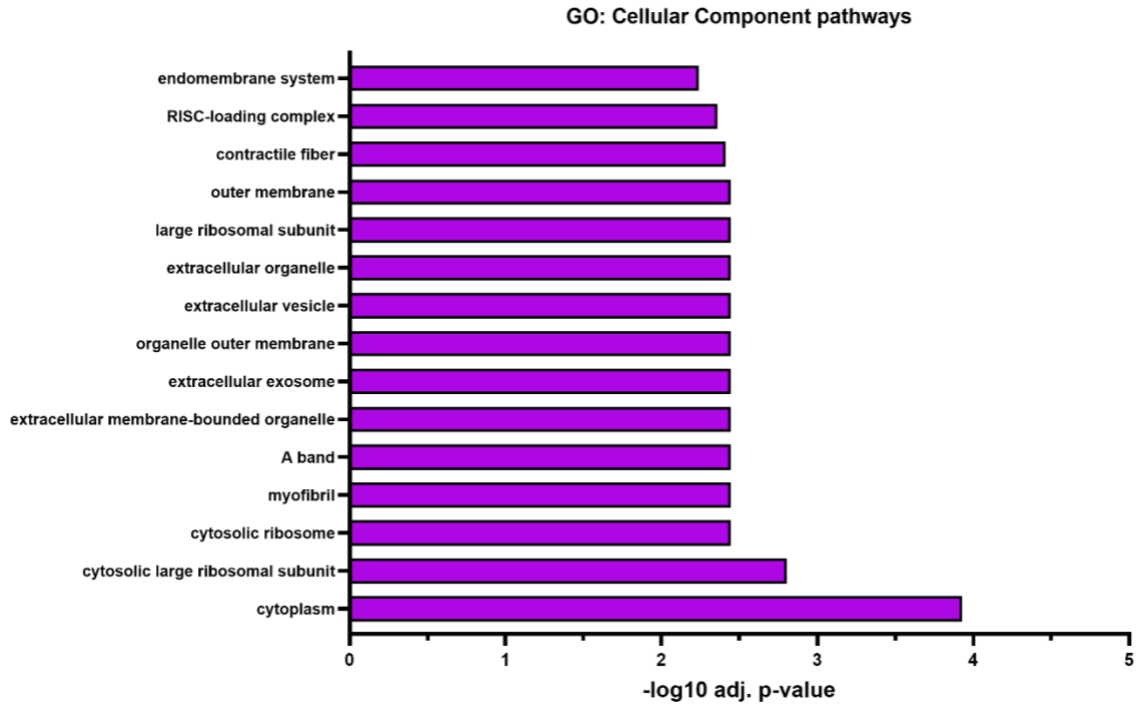
Figure 5-6. Common DEGs between saline and SS-31 treated sepsis survivors reveal remaining alterations are not related to mitochondria.

After subjecting the DEGs that were altered in both saline and SS-31 treated sepsis survivor mice to pathway alteration analyses in gProfiler, it is clear that SS-31 protected mitochondria.

Further emphasizing that SS-31 protects against mitochondrial damage are data from NADH and SDH histological staining (**Figure 5.7**). While sepsis leads to less intense staining in saline treated survivors, animals treated with SS-31 did not demonstrate this negative effect. It is thus clear that the oxidative enzymes NADH and SDH have more activity in non-sepsis control and SS-31 treated sepsis survivors, as noted by more intense staining when compared to saline treated sepsis survivors.
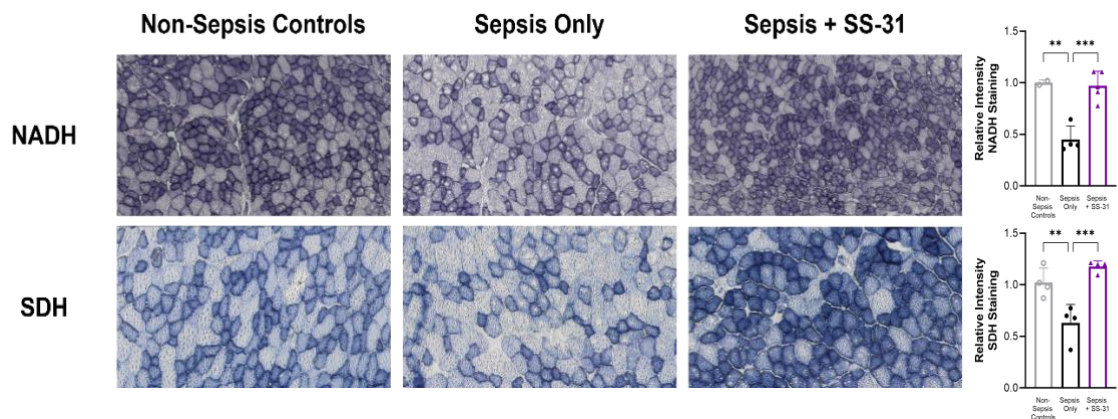
Figure 5-7. NADH/SDH staining in NSC, CS and CS+SS-31 TA sections. NADH (top) and SDH (bottom) staining revealed that while sepsis normally leads to significant decrease in staining intensity, SS-31 protects against this deficit. Quantification of at least 4 different samples from each group confirms this.

While sequencing and histological data indicate mitochondria are protected as a result of SS-31 administration, when probing for mitochondrial complexes I-V, there were no significant differences across any of the samples at day 28—even standard resuscitation sepsis survivors did not show a significant decrease for any protein marker. Further, no significant changes in 3-NT or 4-HNE levels were observed utilizing these 28 day samples. This data indicates that mitochondrial dysfunction may be contributing to persistent muscle weakness in chronic muscle weakness and not just mitochondrial damage.

5.4.1.3   SS-31 treated mice did not exhibit skeletal muscle weakness

Mice treated with SS-31 did not demonstrate post-sepsis skeletal muscle weakness. Indeed, when compared to their non-sepsis controls, SS-31 treated sepsis survivors demonstrated no differences (**Figure 5.8**). Meanwhile, vehicle treated mice suffered 15.3% decreases in maximum specific force. Therefore, it is clear SS-31 treatment during acute sepsis prevented the later development of post-sepsis skeletal muscle weakness.
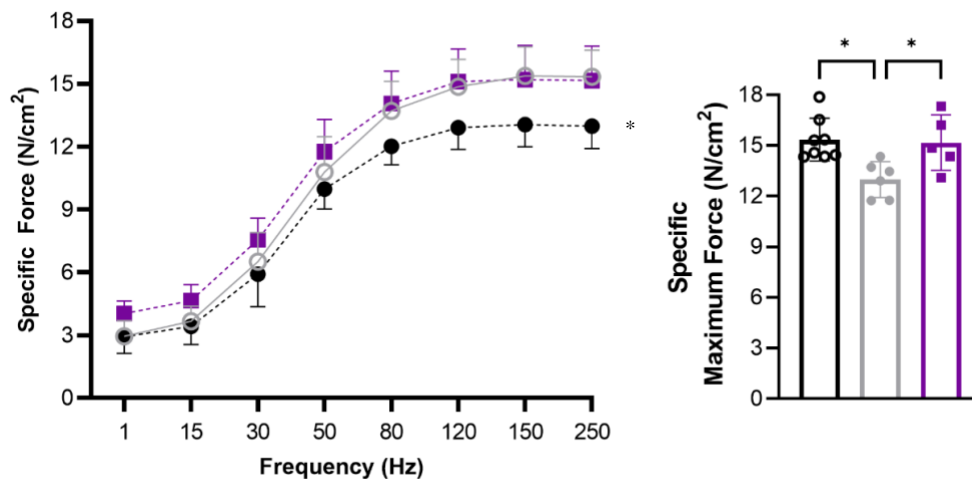
Figure 5-8. SS-31 treated mice did not exhibit any skeletal muscle weakness. (A) Force-frequency curves were significantly different for the non-sepsis control group and sepsis + vehicle group. However, SS-31 treated mice displayed no differences from non-sepsis controls and were even stronger at physiological frequencies (30-50Hz). (B) When looking at maximum force, non-sepsis control mice had no difference than sepsis survivors treated with SS-31, while vehicle treated sepsis survivors suffered 15.3% force loss. When compared to their sepsis surviving controls, SS-31 treated mice were 14.8% stronger.

5.4.2 Hyperoxia therapy during acute sepsis

To evaluate if a lack of oxygen was driving mitochondrial damage, we decided to evaluate if putting mice into a hyperoxia chamber during acute sepsis could (1) improve survival by mediating the effects of acute sepsis, and (2) limit

post-sepsis skeletal muscle weakness. For this study, we induced severe sepsis in late-middle aged mice, and at the 12h mark, mice were separated into a hyperoxia study group and a standard sepsis control group. All mice received resuscitation 2x daily for 5 days with antibiotics and saline beginning at 12h, as usual. Mice in the hyperoxia chamber were slower to return to their baseline temperatures after sepsis induction, and mortality was significantly higher amongst the mice in the chamber. We therefore discontinued this study, as the negative impact on acute sepsis survival could not outweigh any potential improvements in post-sepsis muscle weakness.

5.4.3 Exercise therapy

Following sepsis recovery and development of muscle weakness, mice were allowed access to either a locked or unlocked running wheel connected to monitoring software to record activity over the 6-week running treatment. At the end of the 7th week, (1 week of sepsis and recovery prior to the 6wk running protocol) animals were subjected to both *in vitro* and *in vivo* function testing. However, similar to the clinic, exercising mice did not demonstrate greater function compared to sedentary sepsis survivors (**Figure 5.9 and 5.10**). While mice showed clear weakness even at 7 weeks post-sepsis, they did not demonstrate any difference as a result of exercise treatment. While some of the animal did not run frequently, exclusion of these "sedentary exercisers" from the true "exercisers" did not lead to any differences emerging. However, *in vivo* testing (**Figure 5.10**) indicated that it is possible not all mice demonstrate chronic muscle weakness at the 7-week mark, similar to post-sepsis muscle weakness in human sepsis survivors.
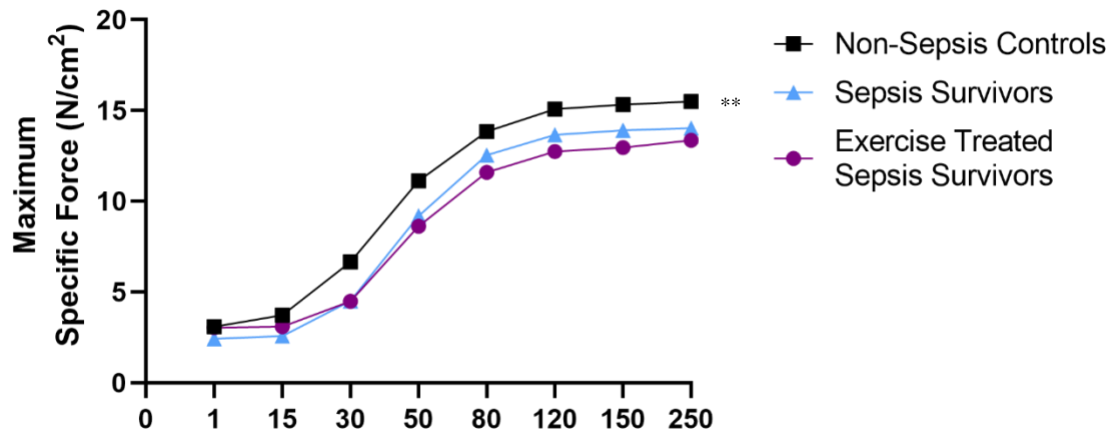
Figure 5-9. *In vitro* **muscle function testing revealed exercise did not resolve post-sepsis skeletal muscle weakness to non-sepsis control levels.**

In vitro testing at 7 weeks revealed no differences in sepsis survivors and exercise treated sepsis surviving mice, though there was a significant effect as a result of sepsis (n=6 per group).
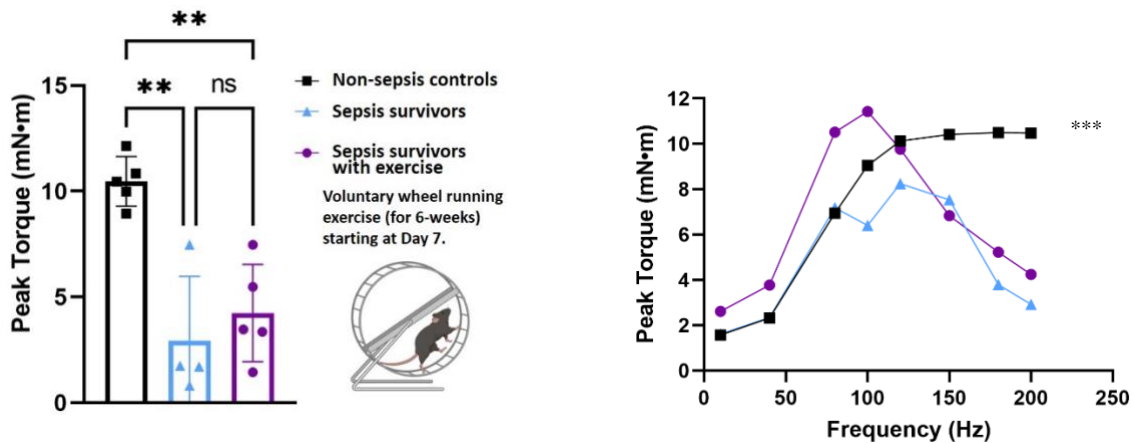
Figure 5-10. *In vivo* **function testing for peak torque following post-sepsis exercise intervention.**

In vivo function testing (n=5 per group) revealed that post-sepsis skeletal muscle weakness is still evident at the 7-week post sepsis mark, noted by significant decreases in the peak torque at 200 Hz of both sepsis survivors and sepsis survivors treated with exercise. While early frequencies indicated a positive effect of exercise, fatigue occurred quickly in post-sepsis animals.

When looking at individual stimulations in **Figure 5.11**, it is clear in the 180-200 Hz range that 3 out of the 4 standard sepsis survivors demonstrate clear chronic weakness. However, one mouse is significantly stronger than the others, despite it also undergoing severe sepsis. This indicates that not all mice develop post-sepsis skeletal muscle weakness, similar to humans. It also emphasizes that a larger cohort of animals should be used for experimental sepsis studies to ensure the results are well-powered.
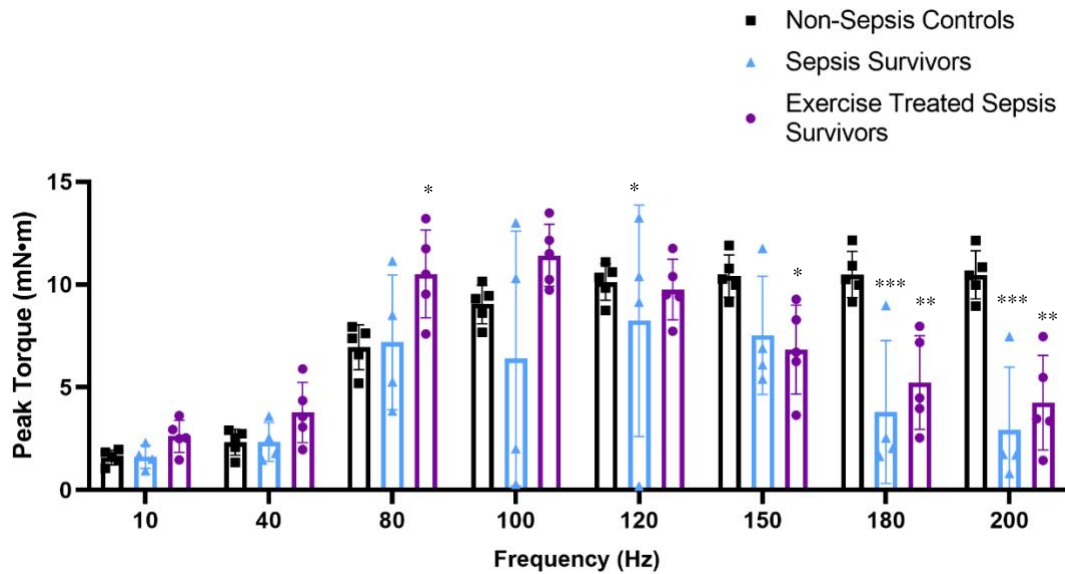
Figure 5-11. *In vivo* **muscle function at each frequency.**

5.4.4 Nicotinamide mononucleotide

Due to its ability to increase mitochondrial quality, NMN was utilized as a true therapeutic to treat already developed muscle weakness. Mice that were 1-week post CS injection (sepsis survivors) were injected with either NMN (300 mg/kg) or saline in equal volumes 1x every day for 1 week. Animals were then euthanized and subjected to *in vitro* function testing. Pre-sepsis bodyweight was similar in all animals (**Figure 5.12**), as was sepsis severity in CS-injected animals. Muscle size was the same for all mice, as indicated by similar PCSAs. When normalized to PCSA, *in vitro* testing for maximum force revealed that mice treated with NMN trended to be similar to their non-sepsis counterparts, while saine treated mice suffered weakness after sepsis. However, due to low sample numbers, no statistical analyses could be performed.
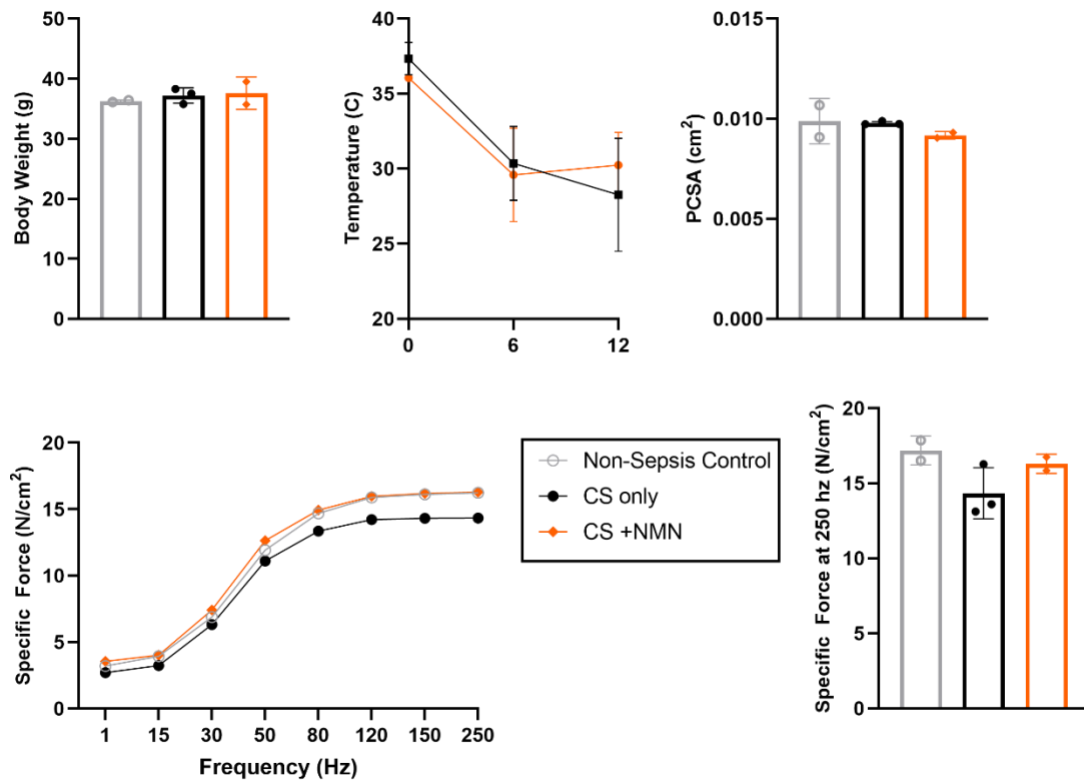
Figure 5-12. NMN treatment after complete recovery from sepsis appeared to help with muscle function.

Mice had equivalent pre-sepsis body weights (**A**) and demonstrated similar degrees of hypothermia as indicated by acute phase hypothermia (**B**). Upon euthanasia for *in vitro* function testing, mice demonstrated no differences in PCSA (**C**), while force trended to be higher in sepsis survivors treated with NMN (**D, E**). However, since n=2-3 per group, no statistics could be calculated.

5.5 Discussion

Therapeutic strategies included attempts at mediating the acute sepsis event itself via access to an oxygen rich-chamber, prevention of muscle weakness through SS-31 administration following severe sepsis development, and treatment of already present post-sepsis muscle weakness with NMN or voluntary wheel-running exercise intervention.

While we attempted to provide mice with higher levels of oxygen for increased consumption during acute sepsis via our hyperoxia chamber study, we found out that this had a negative impact on survival. This finding indicates that instead of too little substrate to prevent proper oxygen use, oxygen may be being misused and actively contribute to worsened sepsis and subsequent significant post-sepsis muscle weakness. Providing more oxygen could have a detrimental effect, worsening overall survival by adding more fuel (oxygen) to the figurative fire (in this case, possible ROS, TLS, and free radical production) This would be similar to what is seen in the clinic when oxygen saturation levels are too high and become toxic (136-139). Indeed, we saw that mice demonstrated worsened outcomes (prolonged decreased body temperature and overall survival rates) as a result of increased oxygen levels, as there were no differences in bacteremia levels (an indicator of sepsis severity) prior to oxygen treatment. Due to this negative impact on survival, we did not further pursue use of a hyperoxia chamber as a therapeutic avenue, nor did we examine how higher oxygen concentration during acute sepsis impacted post-sepsis muscle function.

Exercise, while commonly touted as a "cure all" did not cure post-sepsis muscle weakness. This finding is similar to clinical post-sepsis muscle weakness, where physical therapy and exercise intervention do not show major positive effects (140, 141). While this study lacked a true non-sepsis running control group, the lack of difference between the sedentary and exercised sepsis groups emphasizes voluntary exercise won't alleviate weakness. There were some tendencies that post-sepsis mice did not want to run. Indeed, only half of the animals ran more than 6km/day and were included in post-sepsis function

analyses. However, whether this was a result of sepsis related fatigue is unclear due to the lack of an acclimation period and a non-sepsis running control group. This experiment would therefore be improved by adding these controls to evaluate which mice have a proclivity for running. Allowing a pre-experiment running acclimation period would allow for the exclusion of "non-runners" and enable evaluation of running willingness after sepsis. Resistance exercise has greater impacts on mitochondrial quality. In having mice run on a weighted wheel that increases in weight over the course of the running protocol (142, 143), the animals would engage in progressive resistance training. Overall, though, it is unlikely exercise is the most clinically relevant treatment because of compliance and accessibility issues for the human population, especially aged individuals. This is why I also evaluated pharmacological interventions.

Pharmacological treatment led to the highest success rate in reducing post-sepsis skeletal muscle weakness. SS-31 completely prevented skeletal muscle weakness in sepsis survivors as indicated by no changes in maximum specific force between non-sepsis controls and SS-31 treated sepsis survivors. I also carried out sequencing on gastrocnemius hindlimb tissue to evaluate how SS-31 administration affected gene expression. While these animals were not euthanized until day 28, metabolic changes were still seen in vehicle treated controls, with mitochondria-related terms registering as significantly downregulated (**Table 5.1**). However, these terms did not appear as being altered in the SS-31 treated sepsis survivors, emphasizing the drug protected against mitochondrial abnormalities. Unexpectedly, there were more DEGs for the SS-31 treated sepsis survivor group. However, these DEGs did not translate to mitochondrial pathways, while DEGs for the saline vehicle treated sepsis survivors did. This emphasizes that SS-31 protected against long term mitochondrial alterations. There were some common DEGs for the groups, but upon pathway analysis, mitochondrial abnormalities were not implicated. Instead, myofibrillar and cytoplasmic changes were. This emphasizes that these are sepsis-induced changes that remain unresolved by SS-31. Contrary to my expectations, protection against mitochondrial abnormalities at the genomic level did not translate to protein level changes in the OxPhos

Complexes I-V in SS-31 treated animals. It would be very interesting to repeat this study in a time-course fashion to evaluate if SS-31 protects from early mitochondrial damage that we see by day 4, or if there is an accumulation of mitochondrial abnormalities that are subsequently resolved by treatment. In utilizing high resolution respirometry (Oroboros Oxygraph 2k system), we would be able to evaluate mitochondrial function and ROS production at multiple timepoints throughout sepsis development and recovery. Treating with SS-31 would likely lower ROS production, thereby helping preserve mitochondrial function and preventing long-term skeletal muscle function deficits. Meanwhile, saline/vehicle treatment may confirm that significant mitochondrial damage occurs, driving dysfunction, and these couple to create chronic muscle weakness when not treated with a protecting agent.

When evaluating pharmacological interventions for treating established post-sepsis muscle weakness, SS-31 (given after sepsis resolution, instead of immediately after sepsis development) and NMN were considered. However, while SS-31 can repair damaged mitochondria, it does not have any action in stimulating biogenesis. NMN does have this effect by increasing not just biogenesis, but also fission and fusion. As such, I utilized NMN in a sepsis induced muscle weakness treatment experiment. Contrary to normal, this experiment faced a problem with sepsis survival. While normally attrition rates are high, I lost a majority of animals to sepsis in this experiment. Therefore, no statistical analyses could be carried out in this study. Possibilities for why this issue regarding attrition rate occurred include alterations in individuals performing animal care and sepsis resuscitation, multiple changes in animal location from our separate animal exam room back to the DLAR facility in the basement of HKRB, and leaving the CS stock in the water bath for longer (which could enable increased bacterial growth and greater acute infection with faster subsequent sepsis progression). Repeating this study would provide a better indication on how much function NMN can restore after sepsis, especially if utilizing an *in vivo* function testing approach that also evaluates atrophy.

5.6 Conclusions

Since post-sepsis muscle weakness is largely driven by mitochondrial abnormalities, protecting mitochondria has the ability to prevent and treat this chronic complication. While exercise did not confer clear beneficial effects, similar to clinical manifestations of PSS, pharmacological intervention targeting mitochondria prevented mitochondrial abnormalities and increased muscle function after sepsis. NMN showed promise in treating already developed muscle weakness, while SS-31 completely prevented the conditions development when administered with resuscitation fluids after the development of severe sepsis. This provides hope that intervention may be possible in human chronic muscle weakness during sepsis.

CHAPTER 6. DISCUSSION AND FUTURE DIRECTIONS

6.1 Major findings

Post sepsis skeletal muscle weakness debilitates sepsis survivors and contributes to a negative quality of life. Further, weakness serves as a risk factor for post sepsis complications (56, 57). While previous research has linked mitochondrial abnormalities to post-sepsis weakness, this work is the first to demonstrate that mitochondrial abnormalities *cause* post-sepsis weakness. Further, my work demonstrates that mitochondria can serve as therapeutic targets in preventing and treating post-sepsis complications.

The first aim of this project was to characterize mitochondrial abnormalities as they pertain to post-sepsis muscle weakness over time. Utilizing *in vivo* function testing, we revealed that muscle weakness persists at least 10 weeks in sepsis surviving mice (Chapter 3). This is accompanied by significant changes to the transcriptome and mitochondrial morphology. Next, I utilized a transgenic mouse strain overexpressing the mitochondrial protecting enzyme MnSOD. MnSOD-TG sepsis surviving mice did not demonstrate as many mitochondrial abnormalities which ultimately translated to a lack of muscle weakness following equally severe sepsis when compared to WT controls (Chapter 4). Finally, I evaluated the efficacy of mitochondria-targeting therapeutics (Chapter 5). SS-31 protected against post-sepsis skeletal muscle weakness and mitochondrial dysfunction when given during sepsis. Similar to clinical findings, voluntary exercise therapy had no major benefit. However, pharmacological interventions showed significant promise. NMN, while only tested in a preliminary study, protected against post sepsis muscle weakness.

Together these results implicate mitochondrial damage as *main causes* of post-sepsis skeletal muscle weakness. Further, mitochondria can be targeted therapeutically to prevent (and likely reverse) debilitating post-sepsis complications related to muscle function. These successful pre-clinical results may lead to significant clinical breakthroughs.

6.2 Future directions

6.2.1 Evaluating the role of FFA in post-sepsis metabolism

As mentioned in the discussion of Chapter 3, it is possible that free fatty acids (FFA) serve as the energy substrate for metabolism following sepsis, rather than glucose. While glucose normally serves as the major substrate in metabolism, when energy demands are elevated as they are during sepsis, lipolysis gets upregulated to enable triglyceride conversion to glycerol and free fatty acids (144, 145). The FFAs can then be converted to energy through beta-oxidation and serve as substrates for the TCA cycle. Elevated plasma FFAs are followed by decreases in glucose oxidation and glycogen synthesis, in addition to lower free glucose levels. However, increased plasma FFA does not cause a change in intramuscular glycogen concentrations, something we saw in our metabolomics analyses. Researchers have also found that hepatic gluconeogenesis and glycogenolysis increase as insulin resistance emerges, driving hyperglycemia. In some of the animal experiments in this dissertation, we took the blood glucose levels of the mice throughout sepsis. Hyperglycemic mice had worsened outcomes overall. In the human population, sepsis survivors are known to develop insulin resistance and take on a diabetic phenotype (146-149). Accordingly, it is possible that insulin resistance is worsening post-sepsis skeletal muscle weakness.

It would be ideal to perform a lipidomic experiment to evaluate how lipid levels changes after sepsis. Additionally, utilizing stable isotope tracers would allow for the evaluation of both FFA metabolism and shuttling of G6P to the pentose phosphate pathway. Together, these results would better elucidate how metabolism is altered following sepsis and allow more targeted therapeutic intervention. If this is occurring, preventing the use of alternative metabolic pathways by protecting mitochondria could prevent the energy crisis we see in our plasma metabolomic data. It is possible that a combination of pharmacological agents may need to be used to restore post-sepsis muscle function, and enabling efficient FFA metabolism during acute sepsis may be a key to preventing subsequent damage.

6.2.2 Introducing atrophy into this model during acute sepsis

A criticism the current model faces is that atrophy does not last as long in our murine sepsis survivors as compared to human patients. Introducing a cast to immobilize the limbs and induce severe atrophy at a level similar to bed-ridden ICU patients would further increase the translation of this animal model and enable the evaluation of therapeutic strategies elucidated earlier in this dissertation work when atrophy presence is more of a factor. While long term atrophy status in patients has little relation to muscle strength (42), increasing atrophy during acute sepsis may provide more insight into acute sepsis muscle weakness treatment and how early weakness driven by atrophy affects long-term weakness. In introducing additional acute atrophy, we can see if this induces additional long-term function deficits that we do not currently see, such as significant fibrosis. This would only further increase the clinical relevancy of this model and positive findings regarding interventions reducing post-sepsis weakness.

6.2.3 Later treatment with previously successful therapeutics

SS-31 proved to be a successful therapeutic when administered after the development of sepsis but still during the acute sepsis event itself. However, since muscle weakness develops in a progressive manner, it may be possible to intervene after acute sepsis survival, and not just during the condition. This is particularly important as a majority of sepsis survivors are already suffering from post-sepsis muscle weakness. Administering SS-31 at a higher concentration beginning on day 7 after CS injection may have beneficial effects that could be applied to sepsis survivors who already have developed skeletal muscle weakness. Indeed, when administered to non-sepsis control mice, those given SS-31 instead of a saline vehicle demonstrated increased maximum force production (**Figure 6.2**).

While NMN administration were positive, multiple follow up studies are necessary due to the preliminary nature of the results. Increasing the dose of NMN and/or increasing the frequency with which the drug is administered (either 1x daily

for two weeks instead of 1x every other day for two weeks or 500 g/kg instead of 300/kg) may reverse the significant weakness demonstrated at 10 weeks in sepsis surviving mice. Utilizing the *in vivo* peak isometric torque testing system would allow measurement in the same mice over time to ensure only mice that develop post-sepsis muscle weakness are randomized into the treatment/saline vehicle groups. Then, success of treatment could be established by one of two criteria (1) if drug treatment increases function ability as compared to changes in saline treated mice, and (2) if drug treatment returns function to pre-sepsis function levels. In this sense, drug treatment could be judged on if it helps treat muscle weakness post-sepsis and/or if the intervention cures symptomatic weakness. As such, this testing mechanism should be applied to all future drug study trials where function is a primary outcome.

6.2.4 Mitochondrial transplantation as a therapeutic

This dissertation work established that significant mitochondrial damage occurs during acute sepsis and persists through at least day 28, while functional deficits persist through at least day 70. Mitochondrial abnormalities further accumulate from day 4 through 14 as evidenced by the time-course study discussed in chapter 3. It is therefore likely that providing skeletal muscle with healthy mitochondria capable of utilizing pyruvate efficiently to create ATP without excess free radical and reactive oxygen species production would reduce the overall level of mitochondrial abnormalities and subsequent skeletal muscle weakness. Rather than using pharmacologic strategies as described above, another strategy is to simply provide new, properly functioning mitochondria. In utilizing mitochondrial transplantation, healthy mitochondria could be delivered to the target tissue. Delivering mitochondria via intramuscular injection would prevent a systemic response and specifically target muscle tissue.

6.2.5 Utilizing aged animals for post-sepsis muscle weakness study

While carrying out the bulk of this dissertation study, I also took efforts to refine our animal model of sepsis to work in aged animals (22-24 month-old male C57BL/6 mice). While middle-aged individuals have higher rates of sepsis

compared to young individuals, aged patients have the highest risk for mortality and post sepsis complications. As such, using animals equivalent to aged humans (~80 years of age), would increase the clinical relevancy of this project even further. However, our current sepsis induction and resuscitation protocol used in late-middle-aged mice has limited success in rescuing aged animals. To enable survival, I utilized a variety of approaches, such as increasing fluid levels during resuscitation, decreasing saline levels, and beginning intervention with antibiotics and fluids earlier (i.e., 6h instead of 12h after CS injection), either singly or in combination (**Figure 6.2**). I also investigated if endotoxemia during acute sepsis causes death in aged animals, while it does not in young and middle-aged mice.

First, I confirmed that 250 uL of CS was a nearly lethal dose (LD_{87}) in 22-month-old C57BL/6 male mice. Here, 23/25 mice died after receiving an *i.p.* injection of CS. I then evaluated how many animals could be rescued using our standard late-stage resuscitation protocol beginning at 12 hours to serve as a standard resuscitation control. Here, 700uL of saline is injected subcutaneously and 300 uL of saline mixed with antibiotics. After noting that 36% (9/25) of mice survive, I decreased the waiting period, only allowing 6h to pass before starting resuscitation. In doing so, more mice survived (48%, or 12/25) while still allowing severe sepsis to develop. While CFU analyses utilizing 12h and 6h blood from the standard and early intervention studies were similar, it is likely that organ damage was significantly less in the early intervention group, therefore leading to higher survival from the same dose of CS. Antibiotic administration in aged animals does clear bacterial loads, as bacterial load resolved by 36h in septic animals. Despite clearance of bacteria, mice still died after 36h in both the 6 and 12h groups. These deaths indicate that animals that received 6h resuscitation still suffered from sepsis, not just an acute infection quickly cleared by administration of antibiotics at 6h. The higher survival rate by intervening earlier emphasizes clinical data indicating that mortality increases for every hour sepsis intervention is delayed (41).

To try and keep this model as clinically relevant as possible and thus use late-stage resuscitation, I evaluated whether resuscitation fluid amount had an impact on survival. Dehydration of the animals is an issue during acute sepsis, as they do not move and drink water as normal. Therefore, I tested adding more fluids (1mL of saline instead of .7 mL *s.c.* injection) as part of the standard resuscitation protocol beginning at 12 hours. This strategy, however, worsened survival (only 33% of animals survived) as compared to standard resuscitation. Worried about excess fluid causing kidney damage, I next tried a reduced level of saline (0.3 mL saline instead of 0.7mL *s.c.* injection). This had no impact on survival, so this strategy was not further pursued. Previous attempts in the lab to utilize aged animals included providing heating pads under half of the cage to help maintain a higher core temperature for better survival. This intervention helped with survival, as 5/8 animals survived (62.5%).

Still curious about why death was occurring with early (i.e., 6h) intervention, I evaluated if endotoxin released due to the death of bacteria when antibiotics are introduced could be driving mortality in aged animals in addition to organ damage that accompanies sepsis. I tested this by using heat inactivated cecal slurry as confirmed by bacterial plating of both anaerobic and aerobic bacteria. With only 57% survival, it is likely endotoxemia is contributing to the mortality rate in 22+ month-old mice, and likely means they are not rescuable at all if sepsis is to fully develop prior to resuscitation. Thus, the best way to study long-term muscle dysfunction in aged animals is to utilize an early intervention strategy beginning at 6h instead of 12h. To ensure sepsis and its associated organ damage is occurring, organ damage markers need to investigated utilizing blood taken at 36-48h, such as performing a Western for NGAL, a kidney damage marker. This would enable us to clarify if sepsis occurs within a few hours of CS injection and if intervening at 6h is an appropriate model to allow for the development of a full sepsis event that causes long term dysfunction in aged animals.

This would enable more clinically relevant study, as sepsis occurs at alarmingly higher rates in aged individuals, as does post-sepsis syndrome and

lasting complications. Further, post-sepsis interventions discovered in middle-aged animals may not have the same efficacy as those in aged animals, much less the human population. Aged animals, like humans, have compounding muscle weakness as a result of aging (sarcopenia) that may worsen post-sepsis weakness. Therefore, studies testing both prevention and treatment therapeutics should also be confirmed in aged animals.
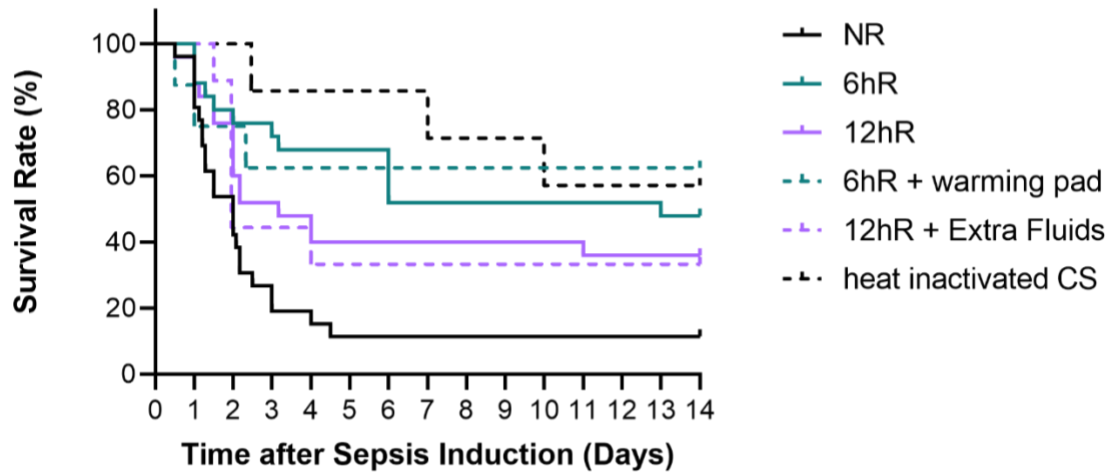
Figure 6-1. Survival comparison of sepsis resuscitation procedures in aged (22–24-month-old) mice

6.3 Conclusions

In utilizing a time-course study, we were able to determine that post-sepsis skeletal muscle weakness occurs in a progressive manner, worsening after the resolution of sepsis and acute phase associated atrophy. Mitochondrial damage in the same time-course study accumulated progressively, with morphological, histological, and transcriptional changes increasing after recovery from acute sepsis. Subsequent sepsis experiments in mice overexpressing MnSOD, a mitochondria-protecting antioxidant enzyme, confirmed that mitochondrial abnormalities cause this post-sepsis skeletal muscle weakness. Further, therapeutics aimed at protecting mitochondria during sepsis prevented this long-term complication. Our results indicate that pharmacological intervention targeting post-sepsis mitochondrial abnormalities may be able to treat lasting skeletal muscle weakness.

APPENDIX 1. ABBREVIATIONS

3-NT: 3-Nitrotyrosine

ADP: Adenosine diphosphate

ATP: Adenosine triphosphate

CFU: Colony forming units

CLP: Cecal ligation and puncture

COX: Cytochrome C oxidase

CS: Cecal clurry

EDL: Extensor digitorum longus

FBS: Fetal bovine serum

FFA: Free fatty acids

GAS: Gastrocnemius

i.p.: Intraperitoneal

ICU: Intensive care unit

IL-6: Interleukin-6

IPM: Imipenem

LD_{100}: 100% lethal dose

LPS: Lipopolysaccharide

MnSOD: Manganese superoxide dismutase

MT: Mitochondrial

NADH: Nicotinamide adenine dinucleotide

NGS: Normal goat serum

NMN: Nicotinamide mononucleotide

PC: Protein carbonyl

PSS: Post-sepsis syndrome

RNS: Reactive nitrogen species

ROS: Reactive oxygen species

s.c.: Subcutaneous

SOL: Soleus

SS-31: Szeto-Schiller-31

TA: Tibialis anterior

TLS: Toxic lipid species

APPENDIX 2. CODE USED FOR DATA PROCESSING IN R 4.2.2

When raw data back from sequencing, it typically comes either as a BAM, SAM, or FASTQ file. To convert these multi-gigabyte files into informative data, building a sequencing pipeline is critical. A pipeline typically consists of trimming, alignment, counting and normalization of the reads, and differential expression to finally identify differentially expressed genes (or DEGs). To accomplish your own RNAseq analysis, you will need a Linux environment or server and R 4.2.2+. You can achieve a Linux environment using a virtual machine on Windows. In terms of your hardware, using a computer with at least 16 GB RAM (preferably 32 GB RAM) and 1 TB of storage is necessary. For reference, if you have 25 samples, you may end up with a data output of 300+ GB, so having ample storage space is necessary. For this pipeline, we will be using the following tools: FastQC, Trimmomatic, STAR, Samtools, FeatureCounts, and DESeq2.

The first step we have to do is check the quality of the reads with FastQC. To do so, you must link the FASTQ (or BAM or SAM) files using the cd command and ensure FastQC is installed into a tools directory.

```
cd/path/to/foldername
```

If your files are zipped, keep them as such to allow for faster processing. To check that you linked the FASTQ files properly, use the ls command. Next, make an output directory to store your output files using the mkdir function.

```
mkdir/path/to/folder-name/
```

Now the files are ready to check for file quality.

```
fastqc your_sample.fastq.gz
```

You then get an output of 5% complete once it has been done, and you will end up with 2 output files, the .html file being of interest. Upon bringing the html files over using FileZilla, you can open them in a browser to see the FastQC Report. You will then be able to view a graph upon which you will want to confirm all your reads are of high quality. After identifying the quality scores on the y-axis, you want to see that at least 80% of your base pairs (found on the x axis) are above Q30, meaning there is about 1 error for every 1,000 base pairs. If you see some base pairs dipping into the yellow area below Q30, it will be necessary to trim your reads prior to continuing.

Trimmomatic, created by Anthony Bolger, is a common adaptor that uses java to trim your Illumina sequence data. To trim your files:

```
java -jar trimmomatic-0.39.jar PE input_forward.fq.gz
input_reverse.fq.gz output_forward_paired.fq.gz
output_forward_unpaired.fq.gz output_reverse_paired.fq.gz
output_reverse_unpaired.fq.gz ILLUMINACLIP:TruSeq3-
PE.fa:2:30:10:2:True LEADING:3 TRAILING:3 MINLEN:36
```

This will remover adaptors, leading low quality bases (LEADING: 3), trailing low quality bases (TRAILING: 3), and drop reads below 36 bases long (MINLEN: 36). After this, you will need to rerun FastQC to check the new quality.

Now it is time to align your files to a genome. STAR, created by Alexander Dobin, is extremely accurate and one of the top aligners used, as it is faster than Tophat. To prep for alignment, you have to load in reference files from STAR's index files. Since mice are commonly used, this example will utilize the Ensembl *Mus musculus* GRCm38 genome. These files are typically in (1) fasta files for the genome itself, and (2) annotated gtf files. It is critical to index the reference genome first:

```
STAR genomeGenerate --genomeDir /data/ref/where you stored
the downloaded genome files --genomeFastaFiles
/data/ref/the downloaded GRCm38 genome file --sjdbGTFfile
data/ref/the downloaded gtf file
```

Fortunately, you only have to index a genome once! The you can recall it and just align the reads to the appropriate genome in future studies. To align the reads:

```
STAR --genomeDir /data/ref/ the downloaded GRCm38 genome
file --readFilesIn path/to/your trimmed FASTQ file --
outFileNamePrefix /path/to/whatever you name the aligned
output files --outSAMtype BAM Unsorted
```

To check the alignment statistics and ensure that you performed these commands properly, check the stats of the STAR aligner that is in the output folder with [Your sample name]Log.final.out. Upon opening, the file you want to see more than 80% uniquely mapped reads in the appropriate column. After checking the quality, organizing the BAM files to prep them for downstream analysis is critical.

```
samtools sort /path/to/your BAM file -o /path/to/your new
file name samtools index /path/to/the file you just created
for output
```

Now we will use Yang Liao's FeatureCounts to determine the abundance of reads for each gene.

```
featureCounts -a /data/ref/the downloaded gtf file -o
/path/to/your new output file.txt --largestOverlap -t exon
-g gene_id /path/to/the sorted bam file you previously
created a step ago
```

By clicking on the newly created stats file, you can check that most of the reads are assigned and not unassigned. For successful analysis, you will need about 20 million reads. The .txt file will enable you to see gene ID in the first column with counts in the last column. It's from these counts that you will perform differential comparison analysis. For this, you will need to swap to R 4.2.2+ for this.

To enable R to read the counts, you will need to create a .csv file using Execl with the gene names in the first column and all of your counts for each sample in subsequent columns. This can be achieved manually in Excel via copy and paste controls, or you can use R scripting. To allow R to compare your different groups, you will also need to create a group assignment table with your sample names as

they appear in the counts file transposed into the first column and the treatment each sample received in the second column (**Figure 1**). By default, R will pick the first condition in alphabetical/numerical order to serve as the comparison point. Thus, you may need to be creative with naming your samples.

Now you are ready to import your files into R and perform differential analyses. To setup R properly you need to install the proper libraries using the install.packages() or BiocManager::install() commands. Once they are installed, you must load them into your library using the library() feature.

```r
library(ggplot2)
library(apeglm)
library(colorRamp2)
library(BiocManager)
library(pheatmap)
library(DESeq2)
```

To load in your files, you need to create a name for them that you can then recall later. To import and store your count data, set up a name such as datCounts or something else descriptive and then call for R to read your csv file. Then you will need to import the condition types for the samples you have the gene counts for by doing the same thing. For the example below, the data is from a timepoint study, so the counts data is "dattp" and the conditions are named infoTP. After you import your files, you will be able to perform differential expression analysis and normalize your counts.

```r
datCounts<-read.csv("SamplesCounts.csv", header = TRUE,
row.names = 1)
infoTP<- read.csv("samplematch.csv", row.names=1)
ddsTP<- DESeqDataSetFromMatrix(countData = round(dattp),
colData = infoTP, design= ~condition)
keep<-rowSums(counts(ddsTP))>=10
ddsTP<-ddsTP[keep,]
ddsTPDE<- DESeq(ddsTP)
normCountsTP<-counts(ddsTPDE, normalized = T)
write.csv(normCountsTP, "normalized.counts.timepoint.csv")
resTP<- results(ddsTPDE, alpha = 0.05)
```

```
resTPOrdered<- resTP[order(resTP$padj),]
write.csv(resTPOrdered,
"DESeq.timepoint.study.ordered.csv")
resultsNames(ddsTPDE)
```

In performing the above "write" tasks, you now have stored the data output in whatever location you assigned your working directory to be. Now you can create files to view DEGs from different conditions compared to your control condition. For this example, the timepoint study contained samples from days 0, 4, and 14, and day 0 served as the control.

```
resultsday4<-results(ddsTPDE, contrast = c("condition",
"Day 04", "Day 0"))
write.csv(resultsday4, "Day4Final.csv")
resultsday14vs0<- results(ddsTPDE, contrast =
c("condition", "Day 14", "Day 0"))

#if it gives you: Error in cleanContrast(object, contrast,
expanded = isExpanded, listValues = listValues,  : as Day 0
is the reference level, was expecting
condition_Day.4_vs_Day.0 to be present in
'resultsNames(object)'
results(ddsTPDE, contrast = c("condition", "Day 04", "Day
0"))
#then run the first two lines of code from the section
above again. It just needs to be reminded it is okay to
show you what you're asking it to show you.
```

After having written these results, you can now prep for principal component analyses to evaluate if the samples from different conditions clustered together.

```
prepTP<-vst(ddsTPDE, blind=FALSE)
matTP<- assay(prepTP)
plotPCA(prepTP, intgroup=c("condition"))
plotPCA(prepTP, intgroup=c("condition")) +
geom_label(aes(label=name))

#alternatively
rlt<-DESeq2::rlogTransformation(ddsTPDE)
```

```
plotPCA(rlt) + stat_ellipse() + geom_text(aes(label=name),
vjust=2)

#to change color
plotPCA(rlt) + stat_ellipse(level = 0.95) +
geom_text(aes(label=name), vjust=2) +
scale_color_brewer(palette = "Set1")
#level changes the confidence interval, we are going with
default 0.95, but it is specified to show where it could go
#to take labeling of the points out, just delete the
geom_text command
```

After creating a PCA plot, you can setup a heatmap to enable better visualization of the differences in the DEGs. For this, you want your rows to cluster, as those are your genes. This will have genes that are up- and down-regulated group together and create a nice heatmap. If you entered your samples in order of their treatments, you will not want the columns to cluster, as this will mess up their groupings in addition to preventing you from being able adjust coloring.

```
deSeqRest<- read.csv("DESeq.timepoint.study.ordered.csv",
row.names =1)
deSeqRest$sig<-ifelse(deSeqRest$padj <= 0.05, "yes", "no")
ggplot(deSeqRest, aes(x=baseMean, y = -log2FoldChange,
color = sig)) + geom_point()
deSeqRest<- na.omit(deSeqRest)
ggplot(deSeqRest, aes(x=baseMean, y = -log2FoldChange,
color = sig)) + geom_point()
subset(deSeqRest, padj <= 0.05)
DeSeq4<- read.csv("Day4Final.csv", row.names =1)
DeSeq4$sig<- ifelse(DeSeq4$padj <= 0.05, "yes", "no")
DeSeq4<- na.omit(DeSeq4)
signi4<- subset(DeSeq4, padj <= 0.05)
signi4
merged<- merge(normCountsTP, signi4, by = 0)
sigCountsAll<- merged[,2:20]
row.names(sigCountsAll) <- merged$Row.names
pheatmap(log2(sigCountsAll + 1), scale = "row")
```

```
heatmap<- pheatmap(log2(sigCountsAll + 1), scale = "row",
treeheight_row = 0, treeheight_col = 0, cluster_cols = F,
show_rownames = F)
```

Now that you have a heatmap, you will want to change its colors so you have a true 0 point with white being the "no change" instead of the default yellow. To do so you will load a new library and perform many of the same functions as above.

```
library(RColorBrewer)

pheatmap(log2(sigCountsAll + 1), scale = "row",
show_rownames = F, treeheight_row = 0, treeheight_col = 0,
color = colorRampPalette(c("slateblue", "white",
"red4"))(7), cluster_cols = FALSE, gaps_col = c(6, 12),
border_color = "black")
```

This code was then adapted for each study (timepoint, CS only sequencing, and my SS-31 drug treatment study). Files were saved to a working directory aptly named for each study and plots were saved as PDFs and PNGs.

REFERENCES

1.   Singer M, Deutschman CS, Seymour CW, Shankar-Hari M, Annane D, Bauer M, Bellomo R, Bernard GR, Chiche JD, Coopersmith CM, Hotchkiss RS, Levy MM, Marshall JC, Martin GS, Opal SM, Rubenfeld GD, van der Poll T, Vincent JL, Angus DC. The Third International Consensus Definitions for Sepsis and Septic Shock (Sepsis-3). JAMA. 2016;315(8):801-10. Epub 2016/02/24. doi: 10.1001/jama.2016.0287. PubMed PMID: 26903338; PMCID: PMC4968574.

2.   Kingren MS, Starr ME, Saito H. Divergent Sepsis Pathophysiology in Older Adults. Antioxid Redox Signal. 2021. Epub 2021/07/03. doi: 10.1089/ars.2021.0056. PubMed PMID: 34210173.

3.   Li Y, Klippel Z, Shih X, Reiner M, Wang H, Page JH. Relationship between severity and duration of chemotherapy-induced neutropenia and risk of infection among patients with nonmyeloid malignancies. Support Care Cancer. 2016;24(10):4377-83. Epub 2016/06/10. doi: 10.1007/s00520-016-3277-0. PubMed PMID: 27278272.

4.   Inoue S, Suzuki K, Komori Y, Morishita Y, Suzuki-Utsunomiya K, Hozumi K, Inokuchi S, Sato T. Persistent inflammation and T cell exhaustion in severe sepsis in the elderly. Crit Care. 2014;18(3):R130. Epub 2014/06/26. doi: 10.1186/cc13941. PubMed PMID: 24962182; PMCID: PMC4230031.

5.   Jevon P, Abdelrahman A, Pigadas N. Management of odontogenic infections and sepsis: an update. Br Dent J. 2020;229(6):363-70. Epub 2020/09/27. doi: 10.1038/s41415-020-2114-5. PubMed PMID: 32978579; PMCID: PMC7517749.

6.   Kelm DJ, Valerio-Rojas JC, Cabello-Garza J, Gajic O, Cartin-Ceba R.
Predictors of Disseminated Intravascular Coagulation in Patients with Septic
Shock. ISRN Critical Care. 2013;2013:219048. doi: 10.5402/2013/219048.

7.   Knoferl MW, Angele MK, Diodato MD, Schwacha MG, Ayala A, Cioffi WG,
Bland KI, Chaudry IH. Female sex hormones regulate macrophage function after
trauma-hemorrhage and prevent increased death rate from subsequent sepsis.
Ann Surg. 2002;235(1):105-12. Epub 2001/12/26. doi: 10.1097/00000658-
200201000-00014. PubMed PMID: 11753049; PMCID: PMC1422402.

8.   Lyons PG, Micek ST, Hampton N, Kollef MH. Sepsis-Associated
Coagulopathy Severity Predicts Hospital Mortality. Crit Care Med.
2018;46(5):736-42. Epub 2018/01/27. doi: 10.1097/ccm.0000000000002997.
PubMed PMID: 29373360.

9.   Martin S, Perez A, Aldecoa C. Sepsis and Immunosenescence in the
Elderly Patient: A Review. Front Med (Lausanne). 2017;4:20. Epub 2017/03/16.
doi: 10.3389/fmed.2017.00020. PubMed PMID: 28293557; PMCID:
PMC5329014.

10.   Iskander KN, Osuchowski MF, Stearns-Kurosawa DJ, Kurosawa S,
Stepien D, Valentine C, Remick DG. Sepsis: multiple abnormalities,
heterogeneous responses, and evolving understanding. Physiol Rev.
2013;93(3):1247-88. Epub 2013/08/01. doi: 10.1152/physrev.00037.2012.
PubMed PMID: 23899564; PMCID: PMC3962548.

11.   Rudd KE, Johnson SC, Agesa KM, Shackelford KA, Tsoi D, Kievlan DR,
Colombara DV, Ikuta KS, Kissoon N, Finfer S, Fleischmann-Struzek C, Machado
FR, Reinhart KK, Rowan K, Seymour CW, Watson RS, West TE, Marinho F, Hay
SI, Lozano R, Lopez AD, Angus DC, Murray CJL, Naghavi M. Global, regional,
and national sepsis incidence and mortality, 1990-2017: analysis for the Global

Burden of Disease Study. Lancet. 2020;395(10219):200-11. Epub 2020/01/20. doi: 10.1016/s0140-6736(19)32989-7. PubMed PMID: 31954465; PMCID: PMC6970225.

12.   Angus DC, Linde-Zwirble WT, Lidicker J, Clermont G, Carcillo J, Pinsky MR. Epidemiology of severe sepsis in the United States: analysis of incidence, outcome, and associated costs of care. Crit Care Med. 2001;29(7):1303-10. Epub 2001/07/11. doi: 10.1097/00003246-200107000-00002. PubMed PMID: 11445675.

13.   Elixhauser A, Friedman B, Stranges E. Septicemia in U.S. Hospitals, 2009: Statistical Brief #122. Healthcare Cost and Utilization Project (HCUP) Statistical Briefs. Rockville (MD)2006.

14.   Andrews RM, Elixhauser A. The National Hospital Bill: Growth Trends and 2005 Update on the Most Expensive Conditions by Payer: Statistical Brief #42. Healthcare Cost and Utilization Project (HCUP) Statistical Briefs. Rockville (MD)2006.

15.   Andrews RM. The National Hospital Bill: The Most Expensive Conditions by Payer, 2006: Statistical Brief #59. Healthcare Cost and Utilization Project (HCUP) Statistical Briefs. Rockville (MD)2006.

16.   Martin GS, Mannino DM, Moss M. The effect of age on the development and outcome of adult sepsis. Crit Care Med. 2006;34(1):15-21. Epub 2005/12/24. doi: 10.1097/01.ccm.0000194535.82812.ba. PubMed PMID: 16374151.

17.   Leviner S. Post-Sepsis Syndrome. Crit Care Nurs Q. 2021;44(2):182-6. Epub 2021/02/18. doi: 10.1097/CNQ.0000000000000352. PubMed PMID: 33595965.

18.   Gritte RB, Souza-Siqueira T, Curi R, Machado MCC, Soriano FG. Why Septic Patients Remain Sick After Hospital Discharge? Frontiers in Immunology. 2021;11(3873). doi: 10.3389/fimmu.2020.605666.

19.   Cuthbertson BH, Elders A, Hall S, Taylor J, MacLennan G, Mackirdy F, Mackenzie SJ, Scottish Critical Care Trials G, Scottish Intensive Care Society Audit G. Mortality and quality of life in the five years after severe sepsis. Crit Care. 2013;17(2):R70. Epub 2013/04/17. doi: 10.1186/cc12616. PubMed PMID: 23587132; PMCID: PMC4057306.

20.   Hofhuis JG, Spronk PE, van Stel HF, Schrijvers AJ, Rommes JH, Bakker J. The impact of severe sepsis on health-related quality of life: a long-term follow-up study. Anesth Analg. 2008;107(6):1957-64. Epub 2008/11/21. doi: 10.1213/ane.0b013e318187bbd8. PubMed PMID: 19020144.

21.   Schefold JC, Bierbrauer J, Weber-Carstens S. Intensive care unit-acquired weakness (ICUAW) and muscle wasting in critically ill patients with severe sepsis and septic shock. J Cachexia Sarcopenia Muscle. 2010;1(2):147-57. Epub 2011/04/09. doi: 10.1007/s13539-010-0010-6. PubMed PMID: 21475702; PMCID: PMC3060654.

22.   Ebashi S. Excitation-contraction coupling and the mechanism of muscle contraction. Annu Rev Physiol. 1991;53:1-16. Epub 1991/01/01. doi: 10.1146/annurev.ph.53.030191.000245. PubMed PMID: 2042955.

23.   Holmes KC. The swinging lever-arm hypothesis of muscle contraction. Curr Biol. 1997;7(2):R112-8. Epub 1997/02/01. doi: 10.1016/s0960-9822(06)00051-0. PubMed PMID: 9081660.

24.   Powers SH, E, Quindry J. Exercise Physiology: Theory and Application to Fitness and Performance, 11th Ed. New York, NY: McGraw-Hill Education; 2021.

25.   Koves TR, Noland RC, Bates AL, Henes ST, Muoio DM, Cortright RN. Subsarcolemmal and intermyofibrillar mitochondria play distinct roles in regulating skeletal muscle fatty acid metabolism. Am J Physiol Cell Physiol. 2005;288(5):C1074-82. Epub 2005/01/14. doi: 10.1152/ajpcell.00391.2004. PubMed PMID: 15647392.

26.   Ferreira R, Vitorino R, Alves RM, Appell HJ, Powers SK, Duarte JA, Amado F. Subsarcolemmal and intermyofibrillar mitochondria proteome differences disclose functional specializations in skeletal muscle. Proteomics. 2010;10(17):3142-54. Epub 2010/07/29. doi: 10.1002/pmic.201000173. PubMed PMID: 20665633.

27.   Swalsingh G, Pani P, Bal NC. Structural functionality of skeletal muscle mitochondria and its correlation with metabolic diseases. Clin Sci (Lond). 2022;136(24):1851-71. Epub 2022/12/23. doi: 10.1042/CS20220636. PubMed PMID: 36545931.

28.   Gan Z, Fu T, Kelly DP, Vega RB. Skeletal muscle mitochondrial remodeling in exercise and diseases. Cell Res. 2018;28(10):969-80. Epub 2018/08/16. doi: 10.1038/s41422-018-0078-7. PubMed PMID: 30108290; PMCID: PMC6170448.

29.   Budzinska M, Zimna A, Kurpisz M. The role of mitochondria in Duchenne muscular dystrophy. J Physiol Pharmacol. 2021;72(2). Epub 2021/08/11. doi: 10.26402/jpp.2021.2.01. PubMed PMID: 34374652.

30.   VanderVeen BN, Fix DK, Carson JA. Disrupted Skeletal Muscle Mitochondrial Dynamics, Mitophagy, and Biogenesis during Cancer Cachexia: A Role for Inflammation. Oxid Med Cell Longev. 2017;2017:3292087. Epub 2017/08/09. doi: 10.1155/2017/3292087. PubMed PMID: 28785374; PMCID: PMC5530417.

31.   Brown JL, Rosa-Caldwell ME, Lee DE, Blackwell TA, Brown LA, Perry RA, Haynie WS, Hardee JP, Carson JA, Wiggs MP, Washington TA, Greene NP. Mitochondrial degeneration precedes the development of muscle atrophy in progression of cancer cachexia in tumour-bearing mice. J Cachexia Sarcopenia Muscle. 2017;8(6):926-38. Epub 2017/08/29. doi: 10.1002/jcsm.12232. PubMed PMID: 28845591; PMCID: PMC5700433.

32.   Ahmed ST, Craven L, Russell OM, Turnbull DM, Vincent AE. Diagnosis and Treatment of Mitochondrial Myopathies. Neurotherapeutics. 2018;15(4):943-53. Epub 2018/11/09. doi: 10.1007/s13311-018-00674-4. PubMed PMID: 30406383; PMCID: PMC6277287.

33.   Talbot J, Maves L. Skeletal muscle fiber type: using insights from muscle developmental biology to dissect targets for susceptibility and resistance to muscle disease. Wiley Interdiscip Rev Dev Biol. 2016;5(4):518-34. Epub 2016/05/21. doi: 10.1002/wdev.230. PubMed PMID: 27199166; PMCID: PMC5180455.

34.   Schiaffino S, Reggiani C. Fiber types in mammalian skeletal muscles. Physiol Rev. 2011;91(4):1447-531. Epub 2011/10/21. doi: 10.1152/physrev.00031.2010. PubMed PMID: 22013216.

35.   Pette D, Staron RS. Myosin isoforms, muscle fiber types, and transitions. Microsc Res Tech. 2000;50(6):500-9. Epub 2000/09/22. doi: 10.1002/1097-0029(20000915)50:6<500::AID-JEMT7>3.0.CO;2-7. PubMed PMID: 10998639.

36.   Sandri M. Protein breakdown in muscle wasting: role of autophagy-lysosome and ubiquitin-proteasome. Int J Biochem Cell Biol. 2013;45(10):2121-9. Epub 2013/05/15. doi: 10.1016/j.biocel.2013.04.023. PubMed PMID: 23665154; PMCID: PMC3775123.

37.   Batt J, dos Santos CC, Cameron JI, Herridge MS. Intensive care unit-acquired weakness: clinical phenotypes and molecular mechanisms. Am J Respir Crit Care Med. 2013;187(3):238-46. Epub 2012/12/04. doi: 10.1164/rccm.201205-0954SO. PubMed PMID: 23204256.

38.   Bonaldo P, Sandri M. Cellular and molecular mechanisms of muscle atrophy. Dis Model Mech. 2013;6(1):25-39. Epub 2012/12/27. doi: 10.1242/dmm.010389. PubMed PMID: 23268536; PMCID: PMC3529336.

39.   Schiaffino S, Dyar KA, Ciciliot S, Blaauw B, Sandri M. Mechanisms regulating skeletal muscle growth and atrophy. FEBS J. 2013;280(17):4294-314. Epub 2013/03/23. doi: 10.1111/febs.12253. PubMed PMID: 23517348.

40.   Walston JD. Sarcopenia in older adults. Curr Opin Rheumatol. 2012;24(6):623-7. Epub 2012/09/08. doi: 10.1097/BOR.0b013e328358d59b. PubMed PMID: 22955023; PMCID: PMC4066461.

41.   Seymour CW, Gesten F, Prescott HC, Friedrich ME, Iwashyna TJ, Phillips GS, Lemeshow S, Osborn T, Terry KM, Levy MM. Time to Treatment and Mortality during Mandated Emergency Care for Sepsis. N Engl J Med. 2017;376(23):2235-44. Epub 2017/05/23. doi: 10.1056/NEJMoa1703058. PubMed PMID: 28528569; PMCID: PMC5538258.

42.   Owen AM, Patel SP, Smith JD, Balasuriya BK, Mori SF, Hawk GS, Stromberg AJ, Kuriyama N, Kaneki M, Rabchevsky AG, Butterfield TA, Esser KA, Peterson CA, Starr ME, Saito H. Chronic muscle weakness and mitochondrial dysfunction in the absence of sustained atrophy in a preclinical sepsis model. Elife. 2019;8. Epub 2019/12/04. doi: 10.7554/eLife.49920. PubMed PMID: 31793435; PMCID: PMC6890461.

43.   Dos Santos C, Hussain SN, Mathur S, Picard M, Herridge M, Correa J, Bain A, Guo Y, Advani A, Advani SL, Tomlinson G, Katzberg H, Streutker CJ, Cameron JI, Schols A, Gosker HR, Batt J, Group MI, Investigators RP, Canadian Critical Care Translational Biology G. Mechanisms of Chronic Muscle Wasting and Dysfunction after an Intensive Care Unit Stay. A Pilot Study. Am J Respir Crit Care Med. 2016;194(7):821-30. Epub 2016/04/09. doi: 10.1164/rccm.201512-2344OC. PubMed PMID: 27058306.

44.   Tamilarasan KP, Temmel H, Das SK, Al Zoughbi W, Schauer S, Vesely PW, Hoefler G. Skeletal muscle damage and impaired regeneration due to LPL-mediated lipotoxicity. Cell Death Dis. 2012;3(7):e354. Epub 2012/07/25. doi: 10.1038/cddis.2012.91. PubMed PMID: 22825472; PMCID: PMC3406590.

45.   Omar A, Marwaha K, Bollu PC. Physiology, Neuromuscular Junction. StatPearls. Treasure Island (FL)2023.

46.   Szent-Gyorgyi AG. Calcium regulation of muscle contraction. Biophys J. 1975;15(7):707-23. Epub 1975/07/01. doi: 10.1016/S0006-3495(75)85849-8. PubMed PMID: 806311; PMCID: PMC1334730.

47.   Korzeniewski B. Regulation of ATP supply during muscle contraction: theoretical studies. Biochem J. 1998;330 (Pt 3)(Pt 3):1189-95. Epub 1998/05/23. doi: 10.1042/bj3301189. PubMed PMID: 9494084; PMCID: PMC1219260.

48.   Vanhorebeek I, Latronico N, Van den Berghe G. ICU-acquired weakness. Intensive Care Med. 2020;46(4):637-53. Epub 2020/02/23. doi: 10.1007/s00134-020-05944-4. PubMed PMID: 32076765; PMCID: PMC7224132.

49.   Abramowitz MK, Paredes W, Zhang K, Brightwell CR, Newsom JN, Kwon HJ, Custodio M, Buttar RS, Farooq H, Zaidi B, Pai R, Pessin JE, Hawkins M, Fry CS. Skeletal muscle fibrosis is associated with decreased muscle inflammation

and weakness in patients with chronic kidney disease. Am J Physiol Renal Physiol. 2018;315(6):F1658-F69. Epub 2018/10/04. doi: 10.1152/ajprenal.00314.2018. PubMed PMID: 30280599; PMCID: PMC6336993.

50.   Steinbacher P, Eckl P. Impact of oxidative stress on exercising skeletal muscle. Biomolecules. 2015;5(2):356-77. Epub 2015/04/14. doi: 10.3390/biom5020356. PubMed PMID: 25866921; PMCID: PMC4496677.

51.   Papanikolaou K, Draganidis D, Chatzinikolaou A, Laschou VC, Georgakouli K, Tsimeas P, Batrakoulis A, Deli CK, Jamurtas AZ, Fatouros IG. The redox-dependent regulation of satellite cells following aseptic muscle trauma (SpEED): study protocol for a randomized controlled trial. Trials. 2019;20(1):469. Epub 2019/08/02. doi: 10.1186/s13063-019-3557-3. PubMed PMID: 31366396; PMCID: PMC6668149.

52.   Kaczmarek A, Kaczmarek M, Cialowicz M, Clemente FM, Wolanski P, Badicu G, Murawska-Cialowicz E. The Role of Satellite Cells in Skeletal Muscle Regeneration-The Effect of Exercise and Age. Biology (Basel). 2021;10(10). Epub 2021/10/24. doi: 10.3390/biology10101056. PubMed PMID: 34681155; PMCID: PMC8533525.

53.   Wallace DC, Fan W. Energetics, epigenetics, mitochondrial genetics. Mitochondrion. 2010;10(1):12-31. Epub 2009/10/03. doi: 10.1016/j.mito.2009.09.006. PubMed PMID: 19796712; PMCID: PMC3245717.

54.   Wallace DC, Fan W, Procaccio V. Mitochondrial energetics and therapeutics. Annu Rev Pathol. 2010;5:297-348. Epub 2010/01/19. doi: 10.1146/annurev.pathol.4.110807.092314. PubMed PMID: 20078222; PMCID: PMC3245719.

55.   Guo C, Sun L, Chen X, Zhang D. Oxidative stress, mitochondrial damage and neurodegenerative diseases. Neural Regen Res. 2013;8(21):2003-14. Epub 2013/07/25. doi: 10.3969/j.issn.1673-5374.2013.21.009. PubMed PMID: 25206509; PMCID: PMC4145906.

56.   Piva S, Fagoni N, Latronico N. Intensive care unit-acquired weakness: unanswered questions and targets for future research. F1000Res. 2019;8. Epub 2019/05/10. doi: 10.12688/f1000research.17376.1. PubMed PMID: 31069055; PMCID: PMC6480958.

57.   Mankowski RT, Laitano O, Clanton TL, Brakenridge SC. Pathophysiology and Treatment Strategies of Acute Myopathy and Muscle Wasting after Sepsis. J Clin Med. 2021;10(9). Epub 2021/05/01. doi: 10.3390/jcm10091874. PubMed PMID: 33926035; PMCID: PMC8123669.

58.   Hermans G, De Jonghe B, Bruyninckx F, Van den Berghe G. Interventions for preventing critical illness polyneuropathy and critical illness myopathy. Cochrane Database Syst Rev. 2014;2014(1):CD006832. Epub 2014/01/31. doi: 10.1002/14651858.CD006832.pub3. PubMed PMID: 24477672; PMCID: PMC7390458 the review. Frans Bruyninckx and Bernard De Jonghe have no known conflicts of interest.

59.   Callahan LA, Supinski GS. Sepsis-induced myopathy. Crit Care Med. 2009;37(10 Suppl):S354-67. Epub 2010/02/06. doi: 10.1097/CCM.0b013e3181b6e439. PubMed PMID: 20046121; PMCID: PMC3967515.

60.   Fredriksson K, Rooyackers O. Mitochondrial function in sepsis: respiratory versus leg muscle. Crit Care Med. 2007;35(9 Suppl):S449-53. Epub 2007/09/22. doi: 10.1097/01.CCM.0000278048.00896.4B. PubMed PMID: 17713392.

61.   Hasselgren PO, Fischer JE. Sepsis: stimulation of energy-dependent protein breakdown resulting in protein loss in skeletal muscle. World J Surg. 1998;22(2):203-8. Epub 1998/02/06. doi: 10.1007/s002689900370. PubMed PMID: 9451937.

62.   Schutz Y. Protein turnover, ureagenesis and gluconeogenesis. Int J Vitam Nutr Res. 2011;81(2-3):101-7. Epub 2011/12/06. doi: 10.1024/0300-9831/a000064. PubMed PMID: 22139560.

63.   Kamei Y, Hatazawa Y, Uchitomi R, Yoshimura R, Miura S. Regulation of Skeletal Muscle Function by Amino Acids. Nutrients. 2020;12(1). Epub 2020/01/23. doi: 10.3390/nu12010261. PubMed PMID: 31963899; PMCID: PMC7019684.

64.   Griesdale DE, Tremblay MH, McEwen J, Chittock DR. Glucose control and mortality in patients with severe traumatic brain injury. Neurocrit Care. 2009;11(3):311-6. Epub 2009/07/29. doi: 10.1007/s12028-009-9249-1. PubMed PMID: 19636972.

65.   Griesdale DE, de Souza RJ, van Dam RM, Heyland DK, Cook DJ, Malhotra A, Dhaliwal R, Henderson WR, Chittock DR, Finfer S, Talmor D. Intensive insulin therapy and mortality among critically ill patients: a meta-analysis including NICE-SUGAR study data. CMAJ. 2009;180(8):821-7. Epub 2009/03/26. doi: 10.1503/cmaj.090206. PubMed PMID: 19318387; PMCID: PMC2665940.

66.   Puthucheary ZA, Rawal J, McPhail M, Connolly B, Ratnayake G, Chan P, Hopkinson NS, Phadke R, Dew T, Sidhu PS, Velloso C, Seymour J, Agley CC, Selby A, Limb M, Edwards LM, Smith K, Rowlerson A, Rennie MJ, Moxham J, Harridge SD, Hart N, Montgomery HE. Acute skeletal muscle wasting in critical

illness. JAMA. 2013;310(15):1591-600. Epub 2013/10/11. doi: 10.1001/jama.2013.278481. PubMed PMID: 24108501.

67.   Gunst J, Vanhorebeek I, Thiessen SE, Van den Berghe G. Amino acid supplements in critically ill patients. Pharmacol Res. 2018;130:127-31. doi: 10.1016/j.phrs.2017.12.007. PubMed PMID: WOS:000433016900012.

68.   Thiessen SE, Van den Berghe G, Vanhorebeek I. Mitochondrial and endoplasmic reticulum dysfunction and related defense mechanisms in critical illness-induced multiple organ failure. Bba-Mol Basis Dis. 2017;1863(10):2534-45. doi: 10.1016/j.bbadis.2017.02.015. PubMed PMID: WOS:000415779100003.

69.   Yen HC, Oberley TD, Vichitbandha S, Ho YS, St Clair DK. The protective role of manganese superoxide dismutase against adriamycin-induced acute cardiac toxicity in transgenic mice. J Clin Invest. 1996;98(5):1253-60. Epub 1996/09/01. doi: 10.1172/JCI118909. PubMed PMID: 8787689; PMCID: PMC507548.

70.   Chapman J, Bansal P, Goyal A, Azevedo AM. Splenomegaly. StatPearls. Treasure Island (FL)2021.

71.   Miller SG, Hafen PS, Law AS, Springer CB, Logsdon DL, O'Connell TM, Witczak CA, Brault JJ. AMP deamination is sufficient to replicate an atrophy-like metabolic phenotype in skeletal muscle. Metabolism. 2021;123:154864. Epub 2021/08/18. doi: 10.1016/j.metabol.2021.154864. PubMed PMID: 34400216; PMCID: PMC8453098.

72.   Singer M. The role of mitochondrial dysfunction in sepsis-induced multi-organ failure. Virulence. 2014;5(1):66-72. Epub 2013/11/05. doi: 10.4161/viru.26907. PubMed PMID: 24185508; PMCID: PMC3916385.

73. Mantzarlis K, Tsolaki V, Zakynthinos E. Role of Oxidative Stress and Mitochondrial Dysfunction in Sepsis and Potential Therapies. Oxid Med Cell Longev. 2017;2017:5985209. Epub 2017/09/15. doi: 10.1155/2017/5985209. PubMed PMID: 28904739; PMCID: PMC5585571.

74. Preau S, Vodovar D, Jung B, Lancel S, Zafrani L, Flatres A, Oualha M, Voiriot G, Jouan Y, Joffre J, Huel F, De Prost N, Silva S, Azabou E, Radermacher P. Energetic dysfunction in sepsis: a narrative review. Ann Intensive Care. 2021;11(1):104. Epub 2021/07/04. doi: 10.1186/s13613-021-00893-7. PubMed PMID: 34216304; PMCID: PMC8254847.

75. Azevedo LC. Mitochondrial dysfunction during sepsis. Endocr Metab Immune Disord Drug Targets. 2010;10(3):214-23. Epub 2010/06/01. doi: 10.2174/187153010791936946. PubMed PMID: 20509844.

76. Moon SJ, Dong W, Stephanopoulos GN, Sikes HD. Oxidative pentose phosphate pathway and glucose anaplerosis support maintenance of mitochondrial NADPH pool under mitochondrial oxidative stress. Bioeng Transl Med. 2020;5(3):e10184. Epub 2020/10/03. doi: 10.1002/btm2.10184. PubMed PMID: 33005744; PMCID: PMC7510474.

77. Gelman SJ, Naser F, Mahieu NG, McKenzie LD, Dunn GP, Chheda MG, Patti GJ. Consumption of NADPH for 2-HG Synthesis Increases Pentose Phosphate Pathway Flux and Sensitizes Cells to Oxidative Stress. Cell Rep. 2018;22(2):512-22. Epub 2018/01/11. doi: 10.1016/j.celrep.2017.12.050. PubMed PMID: 29320744; PMCID: PMC6053654.

78. Geng Y, Faber KN, de Meijer VE, Blokzijl H, Moshage H. How does hepatic lipid accumulation lead to lipotoxicity in non-alcoholic fatty liver disease? Hepatol Int. 2021;15(1):21-35. Epub 2021/02/07. doi: 10.1007/s12072-020-10121-2. PubMed PMID: 33548031; PMCID: PMC7886759.

79.   Frayn KN. The glucose-fatty acid cycle: a physiological perspective. Biochem Soc Trans. 2003;31(Pt 6):1115-9. Epub 2003/12/04. doi: 10.1042/bst0311115. PubMed PMID: 14641007.

80.   Hue L, Taegtmeyer H. The Randle cycle revisited: a new head for an old hat. Am J Physiol Endocrinol Metab. 2009;297(3):E578-91. Epub 2009/06/18. doi: 10.1152/ajpendo.00093.2009. PubMed PMID: 19531645; PMCID: PMC2739696.

81.   Poeze M, Luiking YC, Breedveld P, Manders S, Deutz NE. Decreased plasma glutamate in early phases of septic shock with acute liver dysfunction is an independent predictor of survival. Clin Nutr. 2008;27(4):523-30. Epub 2008/06/17. doi: 10.1016/j.clnu.2008.04.006. PubMed PMID: 18554754.

82.   Cruzat V, Macedo Rogero M, Noel Keane K, Curi R, Newsholme P. Glutamine: Metabolism and Immune Function, Supplementation and Clinical Translation. Nutrients. 2018;10(11). Epub 2018/10/27. doi: 10.3390/nu10111564. PubMed PMID: 30360490; PMCID: PMC6266414.

83.   de Vasconcelos DAA, Giesbertz P, de Souza DR, Vitzel KF, Abreu P, Marzuca-Nassr GN, Fortes MAS, Murata GM, Hirabara SM, Curi R, Daniel H, Pithon-Curi TC. Oral L-glutamine pretreatment attenuates skeletal muscle atrophy induced by 24-h fasting in mice. J Nutr Biochem. 2019;70:202-14. Epub 2019/06/25. doi: 10.1016/j.jnutbio.2019.05.010. PubMed PMID: 31233980.

84.   Holley AK, Bakthavatchalu V, Velez-Roman JM, St Clair DK. Manganese superoxide dismutase: guardian of the powerhouse. Int J Mol Sci. 2011;12(10):7114-62. Epub 2011/11/11. doi: 10.3390/ijms12107114. PubMed PMID: 22072939; PMCID: PMC3211030.

85.   Borrelli A, Schiattarella A, Bonelli P, Tuccillo FM, Buonaguro FM, Mancini
A. The functional role of MnSOD as a biomarker of human diseases and
therapeutic potential of a new isoform of a human recombinant MnSOD. Biomed
Res Int. 2014;2014:476789. Epub 2014/02/11. doi: 10.1155/2014/476789.
PubMed PMID: 24511533; PMCID: PMC3913005.

86.   Jang YC, Perez VI, Song W, Lustgarten MS, Salmon AB, Mele J, Qi W,
Liu Y, Liang H, Chaudhuri A, Ikeno Y, Epstein CJ, Van Remmen H, Richardson
A. Overexpression of Mn superoxide dismutase does not increase life span in
mice. J Gerontol A Biol Sci Med Sci. 2009;64(11):1114-25. Epub 2009/07/28. doi:
10.1093/gerona/glp100. PubMed PMID: 19633237; PMCID: PMC2759571.

87.   Li YB, Huang TT, Carlson EJ, Melov S, Ursell PC, Olson TL, Noble LJ,
Yoshimura MP, Berger C, Chan PH, Wallace DC, Epstein CJ. Dilated
Cardiomyopathy and Neonatal Lethality in Mutant Mice Lacking Manganese
Superoxide-Dismutase. Nat Genet. 1995;11(4):376-81. doi: DOI
10.1038/ng1295-376. PubMed PMID: WOS:A1995TH62900013.

88.   Remick DG, Bolgos GR, Siddiqui J, Shin J, Nemzek JA. Six at six:
interleukin-6 measured 6 h after the initiation of sepsis predicts mortality over 3
days. Shock. 2002;17(6):463-7. Epub 2002/06/19. doi: 10.1097/00024382-
200206000-00004. PubMed PMID: 12069181.

89.   Zhang H, Feng YW, Yao YM. Potential therapy strategy: targeting
mitochondrial dysfunction in sepsis. Mil Med Res. 2018;5(1):41. Epub
2018/11/27. doi: 10.1186/s40779-018-0187-0. PubMed PMID: 30474573;
PMCID: PMC6260865.

90.   Wang K, Qiu Z, Liu J, Fan T, Liu C, Tian P, Wang Y, Ni Z, Zhang S, Luo J,
Liu D, Li W. Analysis of the clinical characteristics of 77 COVID-19 deaths. Sci

Rep. 2020;10(1):16384. Epub 2020/10/04. doi: 10.1038/s41598-020-73136-7. PubMed PMID: 33009426; PMCID: PMC7532142.

91.   Mainali R, Zabalawi M, Long D, Buechler N, Quillen E, Key CC, Zhu X, Parks JS, Furdui C, Stacpoole PW, Martinez J, McCall CE, Quinn MA. Dichloroacetate reverses sepsis-induced hepatic metabolic dysfunction. Elife. 2021;10. Epub 2021/02/23. doi: 10.7554/eLife.64611. PubMed PMID: 33616039; PMCID: PMC7901874.

92.   Kreymann G, Grosser S, Buggisch P, Gottschall C, Matthaei S, Greten H. Oxygen consumption and resting metabolic rate in sepsis, sepsis syndrome, and septic shock. Crit Care Med. 1993;21(7):1012-9. Epub 1993/07/01. doi: 10.1097/00003246-199307000-00015. PubMed PMID: 8319458.

93.   Kao CC, Guntupalli KK, Bandi V, Jahoor F. Whole-body CO_2 production as an index of the metabolic response to sepsis. Shock. 2009;32(1):23-8. Epub 2008/12/09. doi: 10.1097/SHK.0b013e3181970f32. PubMed PMID: 19060787.

94.   Liggett SB, Renfro AD. Energy expenditures of mechanically ventilated nonsurgical patients. Chest. 1990;98(3):682-6. Epub 1990/09/01. doi: 10.1378/chest.98.3.682. PubMed PMID: 2118448.

95.   Reinelt H, Radermacher P, Kiefer P, Fischer G, Wachter U, Vogt J, Georgieff M. Impact of exogenous beta-adrenergic receptor stimulation on hepatosplanchnic oxygen kinetics and metabolic activity in septic shock. Crit Care Med. 1999;27(2):325-31. Epub 1999/03/13. doi: 10.1097/00003246-199902000-00039. PubMed PMID: 10075057.

96.   Boekstegers P, Weidenhofer S, Kapsner T, Werdan K. Skeletal muscle partial pressure of oxygen in patients with sepsis. Crit Care Med. 1994;22(4):640-

50. Epub 1994/04/01. doi: 10.1097/00003246-199404000-00021. PubMed PMID: 8143474.

97.   Holloszy JO. Biochemical adaptations in muscle. Effects of exercise on mitochondrial oxygen uptake and respiratory enzyme activity in skeletal muscle. J Biol Chem. 1967;242(9):2278-82. Epub 1967/05/10. PubMed PMID: 4290225.

98.   Memme JM, Erlich AT, Phukan G, Hood DA. Exercise and mitochondrial health. J Physiol. 2021;599(3):803-17. Epub 2019/11/02. doi: 10.1113/JP278853. PubMed PMID: 31674658.

99.   Bishop DJ, Botella J, Genders AJ, Lee MJ, Saner NJ, Kuang J, Yan X, Granata C. High-Intensity Exercise and Mitochondrial Biogenesis: Current Controversies and Future Research Directions. Physiology (Bethesda). 2019;34(1):56-70. Epub 2018/12/13. doi: 10.1152/physiol.00038.2018. PubMed PMID: 30540234.

100.   Sorriento D, Di Vaia E, Iaccarino G. Physical Exercise: A Novel Tool to Protect Mitochondrial Health. Front Physiol. 2021;12:660068. Epub 2021/05/15. doi: 10.3389/fphys.2021.660068. PubMed PMID: 33986694; PMCID: PMC8110831.

101.   Liang H, Ward WF. PGC-1alpha: a key regulator of energy metabolism. Adv Physiol Educ. 2006;30(4):145-51. Epub 2006/11/17. doi: 10.1152/advan.00052.2006. PubMed PMID: 17108241.

102.   Halling JF, Pilegaard H. PGC-1alpha-mediated regulation of mitochondrial function and physiological implications. Appl Physiol Nutr Metab. 2020;45(9):927-36. Epub 2020/06/10. doi: 10.1139/apnm-2020-0005. PubMed PMID: 32516539.

103.   Vainshtein A, Tryon LD, Pauly M, Hood DA. Role of PGC-1alpha during acute exercise-induced autophagy and mitophagy in skeletal muscle. Am J Physiol Cell Physiol. 2015;308(9):C710-9. Epub 2015/02/13. doi: 10.1152/ajpcell.00380.2014. PubMed PMID: 25673772; PMCID: PMC4420796.

104.   Lu Z, Xu X, Hu X, Fassett J, Zhu G, Tao Y, Li J, Huang Y, Zhang P, Zhao B, Chen Y. PGC-1 alpha regulates expression of myocardial mitochondrial antioxidants and myocardial oxidative stress after chronic systolic overload. Antioxid Redox Signal. 2010;13(7):1011-22. Epub 2010/04/22. doi: 10.1089/ars.2009.2940. PubMed PMID: 20406135; PMCID: PMC2959178.

105.   Hood DA, Memme JM, Oliveira AN, Triolo M. Maintenance of Skeletal Muscle Mitochondria in Health, Exercise, and Aging. Annu Rev Physiol. 2019;81:19-41. Epub 2018/09/15. doi: 10.1146/annurev-physiol-020518-114310. PubMed PMID: 30216742.

106.   Kim Y, Triolo M, Erlich AT, Hood DA. Regulation of autophagic and mitophagic flux during chronic contractile activity-induced muscle adaptations. Pflugers Arch. 2019;471(3):431-40. Epub 2018/10/29. doi: 10.1007/s00424-018-2225-x. PubMed PMID: 30368578.

107.   Vainshtein A, Hood DA. The regulation of autophagy during exercise in skeletal muscle. J Appl Physiol (1985). 2016;120(6):664-73. Epub 2015/12/19. doi: 10.1152/japplphysiol.00550.2015. PubMed PMID: 26679612; PMCID: PMC4796178.

108.   Chen CCW, Erlich AT, Hood DA. Role of Parkin and endurance training on mitochondrial turnover in skeletal muscle. Skelet Muscle. 2018;8(1):10. Epub 2018/03/20. doi: 10.1186/s13395-018-0157-y. PubMed PMID: 29549884; PMCID: PMC5857114.

109.   Lira VA, Okutsu M, Zhang M, Greene NP, Laker RC, Breen DS, Hoehn KL, Yan Z. Autophagy is required for exercise training-induced skeletal muscle adaptation and improvement of physical performance. FASEB J. 2013;27(10):4184-93. Epub 2013/07/05. doi: 10.1096/fj.13-228486. PubMed PMID: 23825228; PMCID: PMC4046188.

110.   Chen CCW, Erlich AT, Crilly MJ, Hood DA. Parkin is required for exercise-induced mitophagy in muscle: impact of aging. Am J Physiol Endocrinol Metab. 2018;315(3):E404-E15. Epub 2018/05/31. doi: 10.1152/ajpendo.00391.2017. PubMed PMID: 29812989.

111.   Erlich AT, Brownlee DM, Beyfuss K, Hood DA. Exercise induces TFEB expression and activity in skeletal muscle in a PGC-1alpha-dependent manner. Am J Physiol Cell Physiol. 2018;314(1):C62-C72. Epub 2017/10/20. doi: 10.1152/ajpcell.00162.2017. PubMed PMID: 29046293; PMCID: PMC5866381.

112.   Porter C, Reidy PT, Bhattarai N, Sidossis LS, Rasmussen BB. Resistance Exercise Training Alters Mitochondrial Function in Human Skeletal Muscle. Med Sci Sports Exerc. 2015;47(9):1922-31. Epub 2014/12/30. doi: 10.1249/MSS.0000000000000605. PubMed PMID: 25539479; PMCID: PMC4478283.

113.   Fang EF. Mitophagy and NAD(+) inhibit Alzheimer disease. Autophagy. 2019;15(6):1112-4. Epub 2019/03/30. doi: 10.1080/15548627.2019.1596497. PubMed PMID: 30922179; PMCID: PMC6526831.

114.   Fang EF, Hou Y, Lautrup S, Jensen MB, Yang B, SenGupta T, Caponio D, Khezri R, Demarest TG, Aman Y, Figueroa D, Morevati M, Lee HJ, Kato H, Kassahun H, Lee JH, Filippelli D, Okur MN, Mangerich A, Croteau DL, Maezawa Y, Lyssiotis CA, Tao J, Yokote K, Rusten TE, Mattson MP, Jasper H, Nilsen H, Bohr VA. NAD(+) augmentation restores mitophagy and limits accelerated aging

in Werner syndrome. Nat Commun. 2019;10(1):5284. Epub 2019/11/23. doi: 10.1038/s41467-019-13172-8. PubMed PMID: 31754102; PMCID: PMC6872719.

115.　Gomes AP, Price NL, Ling AJ, Moslehi JJ, Montgomery MK, Rajman L, White JP, Teodoro JS, Wrann CD, Hubbard BP, Mercken EM, Palmeira CM, de Cabo R, Rolo AP, Turner N, Bell EL, Sinclair DA. Declining NAD(+) induces a pseudohypoxic state disrupting nuclear-mitochondrial communication during aging. Cell. 2013;155(7):1624-38. Epub 2013/12/24. doi: 10.1016/j.cell.2013.11.037. PubMed PMID: 24360282; PMCID: PMC4076149.

116.　Mills KF, Yoshida S, Stein LR, Grozio A, Kubota S, Sasaki Y, Redpath P, Migaud ME, Apte RS, Uchida K, Yoshino J, Imai SI. Long-Term Administration of Nicotinamide Mononucleotide Mitigates Age-Associated Physiological Decline in Mice. Cell Metab. 2016;24(6):795-806. Epub 2017/01/10. doi: 10.1016/j.cmet.2016.09.013. PubMed PMID: 28068222; PMCID: PMC5668137.

117.　Stein LR, Imai S. The dynamic regulation of NAD metabolism in mitochondria. Trends Endocrinol Metab. 2012;23(9):420-8. Epub 2012/07/24. doi: 10.1016/j.tem.2012.06.005. PubMed PMID: 22819213; PMCID: PMC3683958.

118.　Sims CA, Guan Y, Mukherjee S, Singh K, Botolin P, Davila A, Jr., Baur JA. Nicotinamide mononucleotide preserves mitochondrial function and increases survival in hemorrhagic shock. JCI Insight. 2018;3(17). Epub 2018/09/07. doi: 10.1172/jci.insight.120182. PubMed PMID: 30185676; PMCID: PMC6171817.

119.　Hong W, Mo F, Zhang Z, Huang M, Wei X. Nicotinamide Mononucleotide: A Promising Molecule for Therapy of Diverse Diseases by Targeting NAD+ Metabolism. Front Cell Dev Biol. 2020;8:246. Epub 2020/05/16. doi: 10.3389/fcell.2020.00246. PubMed PMID: 32411700; PMCID: PMC7198709.

120.   Shade C. The Science Behind NMN-A Stable, Reliable NAD+Activator and Anti-Aging Molecule. Integr Med (Encinitas). 2020;19(1):12-4. Epub 2020/06/19. PubMed PMID: 32549859; PMCID: PMC7238909.

121.   Whitson JA, Bitto A, Zhang H, Sweetwyne MT, Coig R, Bhayana S, Shankland EG, Wang L, Bammler TK, Mills KF, Imai SI, Conley KE, Marcinek DJ, Rabinovitch PS. SS-31 and NMN: Two paths to improve metabolism and function in aged hearts. Aging Cell. 2020;19(10):e13213. Epub 2020/08/12. doi: 10.1111/acel.13213. PubMed PMID: 32779818; PMCID: PMC7576234.

122.   Yoshino M, Yoshino J, Kayser BD, Patti GJ, Franczyk MP, Mills KF, Sindelar M, Pietka T, Patterson BW, Imai SI, Klein S. Nicotinamide mononucleotide increases muscle insulin sensitivity in prediabetic women. Science. 2021;372(6547):1224-9. Epub 2021/04/24. doi: 10.1126/science.abe9985. PubMed PMID: 33888596.

123.   Szeto HH. First-in-class cardiolipin-protective compound as a therapeutic agent to restore mitochondrial bioenergetics. Br J Pharmacol. 2014;171(8):2029-50. Epub 2013/10/15. doi: 10.1111/bph.12461. PubMed PMID: 24117165; PMCID: PMC3976620.

124.   Liu S, Soong Y, Seshan SV, Szeto HH. Novel cardiolipin therapeutic protects endothelial mitochondria during renal ischemia and mitigates microvascular rarefaction, inflammation, and fibrosis. Am J Physiol Renal Physiol. 2014;306(9):F970-80. Epub 2014/02/21. doi: 10.1152/ajprenal.00697.2013. PubMed PMID: 24553434.

125.   Machiraju P, Wang X, Sabouny R, Huang J, Zhao T, Iqbal F, King M, Prasher D, Lodha A, Jimenez-Tellez N, Ravandi A, Argiropoulos B, Sinasac D, Khan A, Shutt TE, Greenway SC. SS-31 Peptide Reverses the Mitochondrial Fragmentation Present in Fibroblasts From Patients With DCMA, a Mitochondrial

Cardiomyopathy. Front Cardiovasc Med. 2019;6:167. Epub 2019/12/06. doi: 10.3389/fcvm.2019.00167. PubMed PMID: 31803760; PMCID: PMC6873783.

126. Birk AV, Chao WM, Bracken C, Warren JD, Szeto HH. Targeting mitochondrial cardiolipin and the cytochrome c/cardiolipin complex to promote electron transport and optimize mitochondrial ATP synthesis. Br J Pharmacol. 2014;171(8):2017-28. Epub 2013/10/19. doi: 10.1111/bph.12468. PubMed PMID: 24134698; PMCID: PMC3976619.

127. Mitchell W, Ng EA, Tamucci JD, Boyd KJ, Sathappa M, Coscia A, Pan M, Han X, Eddy NA, May ER, Szeto HH, Alder NN. The mitochondria-targeted peptide SS-31 binds lipid bilayers and modulates surface electrostatics as a key component of its mechanism of action. J Biol Chem. 2020;295(21):7452-69. Epub 2020/04/11. doi: 10.1074/jbc.RA119.012094. PubMed PMID: 32273339; PMCID: PMC7247319.

128. Chavez JD, Tang X, Campbell MD, Reyes G, Kramer PA, Stuppard R, Keller A, Zhang H, Rabinovitch PS, Marcinek DJ, Bruce JE. Mitochondrial protein interaction landscape of SS-31. Proc Natl Acad Sci U S A. 2020;117(26):15363-73. Epub 2020/06/20. doi: 10.1073/pnas.2002250117. PubMed PMID: 32554501; PMCID: PMC7334473.

129. Siegel MP, Kruse SE, Percival JM, Goh J, White CC, Hopkins HC, Kavanagh TJ, Szeto HH, Rabinovitch PS, Marcinek DJ. Mitochondrial-targeted peptide rapidly improves mitochondrial energetics and skeletal muscle performance in aged mice. Aging Cell. 2013;12(5):763-71. Epub 2013/05/23. doi: 10.1111/acel.12102. PubMed PMID: 23692570; PMCID: PMC3772966.

130. Campbell MD, Duan J, Samuelson AT, Gaffrey MJ, Merrihew GE, Egertson JD, Wang L, Bammler TK, Moore RJ, White CC, Kavanagh TJ, Voss JG, Szeto HH, Rabinovitch PS, MacCoss MJ, Qian WJ, Marcinek DJ. Improving

mitochondrial function with SS-31 reverses age-related redox stress and improves exercise tolerance in aged mice. Free Radic Biol Med. 2019;134:268-81. Epub 2019/01/01. doi: 10.1016/j.freeradbiomed.2018.12.031. PubMed PMID: 30597195; PMCID: PMC6588449.

131.   Escribano-Lopez I, Diaz-Morales N, Iannantuoni F, Lopez-Domenech S, de Maranon AM, Abad-Jimenez Z, Banuls C, Rovira-Llopis S, Herance JR, Rocha M, Victor VM. The mitochondrial antioxidant SS-31 increases SIRT1 levels and ameliorates inflammation, oxidative stress and leukocyte-endothelium interactions in type 2 diabetes. Sci Rep. 2018;8(1):15862. Epub 2018/10/28. doi: 10.1038/s41598-018-34251-8. PubMed PMID: 30367115; PMCID: PMC6203778.

132.   Sturgeon BE, Sipe HJ, Jr., Barr DP, Corbett JT, Martinez JG, Mason RP. The fate of the oxidizing tyrosyl radical in the presence of glutathione and ascorbate. Implications for the radical sink hypothesis. J Biol Chem. 1998;273(46):30116-21. Epub 1998/11/07. doi: 10.1074/jbc.273.46.30116. PubMed PMID: 9804766.

133.   Marquez LA, Dunford HB. Kinetics of oxidation of tyrosine and dityrosine by myeloperoxidase compounds I and II. Implications for lipoprotein peroxidation studies. J Biol Chem. 1995;270(51):30434-40. Epub 1995/12/22. doi: 10.1074/jbc.270.51.30434. PubMed PMID: 8530471.

134.   Reid Thompson W, Hornby B, Manuel R, Bradley E, Laux J, Carr J, Vernon HJ. A phase 2/3 randomized clinical trial followed by an open-label extension to evaluate the effectiveness of elamipretide in Barth syndrome, a genetic disorder of mitochondrial cardiolipin metabolism. Genet Med. 2021;23(3):471-8. Epub 2020/10/21. doi: 10.1038/s41436-020-01006-8. PubMed PMID: 33077895; PMCID: PMC7935714.

135.   Zhu Y, Luo M, Bai X, Li J, Nie P, Li B, Luo P. SS-31, a Mitochondria-Targeting Peptide, Ameliorates Kidney Disease. Oxid Med Cell Longev. 2022;2022:1295509. Epub 2022/06/17. doi: 10.1155/2022/1295509. PubMed PMID: 35707274; PMCID: PMC9192202.

136.   Durlinger EMJ, Spoelstra-de Man AME, Smit B, de Grooth HJ, Girbes ARJ, Oudemans-van Straaten HM, Smulders YM. Hyperoxia: At what level of SpO(2) is a patient safe? A study in mechanically ventilated ICU patients. J Crit Care. 2017;39:199-204. Epub 2017/03/11. doi: 10.1016/j.jcrc.2017.02.031. PubMed PMID: 28279497.

137.   Wingelaar TT, van Ooij PAM, van Hulst RA. Oxygen Toxicity and Special Operations Forces Diving: Hidden and Dangerous. Front Psychol. 2017;8:1263. Epub 2017/08/10. doi: 10.3389/fpsyg.2017.01263. PubMed PMID: 28790955; PMCID: PMC5524741.

138.   Thomson L, Paton J. Oxygen toxicity. Paediatr Respir Rev. 2014;15(2):120-3. Epub 2014/04/29. doi: 10.1016/j.prrv.2014.03.003. PubMed PMID: 24767867.

139.   Hafner S, Beloncle F, Koch A, Radermacher P, Asfar P. Hyperoxia in intensive care, emergency, and peri-operative medicine: Dr. Jekyll or Mr. Hyde? A 2015 update. Ann Intensive Care. 2015;5(1):42. Epub 2015/11/21. doi: 10.1186/s13613-015-0084-6. PubMed PMID: 26585328; PMCID: PMC4653126.

140.   Iwashyna TJ, Ely EW, Smith DM, Langa KM. Long-term cognitive impairment and functional disability among survivors of severe sepsis. JAMA. 2010;304(16):1787-94. Epub 2010/10/28. doi: 10.1001/jama.2010.1553. PubMed PMID: 20978258; PMCID: PMC3345288.

141.   Iwashyna TJ, Netzer G, Langa KM, Cigolle C. Spurious inferences about long-term outcomes: the case of severe sepsis and geriatric conditions. Am J Respir Crit Care Med. 2012;185(8):835-41. Epub 2012/02/11. doi: 10.1164/rccm.201109-1660OC. PubMed PMID: 22323301; PMCID: PMC3360570.

142.   Dungan CM, Murach KA, Frick KK, Jones SR, Crow SE, Englund DA, Vechetti IJ, Jr., Figueiredo VC, Levitan BM, Satin J, McCarthy JJ, Peterson CA. Elevated myonuclear density during skeletal muscle hypertrophy in response to training is reversed during detraining. Am J Physiol Cell Physiol. 2019;316(5):C649-C54. Epub 2019/03/07. doi: 10.1152/ajpcell.00050.2019. PubMed PMID: 30840493; PMCID: PMC6580158.

143.   Dungan CM, Brightwell CR, Wen Y, Zdunek CJ, Latham CM, Thomas NT, Zagzoog AM, Brightwell BD, VonLehmden GL, Keeble AR, Watowich SJ, Murach KA, Fry CS. Muscle-Specific Cellular and Molecular Adaptations to Late-Life Voluntary Concurrent Exercise. Function (Oxf). 2022;3(4):zqac027. Epub 2022/07/02. doi: 10.1093/function/zqac027. PubMed PMID: 35774589; PMCID: PMC9233305.

144.   Boden G. Interaction between free fatty acids and glucose metabolism. Curr Opin Clin Nutr Metab Care. 2002;5(5):545-9. Epub 2002/08/13. doi: 10.1097/00075197-200209000-00014. PubMed PMID: 12172479.

145.   Tabe Y, Konopleva M, Andreeff M. Fatty Acid Metabolism, Bone Marrow Adipocytes, and AML. Front Oncol. 2020;10:155. Epub 2020/03/07. doi: 10.3389/fonc.2020.00155. PubMed PMID: 32133293; PMCID: PMC7040225.

146.   Frydrych LM, Fattahi F, He K, Ward PA, Delano MJ. Diabetes and Sepsis: Risk, Recurrence, and Ruination. Front Endocrinol (Lausanne). 2017;8:271.

Epub 2017/11/23. doi: 10.3389/fendo.2017.00271. PubMed PMID: 29163354; PMCID: PMC5670360.

147.   Yende S, van der Poll T. Diabetes and sepsis outcomes--it is not all bad news. Crit Care. 2009;13(1):117. Epub 2009/03/18. doi: 10.1186/cc7707. PubMed PMID: 19291261; PMCID: PMC2688126.

148.   Schuetz P, Castro P, Shapiro NI. Diabetes and sepsis: preclinical findings and clinical relevance. Diabetes Care. 2011;34(3):771-8. Epub 2011/03/02. doi: 10.2337/dc10-1185. PubMed PMID: 21357364; PMCID: PMC3041224.

149.   Trevelin SC, Carlos D, Beretta M, da Silva JS, Cunha FQ. Diabetes Mellitus and Sepsis: A Challenging Association. Shock. 2017;47(3):276-87. Epub 2016/10/30. doi: 10.1097/shk.0000000000000778. PubMed PMID: 27787406.

EDUCATION

2019-*present*   University of Kentucky College of Medicine

PhD in Nutritional Science

Thesis Advisor: Hiroshi Saito, Ph.D.

Expected Graduation Date: May 2023

2016-2019   Auburn University

B.S. in Exercise Science

Graduated *Cum Laude*, *University Scholar*

RESEARCH EXPERIENCE

2018-2019   **Auburn University, Department of Kinesiology**

Undergraduate Researcher

Advisers: Bruce Gladden, PhD and Andreas Kavazis, PhD

2019   **University of Kentucky, Department of Biochemistry**

Graduate Research Assistant

Adviser: Haining Zhu, PhD

2020-*present*   **University of Kentucky, Department of Pharmacology and Nutritional Sciences**

Graduate Research Assistant

Adviser: Hiroshi Saito, PhD

TEACHING EXPERIENCE

College Level

Spring 2019   **Auburn University**

KINE 6501: Clinical Exercise Testing Laboratory

Spring 2023   **University of Kentucky College of Medicine**

NS/CNS/AS 602: Integrated Nutritional Sciences

K-12

2019-*present*   **Vestavia Hills High School**

Vestavia, AL

Lecturer, Advanced Placement Civics and Government, We the People Constitutional Debate Section

ADVISING ACTIVITES

Auburn University

06/2018-08/2018   Peer Mentor, Junior Undergraduate Student in Neuroscience, Research Volunteer in Muscle Biochemistry

08/2018-12/2018   Peer Tutor, Sorority Academic Advisory Board

Courses Tutored: KINE 3620; ENGL1100, 1107, 1120, 1127

| 08/2018-05/2019 | Peer Mentor, Junior Undergraduate Student in Biomedical Sciences, Research Volunteer in Muscle Biochemistry |

University of Kentucky College of Medicine

| 06/2020-05/2022 | Graduate Student Advisor, Undergraduate Student in Neuroscience, Research Assistant in Saito Lab |

| 06/2022-05/2023 | Graduate Student Advisor, Senior Undergraduate Student in Biology, Research Assistant in Saito Lab |

ADMINISTRATIVE ACTIVITIES & UNIVERSITY SERVICE

University

Auburn University

| 08/2017-11/2017 | Liaison for Football Seating between campus organizations, Auburn Student Government, and Auburn Athletics |

University of Kentucky

| 01/2022-*present* | Member, Graduate Student Congress |

College

University of Kentucky College of Medicine

05/2020-06/2021	Director of Fundraising, Biomedical Graduate Student Organization (BGSO)
08/2021-04/2022	Planning Committee, Liaison between TRAC and University Event Services, 13th Annual Trainee Poster Session
06/2021-*present*	President, Biomedical Graduate Student Organization
06/2021-*present*	Graduate Student Representative, Trainees in Research Advisory Committee (TRAC)

| 09/2022-*present* | Planning Committee, 14th Annual Trainee Poster Session |

Department

University of Kentucky College of Medicine

Integrated Biomedical Sciences Program

02/2021-03/2021	Panelist, IBS Interview Student Panel Sessions
02/2022-03/2022	Panelist, IBS Interview Student Panel Sessions
02/2022-03/2022	Coordinator, IBS Interview Virtual Happy Hour

Department of Pharmacology and Nutritional Sciences

| 08/2021, 08/2022 | Speaker, Integrated Biomedical Sciences Orientation |
| 07/2022-*present* | Vice President, Nutritional Sciences & Pharmacology Student Association |

HONORS & AWARDS

Academic

2016-2019	Spirit of Auburn Founders Scholarship, Auburn University
2019-2019	Dean's List, College of Education, Auburn University
2019	Auburn University Honors College Honors Scholar
2022	Department of Pharmacology and Nutritional Sciences Special Recognition of Achievement Award, University of Kentucky College of Medicine
2022	Department of Pharmacology and Nutritional Sciences' Nominee for College of Medicine Graduate Trainee of the Year

Research

06/2022	Travel Award, 45th Annual Conference on Shock, Toronto, Canada
05/2023	Arthur Baue Presidential Travel Award, 46th Annual Conference on Shock, Portland Oregon

PROFESSIONAL ACTIVITIES, PUBLIC SERVICE & PROFESSIONAL DEVELOPMENT

Memberships

2016-2019	Auburn University Honors College
2019-*present*	Auburn University Alumni Association
2019-*present*	UK Biomedical Graduate Student Organization *(Currently President, formerly Director of Fundraising)*
2020-*present*	UK Nutritional Sciences & Pharmacology Student Association *(Currently Vice President)*
2020-*present*	UK Women in Medicine and Science
2020-*present*	MITOtalks International Seminar Group
2021-*present*	Students Embracing Equity in Medical Sciences
2021-*present*	US Shock Society
2021-*present*	UK Biomedical Sciences Journal Club
2021-*present*	UK Mito Journal Club
2021-*present*	UK Muscle Forum
2022-*present*	Kentucky Advocates for Science Policy and Research *(Vice President)*
2022-*present*	UK Graduate Student Congress
2022-*present*	Kentucky Academy of Science
2022-*present*	American Physiological Society

Journal Editing

Editor in Chief

08/2022-*present* The Journal of Pharmacology and Nutritional

Sciences (JPNS)

Journal Peer-Reviewing

02/2023-*present* The Journal of Pharmacology and Nutritional Sciences

Collaborative Reviewer *(Supervision provided by Dr. Hiroshi Saito)*

07/2022 SHOCK: Injury, Inflammation, and Sepsis: Laboratory and

Clinical Approaches

Public Service

11/2021 **Girls in Engineering, Math, and Science**

Morehead State University; Morehead, KY

Organized 2 workshops run by graduate students at UK for

the Girl Scouts' attendees to encourage their interest in

science; 6 hours

Professional Development

03/2022   Nutritional Sciences and Pharmacology Student Association

CV & Resume Workshop

08/2022   2022 KY INBRE Electron Microscopy Summer Workshop

University of Kentucky; Lexington, KY

Electron Microscopy Capabilities for Researchers

TEM Imaging Tips & Tricks

Quadriceps mitochondrial dysfunction following

anterior cruciate ligament injury and reconstruction:

TEM analysis of mitochondria

SPEAKING ENGAGEMENTS

03/2022   **Department of Surgery Invited Speaker Research Series**

University of Kentucky; Lexington, KY

Post-Sepsis Muscle Weakness can be mediated by

Mitochondrial Protection

04/2022   **13th Annual College of Medicine Trainee Poster Session**

University of Kentucky; Lexington, KY

Panelist, *Effect of COVID-19 on Biomedical Research*

11/2022   **Invited Speaker**

Arkansas Children's Nutrition Center; Little Rock, AR

Mitochondria as drivers, therapeutic targets in post-sepsis

skeletal muscle weakness

RESEARCH & INTELLECTUAL CONTRIBUTIONS

A. PUBLICATIONS

Peer-Reviewed Research in Professional, Scientific, or Educational Journals

1. Arenas A, Kuang L, Zhang J, **Kingren MS**, Zhu H. FUS regulates autophagy by mediating the transcription of genes critical to the autophagosome formation. *J Neurochem*. 2021 May;157(3)752-763. Doi: 10.1111/jjnc.15281.
2. **Kingren MS**, Starr ME, Saito H. Divergent Sepsis Pathophysiology in Older Adults. *Antioxid Redox Signal*. 2021 Jul 1. Doi: 10.1089/ars.2021.0056. PMID: 34210173
3. Ang JM, **Kingren MS**, Saito H. Comparison of Murine Abdominal Models for Sepsis Studying Chronic Critical Illness. In review, submitted to *Shock* in January 2023.
4. **Kingren MS**. It's Easier than you Think: Building a Pipeline to Analyze your own RNA Sequencing Data. In review, submitted to *JPNS* in March 2023.
5. **Kingren MS,** Owen AM, Keeble AR, Galvan-Lara AM, Mori S, Pu J, Tarantini S, St Clair DK, Ungvari Z, Butterfield TA, Kosmac K, Stromberg A, Fry C, Patel S, Saito H. (2023). *Mitochondrial Abnormalities Cause Progressive Development of Post-Sepsis Chronic Muscle Weakness.* In prep.

Print Media

1. **Kingren MS**, Police S. Forgetfulness in your 40s. *Health and Wellness Magazine*. 2021 October 2021;19(2): 16.

B. ABSTRACT PRESENTATIONS

Local/State/Regional Meetings

1. **Kingren MS**, Harrel M, Sanders E. (2019). *Athlete Performance Optimization: Balancing Sleep, Recovery Techniques, and Nutrition.* Poster presented at the annual School of Kinesiology Research Day, Auburn University.

2. **Kingren MS**, Pu J, Yamashita-Mori S, Galvan-Lara AM, Owen AM, Starr ME, Butterfield TA, Saito H. (2021). *MnSOD Overexpression Mitigates Sepsis-Induced Long-Term Skeletal Muscle Weakness.* Poster presented at the 12th Annual College of Medicine Trainee Poster Session, University of Kentucky.

3. **Kingren MS.** (2021). *Skeletal Muscle Dysfunction Following Sepsis.* Oral departmental seminar presentation given at Spring 2021 Department of Pharmacology & Nutritional Sciences Seminar Series, University of Kentucky College of Medicine.

4. **Kingren MS**, Pu J, Yamashita-Mori S, Owen AM, St Clair DK, Starr ME, Butterfield TA, Tarantini S, Ungvari Z, Saito H. (2022). *Mitochondrial protection ameliorates sepsis-induced skeletal muscle weakness.* Poster presented at the 13th Annual College of Medicine Trainee Poster Session, University of Kentucky.

5. **Kingren MS** (2022). *Mitochondrial Protection Reduces Sepsis-Induced Chronic Muscle Weakness.* Oral seminar presentation given at the spring 2022 Department of Pharmacology & Nutritional Sciences Seminar Series, University of Kentucky College of Medicine.

National/International Meetings

1. Ang JM, Yamashita-Mori S, Lewis ED, **Kingren MS**, Bruno MEC, Starr ME, Saito H. (2021). *Comparison of Murine Abdominal Sepsis Models for Studying Chronic Critical Illness*. Poster presented at the 44th Annual Conference on Shock, Virtual Format.

2. **Kingren MS,** Pu J, Galvan-Lara A., Yamashita-Mori S, Owen AM, St Clair DK, Butterfield TA, Starr ME, Saito H. (2021). *Mitochondrial SOD Overexpression Mitigates Sepsis Induced Chronic Skeletal Muscle Weakness.* Poster presented at the 44th Annual Conference on Shock, Virtual Format.

3. **Kingren MS**, Pu J, Yamashita-Mori S, Owen AM, St Clair DK, Starr ME, Butterfield TA, Tarantini S, Ungvari Z, Saito H. (2022). *Mitochondrial Protection Ameliorates Post-Sepsis Chronic Skeletal Muscle Weakness*. Selected for Oral Presentation at the 45th Annual Conference on Shock, Toronto, Canada.

4. **Kingren MS,** Owen AM, Keeble AR, Galvan-Lara AM, Mori S, Pu J, Tarantini S, St Clair DK, Ungvari Z, Butterfield TA, Kosmac K, Stromberg A, Fry C, Patel S, Saito H. (2023). *Post-Sepsis Chronic Muscle Weakness Occurs Progressively and can be Prevented by Pharmacological Protection of Mitochondria.* Selected for Oral Presentation at the 46th Annual Conference on Shock, Portland, OR, USA.